

AWARD NUMBER: W81XWH-11-1-0600

TITLE: Probing HER2-PUMA and EGFR-PUMA Crosstalks in Aggressive Breast Cancer

PRINCIPAL INVESTIGATOR: Hui-Wen Lo, Ph.D.

RECIPIENT: Duke University
Durham, NC 27708-4640

REPORT DATE: September 2014

TYPE OF REPORT: Final

PREPARED FOR: U.S. Army Medical Research and Materiel Command
Fort Detrick, Maryland 21702-5012

DISTRIBUTION STATEMENT: Approved for Public Release; Distribution
Unlimited

The views, opinions and/or findings contained in this report are those of the author(s) and should not be construed as an official Department of the Army position, policy or decision unless so designated by other documentation.

REPORT DOCUMENTATION PAGE

Form Approved
OMB No. 0704-0188

Public reporting burden for this collection of information is estimated to average 1 hour per response, including the time for reviewing instructions, searching existing data sources, gathering and maintaining the data needed, and completing and reviewing this collection of information. Send comments regarding this burden estimate or any other aspect of this collection of information, including suggestions for reducing this burden to Department of Defense, Washington Headquarters Services, Directorate for Information Operations and Reports (0704-0188), 1215 Jefferson Davis Highway, Suite 1204, Arlington, VA 22202-4302. Respondents should be aware that notwithstanding any other provision of law, no person shall be subject to any penalty for failing to comply with a collection of information if it does not display a currently valid OMB control number. **PLEASE DO NOT RETURN YOUR FORM TO THE ABOVE ADDRESS.**

1. REPORT DATE

September 2014

2. REPORT TYPE

Final

3. DATES COVERED

1Sep2011-31Aug2014

4. TITLE AND SUBTITLE

Probing HER2-PUMA and EGFR-PUMA Crosstalks in Aggressive Breast Cancer

5a. CONTRACT NUMBER

W81XWH-11-1-0600

5b. GRANT NUMBER**5c. PROGRAM ELEMENT NUMBER****5d. PROJECT NUMBER****5e. TASK NUMBER****5f. WORK UNIT NUMBER****6. AUTHOR(S)**

HUI-WEN LO

E-Mail: huiwen.lo@duke.edu

7. PERFORMING ORGANIZATION NAME(S) AND ADDRESS(ES)

Duke University
Durham, NC 27708

8. PERFORMING ORGANIZATION REPORT**9. SPONSORING / MONITORING AGENCY NAME(S) AND ADDRESS(ES)**

U.S. Army Medical Research and Materiel Command
Fort Detrick, Maryland 21702-5012

10. SPONSOR/MONITOR'S ACRONYM(S)**11. SPONSOR/MONITOR'S REPORT NUMBER(S)****12. DISTRIBUTION / AVAILABILITY STATEMENT**

Approved for Public Release; Distribution Unlimited

13. SUPPLEMENTARY NOTES

14. ABSTRACT EGFR and HER2 are overexpressed in 20% and 30% of invasive breast cancer, respectively, and are associated with aggressive tumor subtypes and shortened patient survival. Both receptors are important targets of breast cancer therapy. However, despite the apparent promise of some of these therapies, EGFR- and HER2-based monotherapy and combination regimens have serious limitations and need improvement. The goal of this study is, thus, to gain insights into the biology of EGFR- and HER2-expressing invasive breast cancer in order to provide rationales for more effective EGFR- and HER2-based combination therapy for women with breast cancer. Our proposal is built on novel significant findings made from the initial Idea Award. We discovered that proapoptotic PUMA protein is highly expressed in the breast cancer cell lines and patient tumors that overexpress HER2 and/or EGFR. In addition to co-expression, we found HER2 and EGFR to interact with PUMA constitutively and under the treatment of apoptosis inducers. The HER2-PUMA and EGFR-PUMA interactions are not disrupted when breast cancer cells are treated with the EGFR kinase inhibitors, indicating a kinase-independent interaction. Despite the fact that PUMA has been reported to be primarily located on the mitochondrial membranes and initiate apoptosis upon appropriate stress, our results showed PUMA to be sequestered in the cytoplasm of EGFR-expressing breast cancer cells. Although, the BH3-only proapoptotic proteins can be functionally redundant, we observed PUMA to be essential for apoptotic induction in breast cancer cells. Interestingly, while no reports have investigated PUMA phosphorylation, our preliminary results show that PUMA undergoes tyrosine phosphorylation mediated by HER2 and EGFR. These exiting preliminary observations suggest that EGFR and HER2 may modulate PUMA via two modes of actions: (i) interacting with PUMA to prevent PUMA mitochondrial translocation in a kinase-independent fashion, and (ii) phosphorylating PUMA to affect its functionality in a kinase-dependent phosphorylation. Our hypothesis is that the EGFR-PUMA and HER2-PUMA signaling crosstalks modulate PUMA-mediated apoptotic pathway and cellular functions of EGFR and HER2, together contributing to the aggressive behavior of invasive breast cancer. Based on this, we postulate that restoring intrinsic apoptosis will sensitize breast cancer to EGFR- and HER2-targeted therapy. Specific Aims are (1) Characterize EGFR-PUMA and HER2-PUMA crosstalks in breast cancer overexpressing EGFR and/or HER2. (2) Investigate the biological consequence(s) of the phosphorylation of PUMA by EGFR and HER2 in breast cancer. (3) Determine the extent to which PUMA's apoptotic function is associated with breast cancer response to EGFR- and HER2-targeted therapy. The project sheds light on the malignant phenotype of aggressive breast cancer that overexpress HER2 and/or EGFR which constitutes approximately half of invasive breast cancer and could also provide rationales for new more effective therapy for women with aggressive subtypes of breast cancer.

15. SUBJECT TERMS

NOTHING LISTED

16. SECURITY CLASSIFICATION OF:

U

17. LIMITATION OF ABSTRACT

UU

18. NUMBER OF PAGES

45

19a. NAME OF USAMRMC RESPONSIBLE PERSON

19b. TELEPHONE NUMBER (include area code)

a. REPORT
U

b. ABSTRACT
U

c. THIS PAGE
U

Table of Contents

	<u>Page</u>
1. Introduction	4
2. Keywords	4
3. Overall Project Summary	4
4. Key Research Accomplishments	15
5. Conclusion	15
6. Publications, Abstracts, and Presentations	16
7. Inventions, Patents and Licenses	18
8. Reportable Outcomes	18
9. Other Achievements	18
10. References	18
11. Appendices	19

[SF298]

Note: An abstract is required to be provided in Block 14

EGFR and HER2 are overexpressed in 20% and 30% of invasive breast cancer, respectively, and are associated with aggressive tumor subtypes and shortened patient survival. Both receptors are important targets of breast cancer therapy. However, despite the apparent promise of some of these therapies, EGFR- and HER2-based monotherapy and combination regimens have serious limitations and need improvement. The goal of this study is, thus, to gain insights into the biology of EGFR- and HER2-expressing invasive breast cancer in order to provide rationales for more effective EGFR- and HER2-based combination therapy for women with breast cancer. Our proposal is built on novel significant findings made from the initial Idea Award. We discovered that proapoptotic PUMA protein is highly expressed in the breast cancer cell lines and patient tumors that overexpress HER2 and/or EGFR. In addition to co-expression, we found HER2 and EGFR to interact with PUMA constitutively and under the treatment of apoptosis inducers. The HER2-PUMA and EGFR-PUMA interactions are not disrupted when breast cancer cells are treated with the EGFR kinase inhibitors, indicating a kinase-independent interaction. Despite the fact that PUMA has been reported to be primarily located on the mitochondrial membranes and initiate apoptosis upon appropriate stress, our results showed PUMA to be sequestered in the cytoplasm of EGFR-expressing breast cancer cells. Although, the BH3-only proapoptotic proteins can be functionally redundant, we observed PUMA to be essential for apoptotic induction in breast cancer cells. Interestingly, while no reports have investigated PUMA phosphorylation, our preliminary results show that PUMA undergoes tyrosine phosphorylation mediated by HER2 and EGFR. These exciting preliminary observations suggest that EGFR and HER2 may modulate PUMA via two modes of actions: (i) interacting with PUMA to prevent PUMA mitochondrial translocation in a kinase-independent fashion, and (ii) phosphorylating PUMA to affect its functionality in a kinase-dependent phosphorylation. Our hypothesis is that the EGFR-PUMA and HER2-PUMA signaling crosstalks modulate PUMA-mediated apoptotic pathway and cellular functions of EGFR and HER2, together contributing to the aggressive behavior of invasive breast cancer. Based on this, we postulate that restoring intrinsic apoptosis will sensitize breast cancer to EGFR- and HER2-targeted therapy. Specific Aims are (1) Characterize EGFR-PUMA and HER2-PUMA crosstalks in breast cancer overexpressing EGFR and/or HER2. (2) Investigate the biological consequence(s) of the phosphorylation of PUMA by EGFR and HER2 in breast cancer. (3) Determine the extent to which PUMA's apoptotic function is associated with breast cancer response to EGFR- and HER2-targeted therapy. The project sheds light on the malignant phenotype of aggressive breast cancer that overexpress HER2 and/or EGFR which constitutes approximately half of invasive breast cancer and could also provide rationales for new more effective therapy for women with aggressive subtypes of breast cancer.

1. INTRODUCTION

Approximately half of the human invasive breast carcinomas overexpress HER2 and/or EGFR and the overexpression leads to more aggressive tumor behaviors and shortened patient survival. Both receptors are important targets of breast cancer therapy. However, despite the apparent promise of some of these therapies, HER2- and EGFR-based regimens have their limitations and need improvement. The **goals** of this Idea Expansion Award are to gain insights into the malignant biology and drug-resistant phenotype of EGFR- and/or HER2-overexpressing breast cancer and to use the acquired knowledge for the development of a sensitization strategy that will improve EGFR- and HER2-targeted therapies. The immediate **objective** of this project is to define the biological significance and therapeutic implications of the novel HER2-PUMA and EGFR-PUMA crosstalks in breast cancer. **Our hypothesis is two-fold.** First, we hypothesize that the HER2-PUMA and EGFR-PUMA signaling crosstalks modulate PUMA-mediated apoptotic pathway and regulate cellular functions of HER2 and EGFR, together contributing to the aggressive behavior of HER2- and EGFR-overexpressing breast cancer. Second, we postulate that PUMA's apoptotic function is associated with breast cancer response to HER2- and EGFR-targeted therapies and that restoring PUMA-mediated intrinsic apoptosis will sensitize breast cancer to the therapies. To test the aforementioned hypothesis, we conducted **three Specific Aims:** 1) Characterize the HER2-PUMA and EGFR-PUMA crosstalks in breast cancer cells. 2) Investigate the biological consequence(s) of the phosphorylation of PUMA by HER2 and EGFR in breast cancer. 3) Determine the extent to which PUMA's apoptotic function is associated with breast cancer response to HER2- and EGFR-targeted therapies. Successful accomplishment of these aims could lead to a greater understanding of the malignant biology and the drug-resistant phenotype of nearly half of the invasive breast carcinomas with HER2 and/or EGFR overexpression which makes them more aggressive. The outcome could also provide a rationale to restore PUMA's apoptotic function as a novel strategy that sensitizes aggressive breast cancer to HER2- and EGFR-targeted therapies.

2. KEYWORDS

EGFR, HER2, PUMA, signal crosstalks, apoptosis, phosphorylation, breast cancer

3. OVERALL PROJECT SUMMARY: *Summarize the progress during appropriate reporting period (single annual or comprehensive final). This section of the report shall be in direct alignment with respect to each task outlined in the approved SOW in a summary of Current Objectives, and a summary of Results, Progress and Accomplishments with Discussion. Key methodology used during the reporting period, including a description of any changes to originally proposed methods, shall be summarized. Data supporting research conclusions, in the form of figures and/or tables, shall be embedded in the text, appended, or referenced to appended manuscripts. Actual or anticipated problems or delays and actions or plans to resolve them shall be included. Additionally, any changes in approach and reasons for these changes shall be reported. Any change that is substantially different from the original approved SOW (e.g., new or modified tasks, objectives, experiments, etc.) requires review by the Grants Officer's Representative and final approval by USAMRAA Grants Officer through an award modification prior to initiating any changes.*

Current Objectives: Over the past three years, we were able to complete the proposed research and also expanded the project in a logical and responsible fashion. As proposed, we functionally characterized the interactions between PUMA and EGFR/HER2 and found the interplays to lead to a negative impact on breast cancer response to apoptosis induction. These observations have been published in PLoS One in 2013 [Carpenter, R. L, Han, W., Paw, I. and Lo, H.-W. PLoS ONE

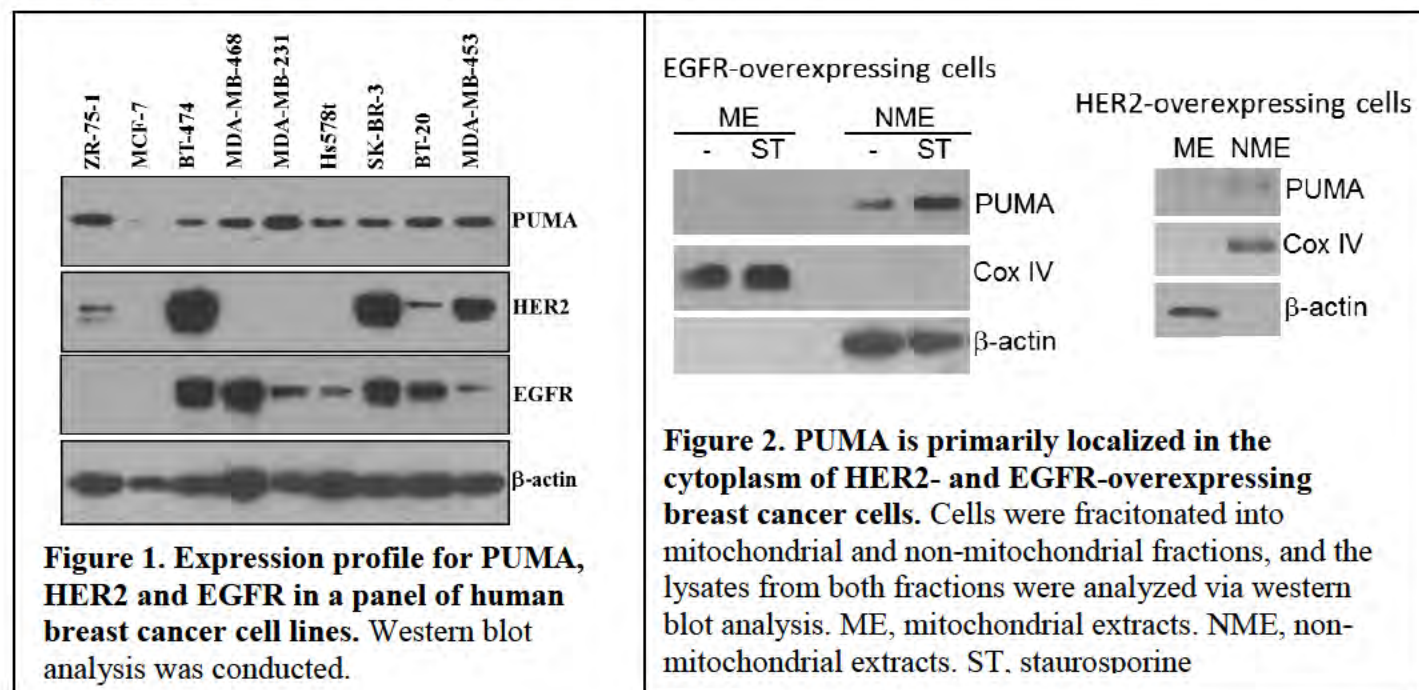
8(11):e78836, 2013]. The results are summarized below. Our future directions are to develop therapeutic strategies to activate PUMA in order to sensitize breast cancer with high levels of EGFR and/or HER2.

We further reported that STAT1 gene expression is enhanced by nuclear EGFR and HER2 via cooperation with STAT3 in breast cancer cells [Han, W., Carpenter, RL., Cao, X. and Lo, H.-W. *Molecular Carcinogenesis* 52:959-969, 2013]. Most recently, we reported that Akt phosphorylates and activates HSF-1 independent of heat shock, leading to Slug overexpression and epithelial-mesenchymal transition (EMT) of HER2-overexpressing breast cancer cells [Carpenter, R. L., Paw, I, Dewhirst, M. W., and Lo, H.-W. *Oncogene*, Published ahead of print, Jan 28, 2014]. The results reported in these publications can be found in the appendix. Building on these observations, our objectives are to further explore the translational implications of these observations. For example, we will examine whether dual targeting of Akt and HSF-1 will effectively prevent metastasis of HER2-driven breast cancer.

Summary of Results

PUMA is primarily localized in the cytoplasm of HER2- and EGFR-overexpressing breast cancer cells, where PUMA is dysfunctional (Task 1-a).

To help determine the extent to which HER2 and EGFR modulate PUMA subcellular locations in breast cancer cells, we first analyzed a panel of human breast cancer cell lines for expression levels of all three proteins. As shown in **Figure 1**, the majority of breast cancer cells lines analyzed expressed PUMA and some of them co-expressed PUMA and HER2/EGFR. Next, we selected a HER2-overexpressing and an EGFR-overexpressing cell lines, fractionated the cells into mitochondrial and non-mitochondrial fractions, extracted lysates from each fraction, and determined PUMA expression levels using western blot analysis. As shown in **Figure 2**, in both cell lines PUMA was primarily localized in the non-mitochondrial extracts (NME), but to a lesser degree in the mitochondrial extracts (ME). Mitochondrial fractionation was effective as indicated by the lack of COX IV expression in the NME and the absence of β -actin expression in the ME. These results indicated that PUMA is primarily localized in the cytoplasm of HER2- and EGFR-overexpressing breast cancer cells, where PUMA is not functional.



PUMA knockdown increased EGFR expression (Task 1-b).

To examine the effects of PUMA on EGFR, we knockdowned PUMA expression using siRNA, treated the cells with and without EGF for 20 minutes, and then determined EGFR levels and activation status using western blot analysis. As shown in **Figure 3**, we found the PUMA siRNA to be effective in reducing PUMA expression while the non-specific (NS) siRNA served as negative controls. Interestingly, our results showed that PUMA downregulation led to increased expression of EGFR, independent of EGF stimulation. Consistent with the increase in EGFR, we observed a higher level of activated EGFR (p-EGFR) in EGF-treated cells with PUMA siRNA compared to those with NS siRNA.

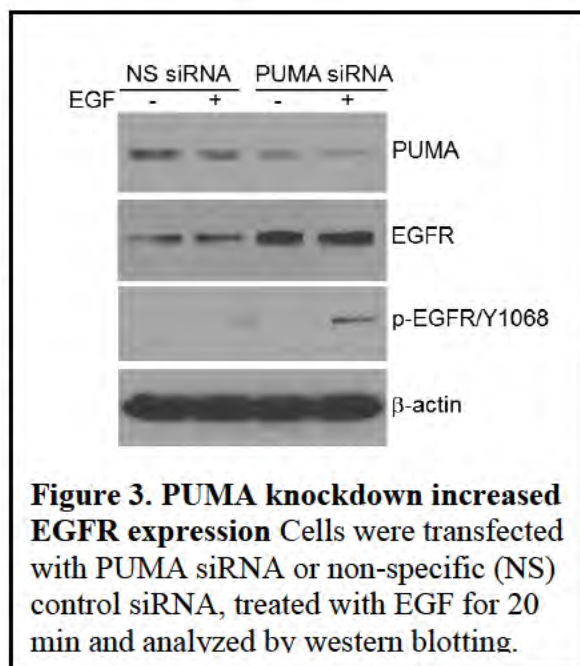


Figure 3. PUMA knockdown increased EGFR expression Cells were transfected with PUMA siRNA or non-specific (NS) control siRNA, treated with EGF for 20 min and analyzed by western blotting.

HER2 interacts with and phosphorylates PUMA in breast cancer cells (Task 2-a).

Using immunoprecipitation/western blotting (IP/WB) and HER2-overexpressing breast cancer cells, we found HER2 to interact with PUMA constitutively (**Figure 4A**). The HER2-PUMA interaction was sustained when breast cancer cells were treated with lapatinib, a dual HER2/EGFR kinase inhibitor that has effectively inhibited HER2 phosphorylation (**Figure 4B**). In line with the results of lapatinib, the HER2-PUMA interaction is independent of heregulin-induced receptor activation (**Figure 4C**). These results indicate that HER2 interacts with PUMA constitutively in a kinase-independent fashion.

Furthermore, we found that PUMA was tyrosine-phosphorylated in heregulin-stimulated HER2-overexpressing MDA-MB-453 cells (**Figure 5A**). We further confirmed this results using cell-free kinase assays in which the reactions contained HER2 (recombinant C-terminal HER2 expressed in Sf9 insect cells; Promega) and pre-dephosphoryated PUMA (from HEK293 cells infected with a PUMA viral vector; OriGene). Reactions were subjected to WB for tyrosine-phosphorylated PUMA using an anti-phosphotyrosine Ab (4G10; Upstate). Importantly, results of the kinase assay (**Figure 5B**) show that HER2 phosphorylated PUMA at the tyrosine residue(s) and the phosphorylation was inhibited by lapatinib. Together, results in Figures 4 and 5 indicate that HER2 interacts with and phosphorylates PUMA.

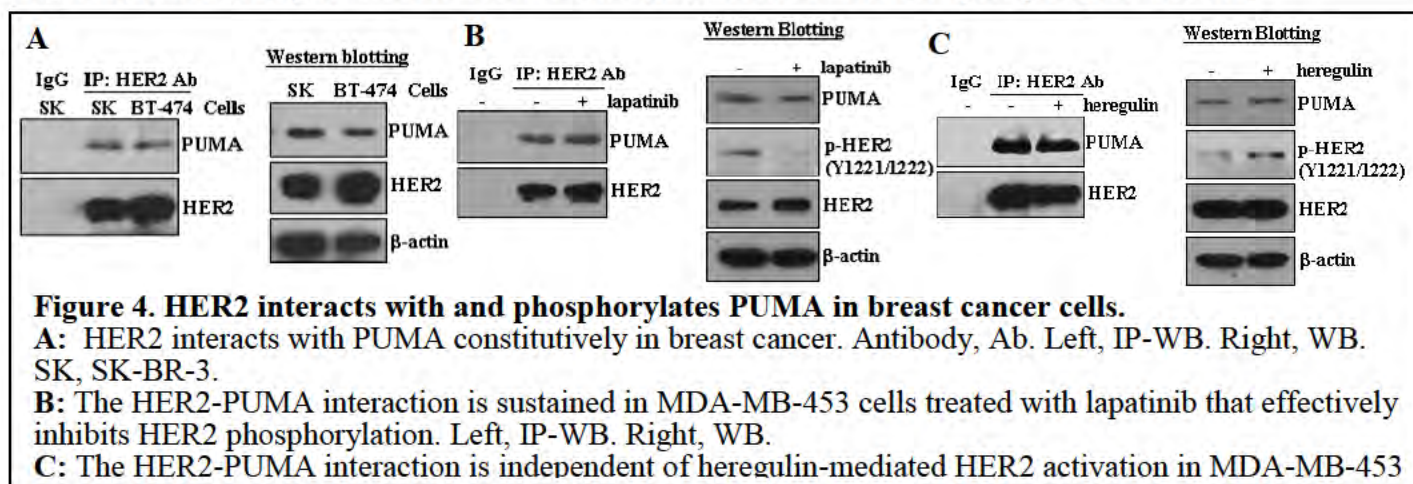


Figure 4. HER2 interacts with and phosphorylates PUMA in breast cancer cells.

A: HER2 interacts with PUMA constitutively in breast cancer. Antibody, Ab. Left, IP-WB. Right, WB. SK, SK-BR-3.

B: The HER2-PUMA interaction is sustained in MDA-MB-453 cells treated with lapatinib that effectively inhibits HER2 phosphorylation. Left, IP-WB. Right, WB.

C: The HER2-PUMA interaction is independent of heregulin-mediated HER2 activation in MDA-MB-453

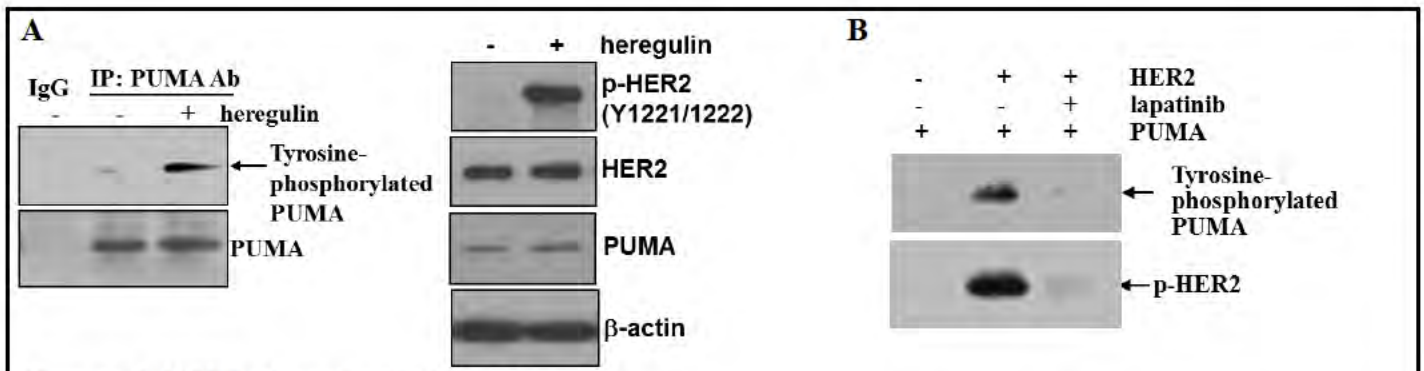


Figure 5. HER2 phosphorylates PUMA.

A: PUMA is tyrosine-phosphorylated in heregulin-stimulated HER2-positive MDA-MB-453 cells. Left, IP-WB. Right, WB.
B: PUMA phosphorylation HER2, as shown by cell-free kinase assay. Reactions were subjected to WB to detect tyrosine-phosphorylated PUMA using an anti-phosphotyrosine Ab. PUMA phosphorylation was inhibited by lapatinib.

EGFR interacts with and phosphorylates PUMA in breast cancer cells (Task 2-a).

As shown by IP/WB in **Figure 6**, EGFR interacts with PUMA constitutively and under the treatments with an apoptosis-inducer, staurosporine (ST), and the EGFR kinase inhibitor, Iressa, in MDA-MB-468 cells with EGFR gene amplification. In the intracellular analyses, serum-starved breast cancer cells were stimulated with and without EGF for 10 minutes. Total proteins were subjected to IP to pull down PUMA followed by WB to detect tyrosine-phosphorylated PUMA. As shown in **Figure 7A-C**, PUMA was tyrosine-phosphorylated in two EGFR-overexpressing cancer cells line and the phosphorylation was enhanced by EGF. In **Figure 7D-E**, we used the cell-free EGFR kinase assay to further show that recombinant PUMA was phosphorylated by EGFR and the phosphorylation was inhibited by the EGFR kinase inhibitor Iressa. Collectively, results in Figures 6 and 7 indicate that PUMA is phosphorylated by EGFR.

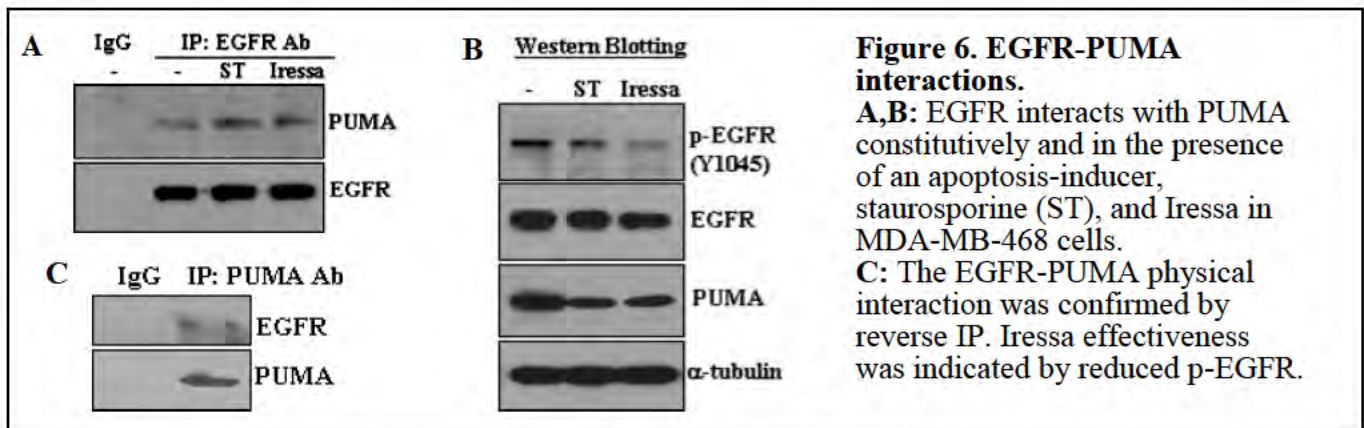
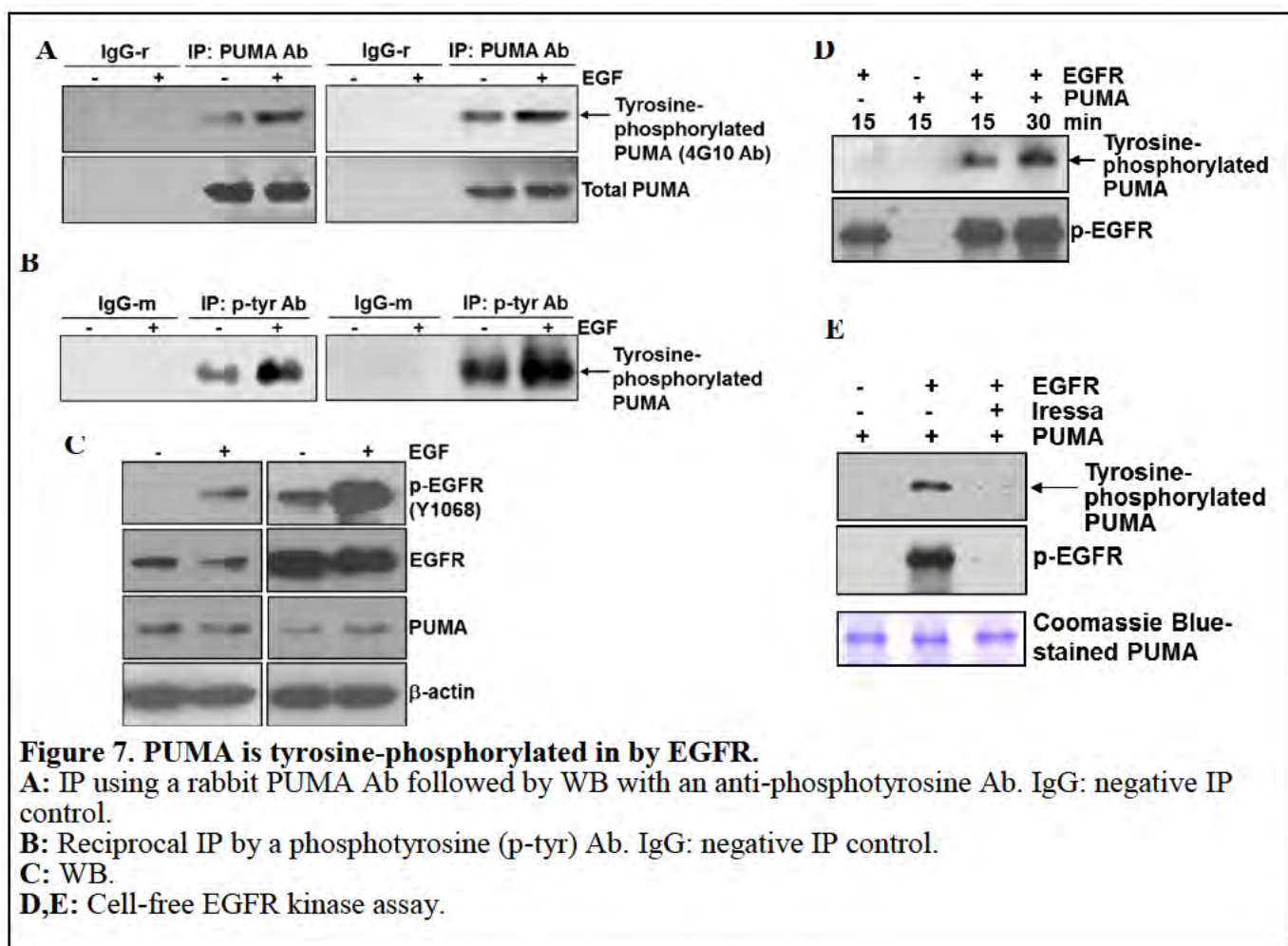


Figure 6. EGFR-PUMA interactions.

A,B: EGFR interacts with PUMA constitutively and in the presence of an apoptosis-inducer, staurosporine (ST), and Iressa in MDA-MB-468 cells.
C: The EGFR-PUMA physical interaction was confirmed by reverse IP. Iressa effectiveness was indicated by reduced p-EGFR.



HER2 phosphorylates PUMA at three tyrosine residues (Task 2-b).

A search of the human PUMA protein sequence revealed the presence of three tyrosine residues, namely Y58, Y152, and Y172 (**Figure 8a**). All three tyrosine residues in PUMA were found to be conserved across multiple mammalian species (**Figure 8a**), indicating these residues are potentially functionally important. To determine which specific PUMA tyrosine residue(s) that HER2 phosphorylates, we conducted site-directed mutagenesis to mutate each tyrosine (Tyr; Y) to phenylalanine (Phe; F) using an expression vector carrying HA-tagged PUMA as the template. Phenylalanine has the same R group as tyrosine without the oxygen to bind phosphate and, thus, cannot be phosphorylated. These PUMA mutants (Y58F-, Y152F-, Y172F-PUMA), along with wild-type PUMA (WT-PUMA), were expressed in cells, immunoprecipitated using an HA-tag antibody, and subjected to the HER2 kinase assay. As shown in **Figure 8b**, WT-PUMA was strongly phosphorylated by recombinant HER2 while all of the mutants showed a low level of phosphorylation, indicating that all three tyrosines can be phosphorylated. To fully understand the biological consequences of PUMA tyrosine phosphorylation we created an additional PUMA mutant, a triple mutant PUMA (TM-PUMA), in which all three tyrosines (Y58, Y152, and Y172) were mutated to phenylalanine. Using the cell-free HER2 kinase assay (**Figure 8b**), WT-PUMA showed phospho-tyrosine bands whereas none were detected with TM-PUMA, indicating the TM-PUMA is not phosphorylated by HER2. To rule out the possibility that TM-PUMA cannot be tyrosine-phosphorylated due to its inability to interact with HER2, we next determined whether TM-PUMA can physically interact with HER2. IP/WB with a HER2 antibody (**Figure 8c**) demonstrated that HER2 interacted with both WT-PUMA and TM-PUMA equally indicating the lack of TM-PUMA phosphorylation by HER2 is not due to decreased

interaction between the two proteins. Taken together, the results in Figures 2 and 3 are the first evidence showing that PUMA undergoes tyrosine phosphorylation and that HER2 can directly phosphorylate PUMA.

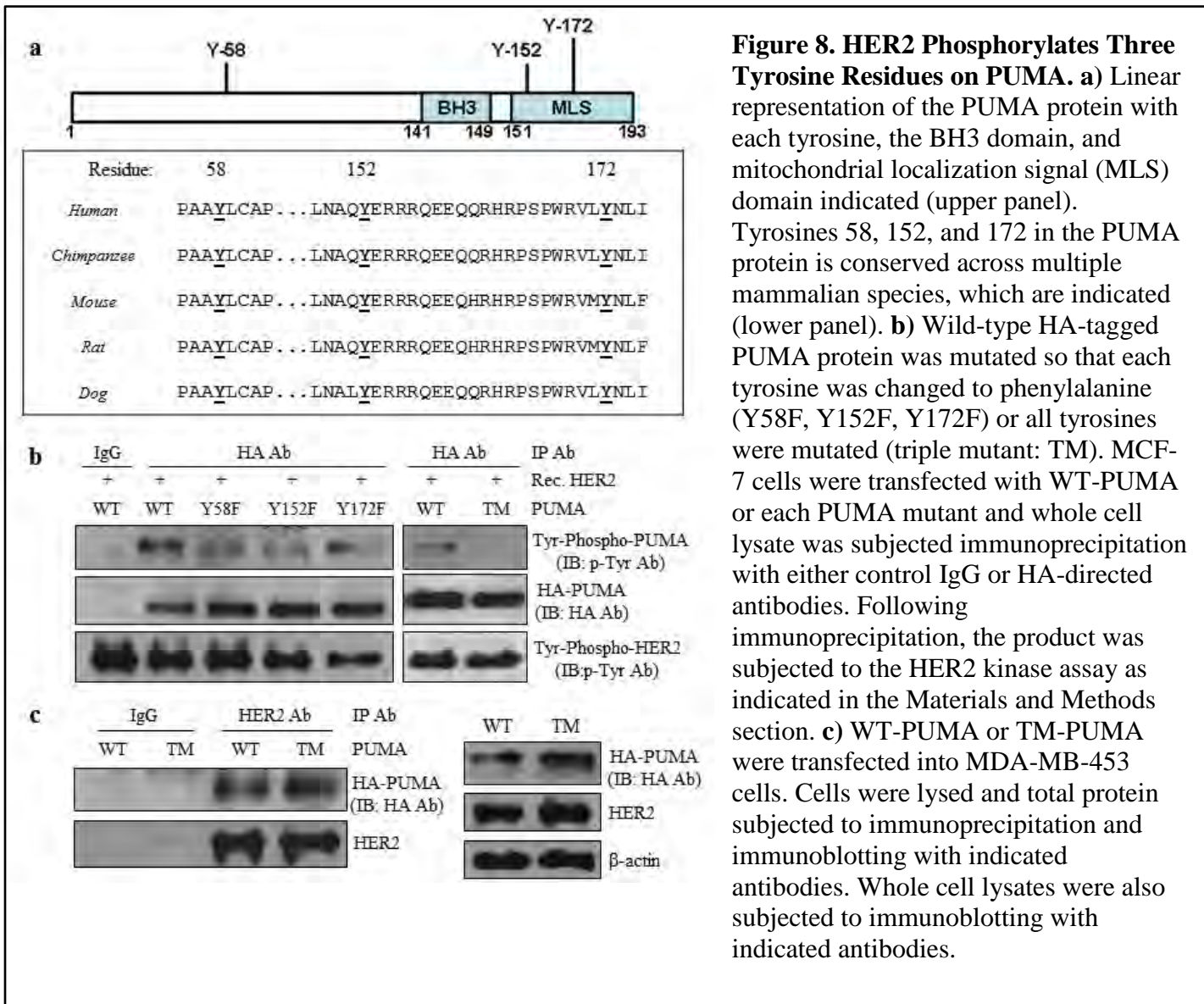


Figure 8. HER2 Phosphorylates Three Tyrosine Residues on PUMA. **a)** Linear representation of the PUMA protein with each tyrosine, the BH3 domain, and mitochondrial localization signal (MLS) domain indicated (upper panel).

Tyrosines 58, 152, and 172 in the PUMA protein is conserved across multiple mammalian species, which are indicated (lower panel). **b)** Wild-type HA-tagged PUMA protein was mutated so that each tyrosine was changed to phenylalanine (Y58F, Y152F, Y172F) or all tyrosines were mutated (triple mutant: TM). MCF-7 cells were transfected with WT-PUMA or each PUMA mutant and whole cell lysate was subjected immunoprecipitation with either control IgG or HA-directed antibodies. Following immunoprecipitation, the product was subjected to the HER2 kinase assay as indicated in the Materials and Methods section. **c)** WT-PUMA or TM-PUMA were transfected into MDA-MB-453 cells. Cells were lysed and total protein subjected to immunoprecipitation and immunoblotting with indicated antibodies. Whole cell lysates were also subjected to immunoblotting with indicated antibodies.

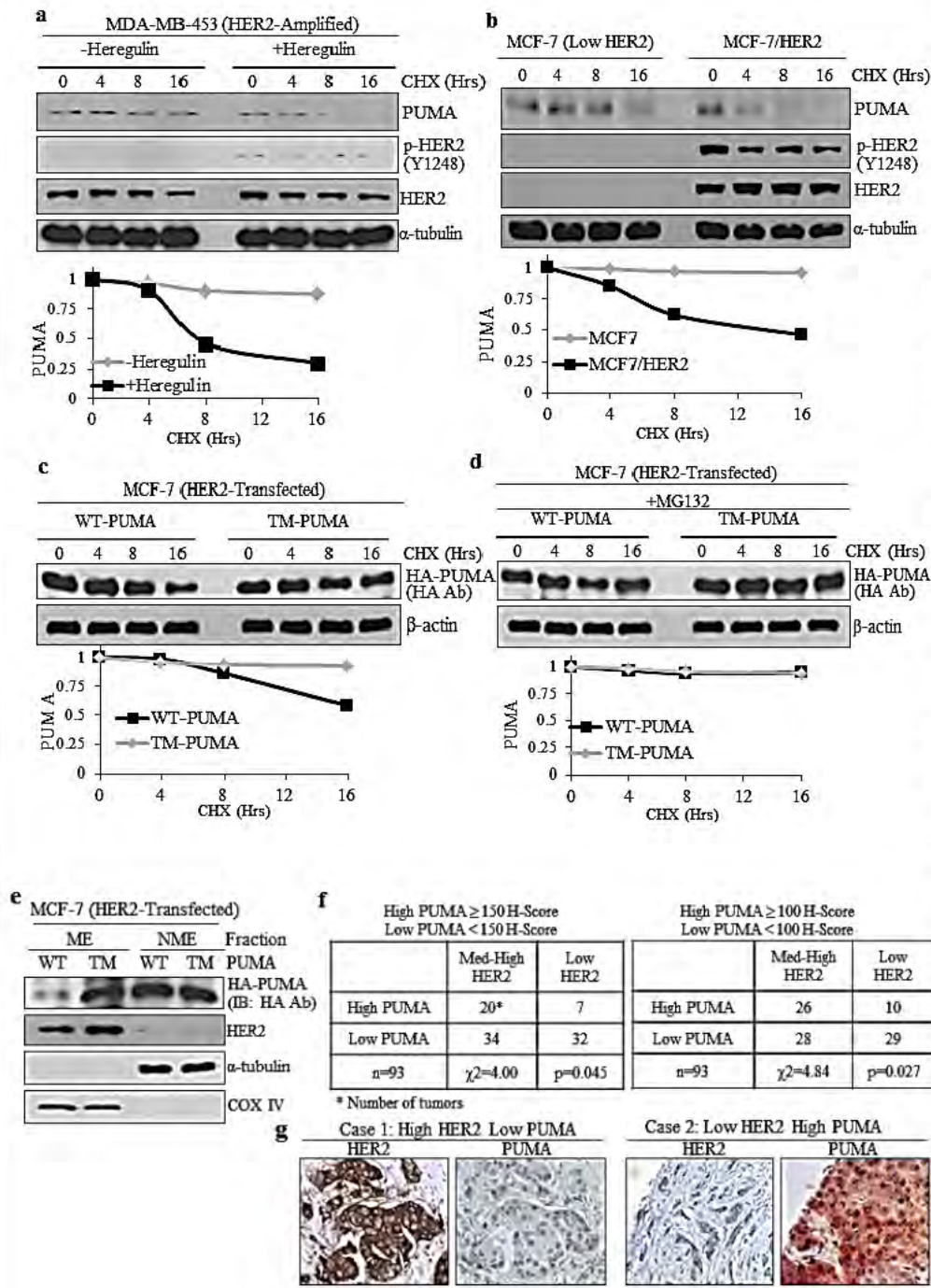
TM-PUMA has a longer half-life than WT-PUMA (Task 2-c).

We next wanted to determine whether PUMA phosphorylation by HER2 altered PUMA stability. To this end, we assessed protein half-life using cycloheximide, which inhibits protein synthesis allowing detection of when proteins are degraded. Cycloheximide is a common method to determine protein stability as several relevant papers have used this method in recent years [1-4]. Thus, HER2-overexpressing MDA-MB-453 cells were treated with cycloheximide for up to 16 hrs in the presence or absence of heregulin to activate HER2. As shown in **Figure 9a**, heregulin induced activation of HER2 in these cells and also led to enhanced PUMA protein degradation. To further examine the stability of PUMA, we assessed PUMA half-life using MCF-7 cells, which have low HER2 expression, or MCF-7/HER2 cells, which have stable overexpression of HER2. **Figure 9b** shows that PUMA is degraded faster in MCF-7/HER2 cells compared to MCF-7 cells indicating HER2 overexpression reduces PUMA stability. We next determined whether the half-life of TM-PUMA, which cannot be tyrosine phosphorylated, differs from that of WT-PUMA. Cells were transfected with either WT-PUMA or TM-PUMA followed by cycloheximide treatment. As shown in **Figure 9c**, WT-PUMA levels significantly decreased at 16 hrs whereas TM-PUMA levels did not substantially decline. Following quantification of PUMA band signals and plotting them over time, we found that the half-life for WT-PUMA was approximately 7 hrs whereas that of TM-PUMA was longer than 16 hrs. It has been previously shown that PUMA can be targeted to the proteasome for degradation [1]. To determine if WT-PUMA or TM-PUMA is regulated by the proteasome, we performed the half-life experiment in the presence of the proteasome inhibitor MG132. As shown in **Figure 9d**, we observed that WT-PUMA half-life could be extended with inhibition of the proteasome confirming previous results [1]. These results suggest HER2-mediated phosphorylation reduces the half-life of PUMA.

We next asked whether TM-PUMA retains the ability to undergo translocation to the mitochondria where PUMA promotes apoptosis. Thus, WT-PUMA or TM-PUMA were transfected into cells followed by isolation of the ME and NME with subsequent immunoblotting. As **Figure 9e** indicates, TM-PUMA retained the ability to undergo mitochondrial localization. Furthermore, we observed greater levels of TM-PUMA compared to WT-PUMA in the ME, which was confirmed by calculation of the mtPUMA Index resulting in 3.3 times more TM-PUMA in the mitochondria than WT-PUMA. A greater TM-PUMA level in the mitochondria is likely the result of enhanced protein stability of TM-PUMA protein in the presence of HER2. Together, these data show that PUMA protein stability is decreased with HER2 activation and blocking PUMA tyrosine phosphorylation enhances PUMA stability and results in greater mitochondrial levels of PUMA.

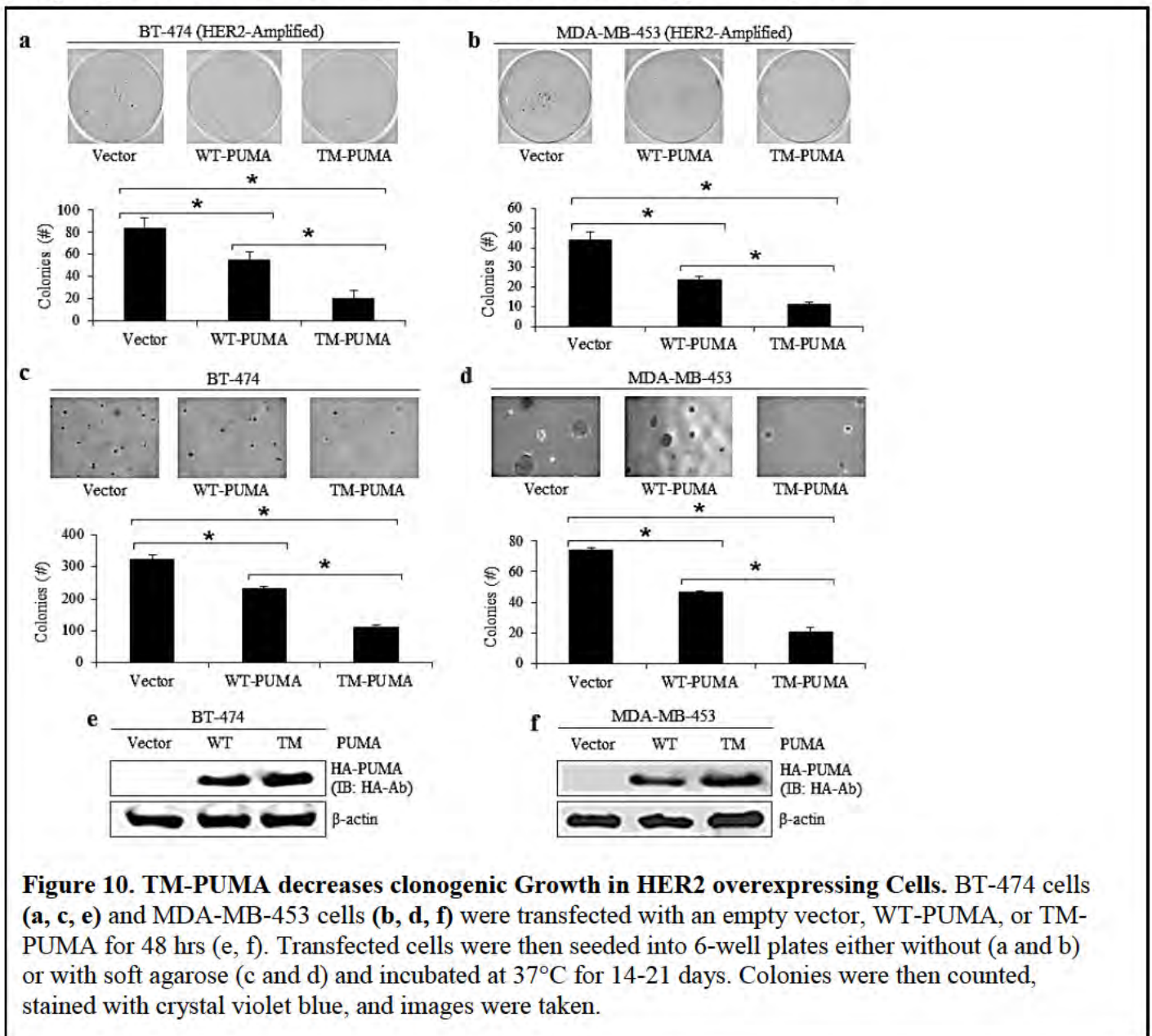
To assess whether this relationship is maintained *in vivo*, we performed immuno-histochemistry on a set of clinical cancer samples (n=93) to detect HER2 and PUMA. After scoring, we divided the samples into low HER2 (0-1+ intensity) or medium to high HER2 (2-3+ intensity). PUMA was divided into high PUMA (either ≥ 150 H-Score or ≥ 100 H-Score) or low PUMA (either < 150 H-Score or < 100 H-Score). We then performed a chi-square analysis to determine the relationship between HER2 and PUMA expression (**Figure 9**). The chi-square analysis using either PUMA barrier (150 H-Score or 100 H-Score) resulted in statistical significance ($p=0.045$ and $p=0.027$, respectively). These data suggest the tissues with high HER2 expression tend to have lower PUMA expression *in vivo* (**Figure 9g**) supporting our data from cell lines that HER2 can downregulate PUMA expression.

Figure 9. HER2 phosphorylation regulates PUMA half-Life and mitochondrial Levels. **a)** MDA-MB-453 cells were incubated in serum-free medium for 16 hrs followed by treatment with heregulin (100 ng/mL) and cycloheximide (10 ug/mL). Whole cell lysate was subjected to immunoblotting with indicated antibodies. **b)** MCF-7 and MCF-7/HER2 cells were incubated in serum-free medium for 16 hrs followed by treatment with heregulin (100 ng/mL) and cycloheximide (10 ug/mL). Whole cell lysate was subjected to immunoblotting with indicated antibodies. **c,d)** MCF-7 cells were transfected with HER2 and either WT-PUMA or TM-PUMA. Cells were incubated in serum-free medium for 16 hrs followed by treatment with heregulin (100 ng/mL) and cycloheximide (10 ug/mL) without **(c)** or with MG132 (10 μ M) co-treatment **(d)**. Whole cell lysate was subjected to immunoblotting with indicated antibodies. **e)** MCF-7 cells were transfected with WT-PUMA or TM-PUMA and mitochondria were isolated. ME and NME were subjected to immunoblotting with indicated antibodies. **f)** Chi-square tables for analysis of clinical cancer samples. Med-High HER2=2-3+. Low HER2=0-1+. **g)** Sample IHC images of clinical cancer samples for High HER2 + Low PUMA (case 1) and Low HER2 + High PUMA (case 2).



TM-PUMA has a stronger effect than WT-PUMA on suppressing clonogenic growth (Task 2-c).

Figure 9 indicated that TM-PUMA had greater protein stability and greater protein levels in the mitochondria, which may indicate that TM-PUMA has an enhanced ability to promote apoptosis. To examine the effect of TM-PUMA on cell viability, we expressed an empty vector, WT-PUMA or TM-PUMA in two different HER2-overexpressing breast cancer cell lines, namely BT-474 (Figure 10a,c,e) and MDA-MB-453 (Figure 10b,d,f) cells, and monitored the ability of these cells to form colonies. As shown by the anchorage-dependent colony assay (Figures 10a and 10b), TM-PUMA significantly decreased colony formation compared to WT-PUMA, indicating that TM-PUMA had a stronger growth suppression than WT-PUMA. As expected, compared to the empty vector, WT-PUMA had a stronger propensity to decrease the colony formation ability of both cell lines. Both of these cells are aggressive and will grow independent of attachment. Therefore, a similar experiment was also performed with the same cell lines but using an anchorage-independent soft agarose colony assay. TM-PUMA significantly reduced soft agarose colony formation compared to WT-PUMA (Figures 10c and 10d). WT-PUMA also reduced colony formation compared to vector in both cell lines. Together, these data demonstrate that TM-PUMA has a greater effect than WT-PUMA on decreasing clonogenic growth of breast cancer cells and suggests tyrosine phosphorylation of PUMA decreases the ability of PUMA to suppress cell growth.



TM-PUMA induces apoptosis to a greater degree than WT-PUMA (Task 2-c).

We observed that TM-PUMA has a greater effect on cell growth than WT-PUMA in the context of HER2 overexpressing cells. However, whether this decrease in cell growth with TM-PUMA was due to enhanced apoptosis cannot be determined from analysis of the colony assays. To determine the effect of TM-PUMA on apoptosis, BT-474 cells were transfected with an empty vector, WT-PUMA, or TM-PUMA followed by treatment with heregulin to ensure HER2 activation. We then assessed the extent of apoptosis in the treated cells by the Annexin V binding assay using flow cytometry. **Figures 11a and 11c** show that TM-PUMA induced the greatest levels of apoptosis compared to WT-PUMA or empty vector. PUMA has been shown previously to sensitize cancer cells to treatment with apoptosis-inducing chemotherapeutic agents [5]. Therefore, we next assessed whether TM-PUMA could further enhance apoptosis in the presence of a low dose of anisomycin, an apoptosis inducer [6]. To this end, cancer cells were transfected with vector, WT-PUMA, or TM-PUMA followed by exposure to heregulin and anisomycin with subsequent assessment of Annexin V binding. As shown in **Figures 11b and 11c**, TM-PUMA expression significantly promoted apoptosis in the presence of anisomycin compared to vector and WT-PUMA. As expected, we observed modest increases in apoptosis in anisomycin-treated cells expressing vector or WT-PUMA compared to untreated cells. To confirm the effects of WT-PUMA and TM-PUMA on apoptosis, cell lysates were analyzed by WB for the presence of PARP-1 cleavage. Consistent with the results of the Annexin V staining, the results revealed that TM-PUMA induced the greatest levels of cleaved PARP-1 (**Figure 11d**). Together, results presented in Figure 6 indicate TM-PUMA as a stronger apoptosis inducer than WT-PUMA and that tyrosine phosphorylation of PUMA reduces the ability of PUMA to promote apoptosis.

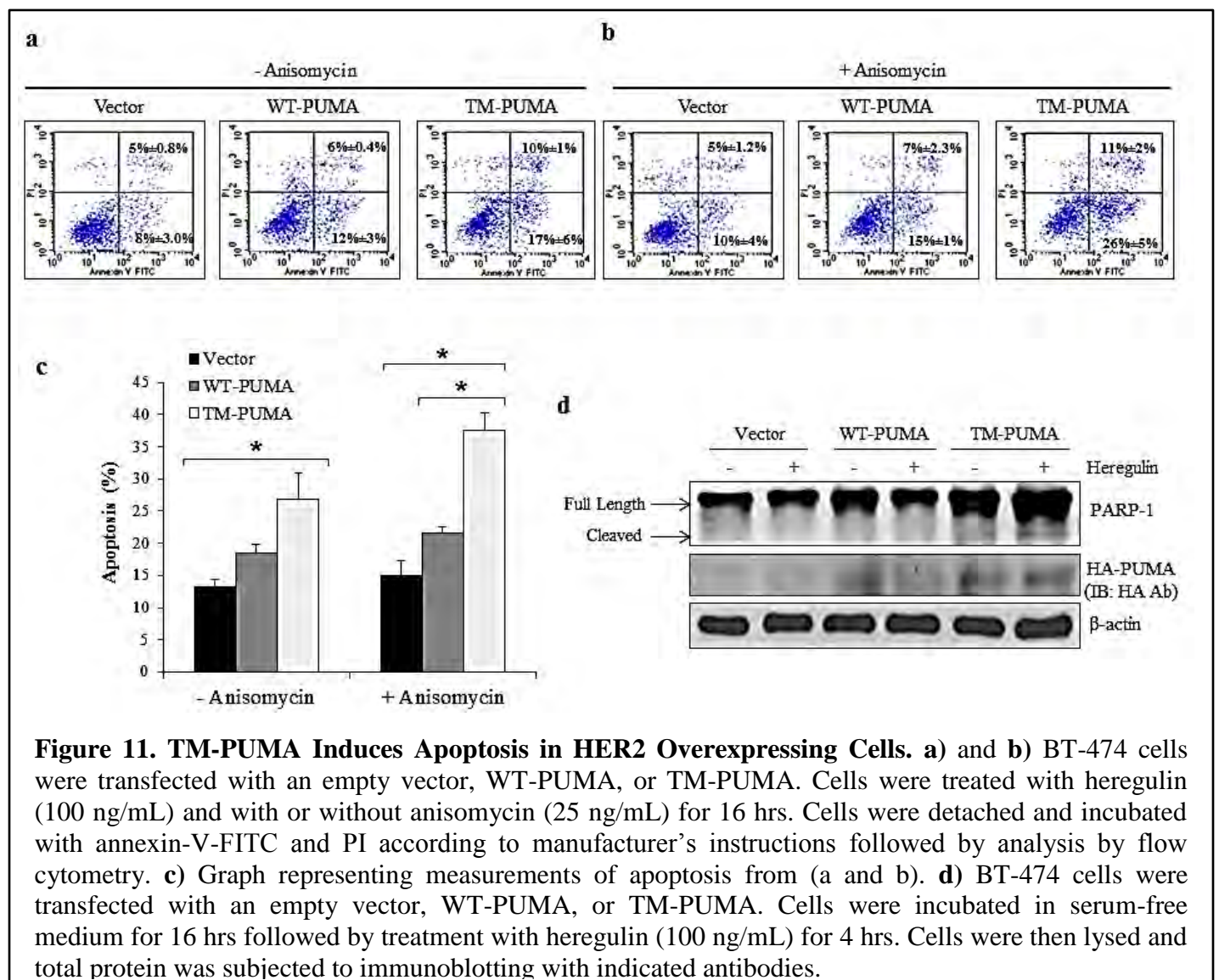
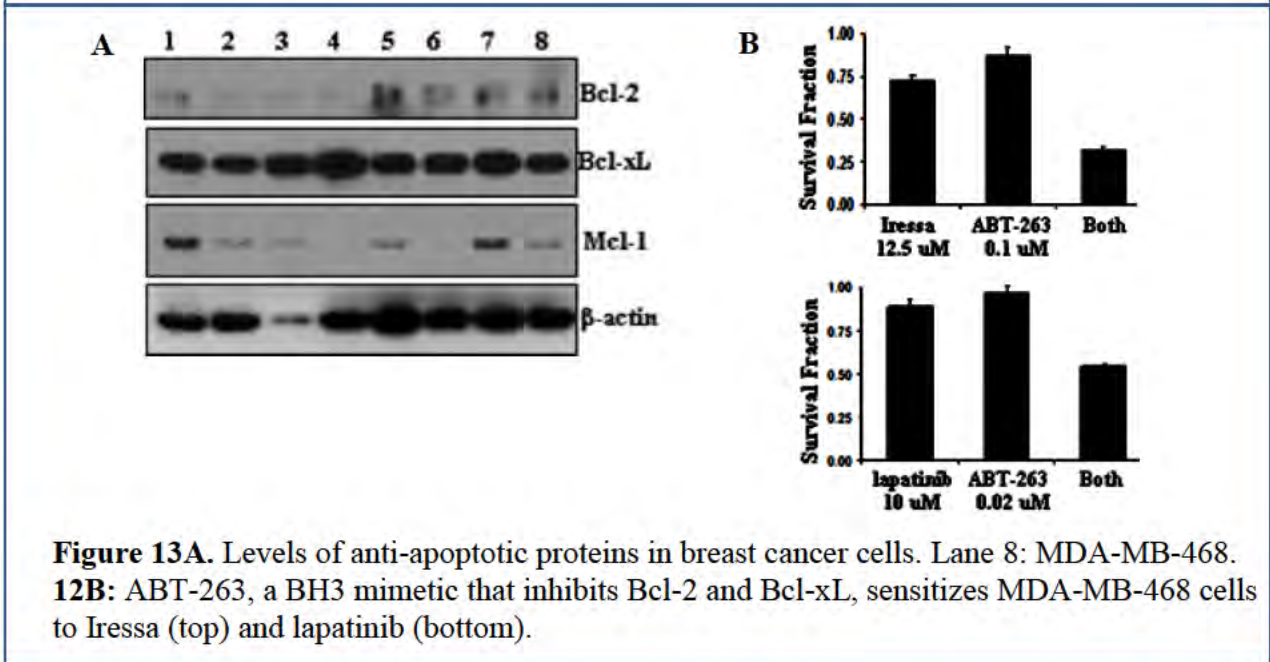
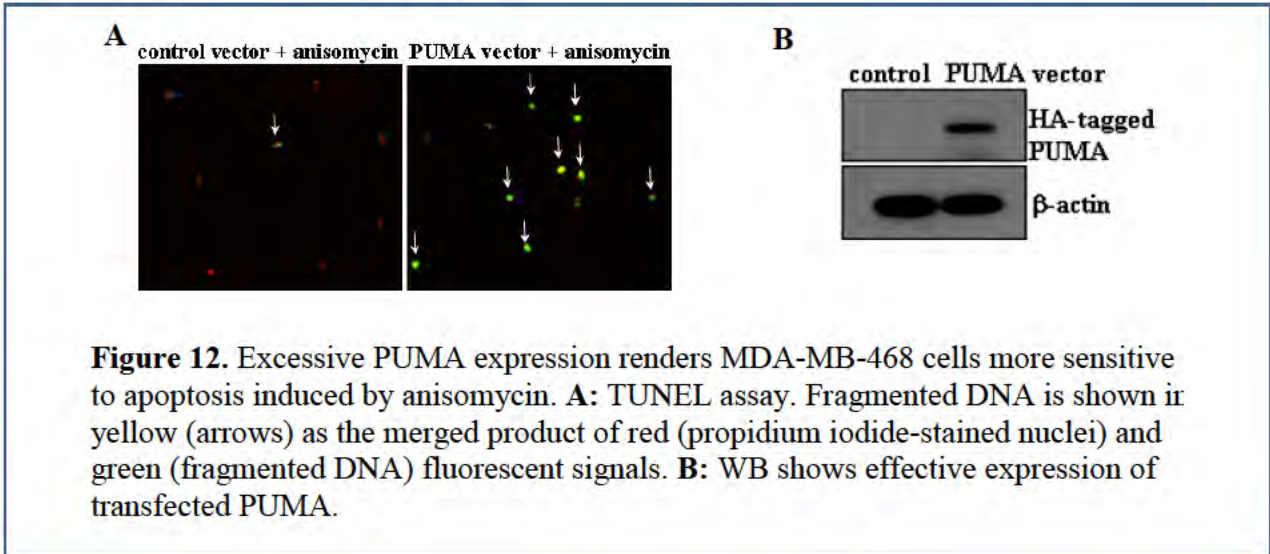


Figure 11. TM-PUMA Induces Apoptosis in HER2 Overexpressing Cells. a) and b) BT-474 cells were transfected with an empty vector, WT-PUMA, or TM-PUMA. Cells were treated with heregulin (100 ng/mL) and with or without anisomycin (25 ng/mL) for 16 hrs. Cells were detached and incubated with annexin-V-FITC and PI according to manufacturer's instructions followed by analysis by flow cytometry. c) Graph representing measurements of apoptosis from (a and b). d) BT-474 cells were transfected with an empty vector, WT-PUMA, or TM-PUMA. Cells were incubated in serum-free medium for 16 hrs followed by treatment with heregulin (100 ng/mL) for 4 hrs. Cells were then lysed and total protein was subjected to immunoblotting with indicated antibodies.

Ectopic PUMA expression and a BH3 mimetic sensitize EGFR-expressing breast cancer cells to EGFR kinase inhibitors (Task 3-a).

Although BH3-only proapoptotic proteins can be functionally redundant, we found that increased PUMA expression rendered MDA-MB-468 cells (with endogenous EGFR and PUMA) more sensitive to apoptosis induction (**Figure 12**). We also found that breast cancer cells expressed anti-apoptotic proteins (**Figure 13A**), making them susceptible to the BH3 mimetics that typically target Bcl-2/Bcl-xL/Mcl-1. As shown in **Figure 13B**, ABT-263 (a BH3 mimetic [7] being tested in the clinic) sensitizes MDA-MB-468 cells to Iressa (top) and lapatinib (bottom).



4. KEY RESEARCH ACCOMPLISHMENTS: *Bulleted list of key research accomplishments emanating from this research. Project milestones, such as simply completing proposed experiments, are not acceptable as key research accomplishments. Key research accomplishments are those that have contributed to the major goals and objectives and that have potential impact on the research field.*

- The project sheds light on the malignant phenotype of aggressive breast cancer that overexpress HER2 and/or EGFR which constitutes approximately half of invasive breast cancer, and also provides rationales for new more effective therapy for women with aggressive subtypes of breast cancer.
- We have gained novel insights into the malignant biology and drug-resistant phenotype of EGFR- and/or HER2-overexpressing breast cancer and to use the acquired knowledge for the development of a sensitization strategy that will improve EGFR- and HER2-targeted therapies.
- EGFR and HER2 antagonize breast cancer response to apoptosis-inducing therapy by phosphorylating and destabilizing the proapoptotic PUMA protein.
- Combining BH3 mimetics with EGFR/HER2 targeted agents can be an effective therapy with better efficacy than monotherapy in breast cancer.
- Akt phosphorylates and activates heat shock factor-1 (HSF-1) independent of heat shock, leading to Slug overexpression and epithelial-mesenchymal transition (EMT) of HER2-overexpressing breast cancer cells.

5. CONCLUSION: *Summarize the importance and/or implications with respect to medical and/or military significance of the completed research including distinctive contributions, innovations, or changes in practice or behavior that has come about as a result of the project. A brief description of future plans to accomplish the goals and objectives shall also be included.*

EGFR and HER2 are major molecular targets for breast cancer therapy. However, EGFR-targeted therapy needs urgent improvements while HER2-targeted treatments do not consistently produce satisfactory clinical outcomes. The goal of this study is, thus, to gain insights into the biology of EGFR- and HER2-expressing invasive breast cancer in order to provide rationales for more effective EGFR- and HER2-based combination therapy for women with breast cancer. As proposed, we functionally characterized the interactions between PUMA and EGFR/HER2 and found the interplays to lead to a negative impact on breast cancer response to apoptosis induction. We also produced evidence suggesting that combining BH3 mimetics with EGFR/HER2 targeted agents can be an effective therapy with better efficacy than monotherapy in treating breast cancer. These novel observations laid the foundation for future research to develop therapeutic strategies that activate PUMA in order to sensitize breast cancer with high levels of EGFR and/or HER2.

We reported that Akt phosphorylates and activates heat shock factor-1 (HSF-1) independent of heat shock, leading to Slug overexpression and epithelial-mesenchymal transition (EMT) of HER2-overexpressing breast cancer cells. EMT is an essential step for tumor progression, although the mechanisms driving EMT are still not fully understood. In an effort to investigate these mechanisms, we observed that heregulin-mediated activation of HER2, or HER2 overexpression, resulted in EMT, which is accompanied with increased expression of a known EMT regulator Slug, but not TWIST or Snail. We then investigated how HER2 induced Slug expression and found, for the first time, that there are four consensus HSF Sequence-binding Elements, the binding sites for HSF-1, located in the Slug promoter. HSF-1 bound to and transactivated the Slug promoter independent of heat shock, leading to Slug

expression in breast cancer cells. Knockdown of HSF-1 expression by siRNA reduced Slug expression and heregulin-induced EMT. The positive association between HSF-1 and Slug was confirmed by immunohistochemical staining of a cohort of 100 invasive breast carcinoma specimens. While investigating how HER2 activated HSF-1 independent of heat shock, we observed that HER2 activation resulted in concurrent phosphorylation of Akt and HSF-1. We then observed, also for the first time, that Akt directly interacted with HSF-1 and phosphorylated HSF-1 at S326. Inhibition of Akt using siRNA, dominant-negative Akt mutant, or small molecule inhibitors prevented heregulin-induced HSF-1 activation and Slug expression. Conversely, constitutively active Akt induced HSF-1 phosphorylation and Slug expression. HSF-1 knockdown reduced the ability of Akt to induce Slug expression, indicating an essential that HSF-1 plays in Akt-induced Slug upregulation. Together, we uncovered the existence of a novel Akt-HSF-1 signaling axis that leads to Slug upregulation and EMT, and potentially contributes to progression of HER2-positive breast cancer. Building on these observations, our future directions are to further explore the translational implications of these observations. For example, we will examine whether dual targeting of Akt and HSF-1 will effectively prevent metastasis of HER2-driven breast cancer.

6. PUBLICATIONS, ABSTRACTS, AND PRESENTATIONS:

a. List all manuscripts submitted for publication during the period covered by this report resulting from this project. Include those in the categories of lay press, peer-reviewed scientific journals, invited articles, and abstracts. Each entry shall include the author(s), article title, journal name, book title, editors(s), publisher, volume number, page number(s), date, DOI, PMID, and/or ISBN.

(1) Lay Press: None

(2) Peer-Reviewed Scientific Journals:

- Cao, X., Zhu, H., Ali-Osman, F. and Lo, H.-W. EGFR and EGFRvIII undergo stress- and EGFR kinase inhibitor-induced mitochondrial translocation: A novel mechanism of EGFR-driven antagonism of apoptosis. PMID:21388543. PMCID:PMC3063231. Molecular Cancer 10:26, 2011. [8]
- Cao, X., Geradts, J., Dewhirst, M. and Lo, H.-W. Upregulation of VEGF-A and CD24 gene expression by the tGLI1 transcription factor contributes to the aggressive behavior of breast cancer cells. PMID: 21666711. PMCID:PMC3175334. Oncogene 31:104-115, 2012. [9]
- Carpenter, R. L., Han, W., Paw, I. and Lo, H.-W. HER2 phosphorylates and destabilizes proapoptotic PUMA, leading to antagonized apoptosis in cancer cells. PMID: 24236056. PMCID: PMC3827261 PLoS ONE 8(11):e78836, 2013. [10]
- Han, W., Carpenter, RL., Cao, X. and Lo, H.-W. STAT1 gene expression is enhanced by nuclear EGFR and HER2 via cooperation with STAT3. PMID:22693070. Molecular Carcinogenesis 52:959-969, 2013. [11]
- Han, W., Carpenter, RL, and Lo, H.-W. TGLI1 upregulates expression of VEGFR2 and VEGF-A, leading to a robust VEGF-VEGFR2 autocrine loop and cancer cell growth. doi:10.1166/ch.2013.1006. Cancer Hallmarks 1: 28-37, 2013. [12]

• Zhu, H., Carpenter, R. L., Han, W., and Lo, H.-W. The GLI1 splice variant TGLI1 is a novel mediator of glioblastoma angiogenesis and growth. PMID: 24045042. PMCID: PMC3874262. Cancer Letters 343(1):51-61. 2014. [13]

• Carpenter, R. L., Paw, I., Dewhirst, M. W., and Lo, H.-W. Akt phosphorylates and activates HSF-1 independent of heat shock, leading to Slug overexpression and epithelial-mesenchymal transition (EMT) of HER2-overexpressing breast cancer cells. PMID: 24469056 Oncogene, Published ahead of print, Jan 28, 2014. [14]

(3) Invited Articles:

• Han, W. and Lo, H.-W. Landscape of EGFR Signaling Network in Human Cancers: Biology and Therapeutic Response in Relation to Receptor Subcellular Locations. Cancer Letters 318:124-134, 2012. (invited review) [15]

• Lo, H.-W. Akt destabilizes p57Kip2: Akt at the converging crossroad? Cell Cycle 12(6):870-871, 2013. I(invited News & Views) [16]

• Carpenter, R. L. and Lo, H.-W. Regulation of Apoptosis by HER2 in Breast Cancer. Journal of Carcinogenesis & Mutagenesis S7:300, 2013. (invited review) [17]

• Carpenter, R. L. and Lo, H.-W. STAT3-regulated Genes Relevant to Human Cancers. PMID: 24743777. In Special Issue: STAT3 Signalling in Cancer: Friend or Foe. Cancers 6:897-925, 2014. [18]

(4) Abstracts: None

b. List presentations made during the last year (international, national, local societies, military meetings, etc.). Use an asterisk () if presentation produced a manuscript.*

* Global Breast Cancer Conference, October 7, 2011; Seoul , Korea

Title: Upregulation of VEGF-A Gene Expression by the tGLI1 Transcription Factor Contributes to Aggressive Breast Cancer

* Breast Cancer Research Forum at Duke University School of Medicine, January 20, 2012

Title: Non-canonical EGFR Signaling Pathways in Breast Cancer

• Virginia Commonwealth University, Department of Neurosurgery, June 18, 2012

Title: Targeting novel signaling pathways and their crosstalks in glioblastoma

* North Carolina State University, Department of Environmental and Molecular Toxicology, Sept. 18, 2012

Title: Landscape of the EGFR signaling network in relation to carcinogenesis, tumor progression and therapeutic resistance

* University of Wisconsin at Madison, Seminar of Cancer Biology, Feb. 21, 2013

Title: Atypical Transcriptional Mechanisms for Tumor Progression

• Invited Seminar, March 19, 2014, Wake Forest University, Winston-Salem, NC

Title: Truncated Glioma-associate Oncogene Homolog 1 (tGLI1) in Tumor Progression

7. INVENTIONS, PATENTS AND LICENSES: *List all inventions made and patents and licenses applied for and/or issued. Each entry shall include the inventor(s), invention title, patent application number, filing date, patent number if issued, patent issued date, national, or international.*

Nothing to report

8. REPORTABLE OUTCOMES: *Provide a list of reportable outcomes that have resulted from this research. Reportable outcomes are defined as a research result that is or relates to a product, scientific advance, or research tool that makes a meaningful contribution toward the understanding, prevention, diagnosis, prognosis, treatment and /or rehabilitation of a disease, injury or condition, or to improve the quality of life. This list may include development of prototypes, computer programs and/or software (such as databases and animal models, etc.) or similar products that may be commercialized.*

The project has advanced our current understanding of breast cancer with high levels of EGFR and/or HER2. The results have been reported in a number of publications.

9. OTHER ACHIEVEMENTS: *This list may include degrees obtained that are supported by this award, development of cell lines, tissue or serum repositories, funding applied for based on work supported by this award, and employment or research opportunities applied for and/or received based on experience/training supported by this award.*

Nothing to report

10. REFERENCES: *List all references pertinent to the report using a standard journal format (i.e., format used in Science, Military Medicine, etc.).*

1. Fricker, M., J. O'Prey, A.M. Tolkovsky, and K.M. Ryan *Phosphorylation of Puma modulates its apoptotic function by regulating protein stability.* Cell Death Dis, 2010. **1**, e59 DOI: 10.1038/cddis.2010.38.
2. Ji, Z., F.C. Mei, J. Xie, and X. Cheng, *Oncogenic KRAS activates hedgehog signaling pathway in pancreatic cancer cells.* J Biol Chem, 282:14048-55, 2007.
3. Lakhter, A.J., R.P. Sahu, Y. Sun, W.K. Kaufmann, E.J. Androphy, J.B. Travers, and S.R. Naidu, *Chloroquine Promotes Apoptosis in Melanoma Cells by Inhibiting BH3 Domain-Mediated PUMA Degradation.* J Invest Dermatol, 133:2247-54, 2013.
4. Sandow, J.J., A.M. Jabbour, M.R. Condina, C.P. Daunt, F.C. Stomski, B.D. Green, C.D. Riffkin, P. Hoffmann, M.A. Guthridge, J. Silke, A.F. Lopez, and P.G. Ekert, *Cytokine receptor signaling activates an IKK-dependent phosphorylation of PUMA to prevent cell death.* Cell Death Differ, 19:633-41, 2012.
5. Yu, J., W. Yue, B. Wu, and L. Zhang, *PUMA sensitizes lung cancer cells to chemotherapeutic agents and irradiation.* Clin Cancer Res, 12:2928-36, 2006.
6. Faris, M., N. Kokot, K. Latinis, S. Kasibhatla, D.R. Green, G.A. Koretzky, and A. Nel, *The c-Jun N-Terminal Kinase Cascade Plays a Role in Stress-Induced Apoptosis in Jurkat Cells by Up-Regulating Fas Ligand Expression.* The Journal of Immunology, 160:134-144, 1998.
7. Tse, C., A.R. Shoemaker, J. Adickes, M.G. Anderson, J. Chen, S. Jin, E.F. Johnson, K.C. Marsh, M.J. Mitten, P. Nimmer, L. Roberts, S.K. Tahir, Y. Xiao, X. Yang, H. Zhang, S.

- Fesik, S.H. Rosenberg, and S.W. Elmore, *ABT-263: a potent and orally bioavailable Bcl-2 family inhibitor*. *Cancer Res*, 68:3421-8, 2008.
8. Cao, X., H. Zhu, F. Ali-Osman, and H.W. Lo, *EGFR and EGFRvIII undergo stress- and EGFR kinase inhibitor-induced mitochondrial translocation: a potential mechanism of EGFR-driven antagonism of apoptosis*. *Mol Cancer*, 10:26, 2011.
 9. Cao, X., J. Geradts, M.W. Dewhirst, and H.W. Lo, *Upregulation of VEGF-A and CD24 gene expression by the tGLII transcription factor contributes to the aggressive behavior of breast cancer cells*. *Oncogene*, 31:104-15, 2012.
 10. Carpenter, R.L., W. Han, I. Paw, and H.-W. Lo, *HER2 Phosphorylates and Destabilizes Pro-Apoptotic PUMA, Leading to Antagonized Apoptosis in Cancer Cells*. *PLoS ONE*, 8:e78836, 2013.
 11. Han, W., R.L. Carpenter, X. Cao, and H.W. Lo, *STAT1 gene expression is enhanced by nuclear EGFR and HER2 via cooperation with STAT3*. *Mol Carcinog*, 52:959-69, 2013.
 12. Han, W., R.L. Carpenter, and H.-W. Lo, *TGLII upregulates expression of VEGFR2 and VEGF-A, leading to a robust VEGF-VEGFR2 autocrine loop and cancer cell growth*. *Cancer Hallmarks*, 1:28-37, 2013.
 13. Zhu, H., R.L. Carpenter, W. Han, M.W. Dewhirst, and H.W. Lo, *The GLII Splice Variant TGLII Promotes Glioblastoma Angiogenesis and Growth*. *Cancer Lett*, 343:51-61, 2014.
 14. Carpenter, R.L., I. Paw, M.W. Dewhirst, and H.W. Lo, *Akt phosphorylates and activates HSF-1 independent of heat shock, leading to Slug overexpression and epithelial-mesenchymal transition (EMT) of HER2-overexpressing breast cancer cells*. *Oncogene*, 2014.
 15. Han, W. and H.-W. Lo, *Landscape of EGFR signaling network in human cancers: Biology and therapeutic response in relation to receptor subcellular locations*. *Cancer Letters*, 318:124-134, 2012.
 16. Lo, H.W., *Akt destabilizes p57 (Kip2) : Akt at the converging crossroad?* *Cell Cycle*, 12:870-1, 2013.
 17. Carpenter, R.L. and H.-W. Lo, *Regulation of Apoptosis by HER2 in Breast Cancer. Invited review*. *Journal of Carcinogenesis & Mutagenesis* S7:300, 2013.
 18. Carpenter, R.L. and H.W. Lo, *STAT3 Target Genes Relevant to Human Cancers*. *Cancers (Basel)*, 6:897-925, 2014.

11. APPENDICES: Attach all appendices that contain information that supplements, clarifies or supports the text. Examples include original copies of journal articles, reprints of manuscripts and abstracts, a curriculum vitae, patent applications, study questionnaires, and surveys, etc.

Two manuscript reprints are included.

- Carpenter, R. L., Han, W., Paw, I. and Lo, H.-W. HER2 phosphorylates and destabilizes proapoptotic PUMA, leading to antagonized apoptosis in cancer cells. PMID: 24236056. PMCID: PMC3827261 *PLoS ONE* 8(11):e78836, 2013. [10]
- Carpenter, R. L., Paw, I, Dewhirst, M. W., and Lo, H.-W. Akt phosphorylates and activates HSF-1 independent of heat shock, leading to Slug overexpression and epithelial-mesenchymal transition (EMT) of HER2-overexpressing breast cancer cells. PMID: 24469056 *Oncogene*, Published ahead of print, Jan 28, 2014. [14]

HER2 Phosphorylates and Destabilizes Pro-Apoptotic PUMA, Leading to Antagonized Apoptosis in Cancer Cells

Richard L. Carpenter¹, Woody Han¹, Ivy Paw¹, Hui-Wen Lo^{1,2,3*}

1 Division of Surgical Sciences, Department of Surgery, Duke University School of Medicine, Durham, North Carolina, United States of America, **2** Duke Cancer Institute, Duke University School of Medicine, Durham, North Carolina, United States of America, **3** Duke Center for RNA Biology, Duke University School of Medicine, Durham, North Carolina, United States of America

Abstract

HER2 is overexpressed in 15–20% of breast cancers. HER2 overexpression is known to reduce apoptosis but the underlying mechanisms for this association remain unclear. To elucidate the mechanisms for HER2-mediated survival, we investigated the relationship between HER2 and p53 upregulated modulator of apoptosis (PUMA), a potent apoptosis inducer. Our results showed that HER2 interacts with PUMA, which was independent of HER2 activation. In addition, we observed that HER2 interacted with PUMA in both mitochondrial and non-mitochondrial compartments. We next examined whether HER2 phosphorylates PUMA. Notably, PUMA tyrosine phosphorylation has never been reported. Using an intracellular assay, we found PUMA to be phosphorylated in breast cancer cells with activated HER2. Via cell-free HER2 kinase assay, we observed that PUMA was directly phosphorylated by HER2. Activation of HER2 decreased PUMA protein half-life. To identify which of the three tyrosines within PUMA are targeted by HER2, we generated three PUMA non-phosphorylation mutants each with a single Tyr→Phe substitution. Results indicated that each PUMA single mutant had lost some, but not all phosphorylation by HER2 indicating that HER2 targets all three tyrosines. Consequently, we created an additional PUMA mutant with all three tyrosines mutated (TM-PUMA) that could not be phosphorylated by HER2. Importantly, TM-PUMA was found to have a longer half-life than PUMA. An inverse association was observed between HER2 and PUMA in 93 invasive breast carcinoma samples. We further found that TM-PUMA suppressed growth of breast cancer cells to a greater degree than PUMA. Also, TM-PUMA had a stronger propensity to induce apoptosis than PUMA. Together, our results demonstrate, for the first time, that PUMA can be tyrosine phosphorylated and that HER2-mediated phosphorylation destabilizes PUMA protein. The HER2-PUMA interplay represents a novel mechanism by which PUMA is regulated and a new molecular basis for HER2-mediated growth and survival of cancer cells.

Citation: Carpenter RL, Han W, Paw I, Lo H W (2013) HER2 Phosphorylates and Destabilizes Pro Apoptotic PUMA, Leading to Antagonized Apoptosis in Cancer Cells. PLoS ONE 8(11): e78836. doi:10.1371/journal.pone.0078836

Editor: Jingwu Xie, Indiana University School of Medicine, United States of America

Received: August 15, 2013; **Accepted:** September 24, 2013; **Published:** November 13, 2013

Copyright: © 2013 Carpenter et al. This is an open access article distributed under the terms of the Creative Commons Attribution License, which permits unrestricted use, distribution, and reproduction in any medium, provided the original author and source are credited.

Funding: This study was supported by the National Institutes of Health grant K01 CA118423, and W81XWH 11 1 0600 from the United States Department of Defense, the Pediatric Brain Tumor Foundation, the Beez Foundation and the Intramural Division of Surgical Sciences Dani P. Bolognesi, Ph.D. Award and Clarence Gardner, Ph.D. Award (to H WL). The funders had no role in study design, data collection and analysis, decision to publish, or preparation of the manuscript.

Competing Interests: The authors have declared that no competing interests exist.

* E mail: huiwen.lo@duke.edu

Introduction

Breast cancer rates are declining but it remains a significant public health threat. Current estimates indicate there will be 300,000 new cases and 40,000 deaths from breast cancer in 2013 [1]. It is estimated that there will be more new breast cancer cases in women than any other type of cancer in 2013 [1]. HER2 is overexpressed in 15–20% of human breast cancers and this overexpression is associated with poor patient outcomes including decreased overall survival, increased tumor relapse, and more aggressive disease [2–4]. HER2 activation occurs by heterodimerization with other ERBB family receptors, such as heregulin binding to HER3 that will then heterodimerize with HER2 to activate downstream HER2 pathways [5].

Overexpression of HER2 is known to reduce apoptosis. Pro-apoptotic and anti-apoptotic Bcl 2 proteins control the intrinsic apoptotic pathway at the mitochondria. Positive correlations have been found between HER2 expression and anti-apoptotic proteins such as Bcl xL, Mcl 1, and Bcl 2 [6–8]. In addition, forced expression of HER2 caused increased protein levels of anti-

apoptotic proteins such as Bcl 2 and Bcl xL while inhibition of HER2 reduced Mcl 1 and increased Bax expression [6,7,9]. HER2 can also activate PI3K AKT and ERK1/2 signaling, which can regulate apoptosis by controlling gene expression, such as upregulation of survivin, and post-translational regulation, such as phosphorylation and inactivation of pro-apoptotic Bad [10,11]. HER2 regulation of apoptosis has primarily been observed to be mediated by downstream signaling while direct regulation of Bcl 2 proteins by HER2 has not been assessed.

The PUMA gene was first identified in 2001 [12,13] as a screen for transcriptional targets of p53. The *BBC3* gene was identified soon after by yeast two-hybrid screening and cDNA for this gene matched that of PUMA [14]. This later discovery of the *BBC3* gene also established that PUMA expression could be induced by apoptotic stimuli independent of p53 [14]. PUMA contains two functional domains on the C-terminus, the BH3 domain and the mitochondrial localization signal (MLS) [15,16]. Functional activity of PUMA is initiated by protein targeting to the outer mitochondrial membrane where PUMA interacts with anti-apoptotic Bcl 2 family members inhibiting their suppression of

Bax and Bak [12,17]. Inhibition of anti apoptotic Bcl 2 family members leads to activation of pro apoptotic proteins Bax/Bak triggering mitochondrial outer membrane permeabilization (MOMP) and release of cytochrome C [12,16,17]. Cytoplasmic cytochrome C ultimately forms the apoptosome leading to activation of effector caspases 3/9 and apoptosis. Loss of PUMA activity has been associated with multiple cancer types. Deletion of a portion of chromosome 19, where the *PUMA* gene is located, has been reported in multiple cancer types [13,18,19]. In addition, *PUMA* is a p53 inducible gene and p53 has mutations in more than 40% of cancers [20]. Consequently, impaired PUMA induction has been observed with p53 mutation or deletion [13,21]. Also, cancer cells with PUMA deleted have high resistance to p53 inducible therapies such as DNA damaging agents, UV, and gamma irradiation among others [19]. However, a number of studies have reported that PUMA expression can be induced by p53 independent mechanisms [19,22–25].

A direct link between HER2 and PUMA has not been investigated. Also unknown is whether PUMA undergoes tyrosine phosphorylation. In this study, we discovered a novel finding that PUMA can be phosphorylated on tyrosine residues directly by HER2. Furthermore, PUMA phosphorylation by HER2 leads to PUMA destabilization and cell survival. We also show that a PUMA mutant that cannot be phosphorylated on tyrosine residues (TM PUMA) has an enhanced ability to induce apoptosis. Taken together, our study uncovered a novel HER2→PUMA signaling axis that represents a novel mechanism by which PUMA protein and PUMA mediated cell death are regulated. Our findings also provide evidence implicating PUMA down regulation as a new molecular basis for HER2 mediated growth and survival.

Materials and Methods

Cells and Cell Culture

MDA MB 453, MCF 7, BT 474, and SK BR3 human breast cancer cell lines were obtained from American Type Culture Collection, ATCC (Manassas, VA). MDA MB 453 cells were maintained in Leibovitz L 15 medium supplemented with 10% fetal bovine serum (FBS) at 0% carbon dioxide. MCF 7 cells were maintained in MEM medium supplemented with 10% FBS, 1 mM sodium pyruvate, 0.1 mM non essential amino acids, and 10 µg/mL bovine insulin. BT 474 cells were maintained in DMEM medium supplemented with 10% FBS. SK BR3 cells were maintained in McCoy's 5a medium supplemented with 10% FBS. MCF 7/HER2 cells were maintained in MEM medium supplemented with 10% FBS, 1 mM sodium pyruvate, 0.1 mM non essential amino acids, 10 µg/mL bovine insulin, and 350 µg/mL G418.

Chemicals and Reagents

All chemicals were purchased from Sigma (St. Louis, MO) unless otherwise stated. Cycloheximide was purchased from Amresco (Solon, OH), MG132 was purchased from CalBiochem (San Diego, CA), anisomycin was purchased from Enzo Life Sciences (Farmingdale, NY), and Lapatinib was purchased from LC Laboratories (Woburn, MA). Tubulin, β actin, and IgG antibodies were purchased from Sigma. HA antibody was purchased from Roche (Indianapolis, IN), PARP 1 antibody was purchased from Santa Cruz Biotechnology (Santa Cruz, CA), COX IV antibody was purchased from Abcam (Cambridge, MA), and 4G10 antibody was purchased from Millipore (Billerica, MA). PUMA, HER2, and phospho HER2 (Y1248) antibodies were purchased from Cell Signaling Technologies (Danvers, MA).

Plasmids

The pHA PUMA plasmid was kindly provided by Dr. Bert Vogelstein via Addgene plasmid 16588 [13]. Generation of single mutant PUMAs (Y58F PUMA, Y152F PUMA, and Y172F PUMA) as well as the triple mutant (Y58F/Y152F/Y172F PUMA) was done using a QuikChange Site Directed Mutagenesis kit (Agilent Technologies, Santa Clara, CA) per manufacturer's instructions. Primers used for mutagenesis were the following:
 Y58F Forward 5'
 TGCCCCGCTGCCTTTTCTCTGCGCCCCCA 3', Y58F Reverse 5' TGGGGGCGCAGA GAAAGGCAGCGGGCA 3',
 Y152F Forward 5' CTCAACGCACAGTTTGAGCGGCG GAGA 3', Y152F Reverse 5'
 TCTCCGCCGCTCAAACCTGTGCGTTGAG 3', Y172F Forward 5' TCACCTGGAGGGTCCCTGTTCAATCTCATCAT 3', and Y172F Reverse 5' ATGATGAGATTGAACAG GACCCTCCAGGGTGA 3'. Mutation was confirmed by sequencing.

Immunoprecipitation/Western Blotting (IP/WB)

Cells were lysed with RIPA buffer (50 mM Tris, 150 mM NaCl, 1 mM EDTA, 1% NP 40, 0.1% SDS, 1% sodium deoxycholate) supplemented with protease/phosphatase inhibitors followed by sonication and collection of supernatant. Whole cell extracts were pre cleared with 1 µg rabbit IgG and 20 µL protein A agarose for 1 hr at 4°C. Cleared lysates were then incubated with 1 µg HER2 or PUMA antibody or control rabbit IgG at 4°C overnight with agitation. Protein A agarose was then added and incubated at 4°C for 60 minutes with agitation. Protein A agarose pellets were collected and washed multiple times with RIPA buffer at 4°C. Washed pellets were boiled and subjected to SDS PAGE and immunoblotting as described previously [26]. Determination of PUMA tyrosine phosphorylation was determined by immunoprecipitation of PUMA followed by immunoblotting using anti phospho tyrosine 4G10 Platinum antibody (Millipore).

Cell-free HER2 Kinase Assays

Recombinant human PUMA protein (Origene, Rockville, MD) was dephosphorylated with recombinant human PTP1B protein at 30°C followed by PTP1B inactivation at 65°C. Dephosphorylated PUMA was then incubated with recombinant human HER2 protein (Promega, Madison, WI) and ATP at 30°C. Sample was then boiled and subjected to SDS PAGE and immunoblotting using anti phospho tyrosine 4G10 Platinum antibody (Millipore).

Immunoprecipitation-kinase Assay

Cells were transfected with HA tagged PUMA plasmids and cell lysates were collected as described above. Immunoprecipitated was done with HA antibody as described above. Following washes, protein A agarose pellets were dephosphorylated with recombinant human PTP1B followed by incubation with recombinant human HER2 as described above. Samples were then boiled and subjected to SDS PAGE and immunoblotting using anti phospho tyrosine 4G10 Platinum antibody (Millipore).

Colony Formation Assays

Following transfection of indicated plasmids cells were seeded into 6 well culture plates to determine anchorage dependent clonogenic growth as we described previously [27]. Following transfection, cells were also seeded into 6 well plates with agarose to determine anchorage independent clonogenic growth. Wells pre coated with a bottom layer of 0.5% agarose and cells were seeded into top layer with 0.35% agarose. After 2–4 weeks,

colonies with or without agarose were stained with crystal violet blue solution (Sigma) for 1 hr and colonies were counted under a microscope. Experiments were performed in triplicate.

Assessment of Apoptosis

Cells were transfected with indicated plasmids, treated with indicated compounds, and harvested with trypsin/EDTA. Apoptosis was then determined using FITC Annexin V/propidium iodide detection kit from BD Pharmingen (San Jose, CA) per manufacturer's instructions. Cells were then analyzed by flow cytometry using a BD FACSCalibur flow cytometer. PARP 1 cleavage was determined using immunoblotting of cell lysates following indicated transfection and treatment.

Determination of PUMA Mitochondrial Levels

Mitochondrial fractionation was performed using an assay kit from Pierce/Thermo Scientific (Rockford, IL), according to manufacturer's instructions as we have described previously [26]. Briefly, protein was isolated from the mitochondrial extract (ME) and the non mitochondrial extract (NME). The ME and NME were then subjected to SDS PAGE and immunoblotting. Band intensities were then measured using NIH ImageJ software. The extent of PUMA mitochondrial localization (mtPUMA Index) was computed using band densities with the following equation:

$$mtPUMAIndex \equiv \frac{\frac{\text{mitochondrialPUMA}}{\%ME}}{\left(\frac{\text{mitochondrialPUMA}}{\%ME}\right) + \left(\frac{\text{non-mitochondrialPUMA}}{\%NME}\right)}$$

%ME is the percent of the total ME loaded and %NME is the percent of the total NME loaded for immunoblotting.

Immunohistochemistry of Clinical Tumor Samples

Slides were purchased from US Biomax (Rockville, MD). Assessment of HER2 intensity (0-3+) was completed by US Biomax. PUMA detection was conducted as we described previously [28]. Slides were incubated with PUMA antibody (Cell Signaling Technology, Danvers, MA). Histologic scores (H Scores) were computed from both percent positivity (A%, A = 1-100) and intensity (B = 0-3+) using the following equation: H Score = A × B. Chi square analysis was used to determine relationship between HER2 intensity and PUMA H Score.

Statistical Analyses

Data are presented as Mean ± SE. Differences were determined via One Way ANOVA with Tukey's post hoc test or student's t test where appropriate. Chi Square analysis was performed for the IHC results. Significance was set at p < 0.05.

Results

HER2 Physically Associates with PUMA

To investigate whether HER2 has any interplay with PUMA, we first assessed whether HER2 can physically interact with PUMA using immunoprecipitation/western blotting (IP/WB). We used SK BR3 and BT 474 breast cancer cells as they overexpress HER2 due to HER2 gene amplification. We immunoprecipitated HER2 from these cells and found that PUMA could be detected with HER2 pull down in both cell lines (Figure 1a). This indicated a novel finding that HER2 physically interacts with PUMA. It is worth noting that we did not detect an interaction between HER2 and Bad or Bmf, other BH3 only proteins, suggesting the

interaction with HER2 is specific to PUMA (Figure 1a). We next assessed whether HER2 kinase activity was required for the interaction with PUMA. For this, cells were treated with or without heregulin as a means of activating HER2 kinase activity. Of note, HER2 does not have obvious ligands and relies on binding to heregulin bound HER3 for activation; HER3 does not have kinase activity [5]. As shown in Figure 1b, HER2 was activated by heregulin but this did not significantly change the interaction of HER2 with PUMA. Cells were then treated with or without lapatinib, which inhibits HER2 activation [29]. Lapatinib decreased HER2 activation but also did not significantly affect the interaction of HER2 and PUMA (Figure 1c). Collectively, these data indicate that HER2 can physically interact with PUMA and this interaction is not dependent on kinase activity of HER2.

PUMA primarily localizes to the mitochondria as it contains a mitochondrial localization signal [12,16] but PUMA has also been observed to promote apoptosis without mitochondrial localization [15]. In addition, HER2 is primarily localized to the plasma membrane but has recently been found to localize to the mitochondria where it influences cellular metabolism and promotes resistance of trastuzumab [30]. Therefore, we next determined where PUMA and HER2 physically interact. Mitochondrial (ME) and non mitochondrial extracts (NME) were isolated from BT 474 cells and immunoblotting for α tubulin and COX IV confirmed there was effective isolation of mitochondrial and non mitochondrial fractions (Figure 1d). Figure 1d shows that PUMA and HER2 were detected in both the ME and the NME confirming previous observations [30]. Despite loading of equal amounts of protein (60 μ g), there appeared to be greater PUMA and HER2 levels in the ME than the NME. However, this apparent imbalance is due to the fact that 60 μ g is 80% of the ME harvested but only 2% of the NME harvested. To determine interaction between HER2 and PUMA, HER2 was immunoprecipitated from equal amounts of the ME and NME followed by immunoblotting. We observed interaction between HER2 and PUMA in both the ME and the NME (Figure 1d). These are the first data indicating HER2 physically interacts with PUMA and that this interaction occurs in and out of the mitochondrial compartment.

HER2 Directly Phosphorylates PUMA

Following detection of a direct interaction between HER2 and PUMA, we next determined whether PUMA could be phosphorylated by HER2. To the best of our knowledge, PUMA tyrosine phosphorylation has not been previously reported. To first assess whether PUMA can be tyrosine phosphorylated intracellularly, we starved HER2 overexpressing cells for 16 hrs and then treated the cells with or without heregulin to activate HER2. We subjected the cell lysates to IP/WB using a PUMA antibody for IP and immunoblotted with anti phospho tyrosine antibodies. As shown in Figure 2a, tyrosine phosphorylated PUMA was readily detected in heregulin stimulated cells which expressed activated phosphorylated HER2 (p HER2). However, MCF 7 cells, which express low levels of HER2, did not respond to heregulin and did not show significant PUMA tyrosine phosphorylation (Figure 2b). In contrast, MCF 7 cells with stable, forced HER2 overexpression (MCF 7/HER2 cells) shows PUMA tyrosine phosphorylation in response to heregulin (Figure 2c). These results are the first to show that PUMA can be phosphorylated on tyrosine residues and this occurred with HER2 stimulation by heregulin.

We next wanted to determine whether HER2 could directly phosphorylate PUMA. To this end, we used commercially available purified recombinant PUMA and HER2 proteins to perform a cell free kinase assay. As shown in Figure 2d, PUMA

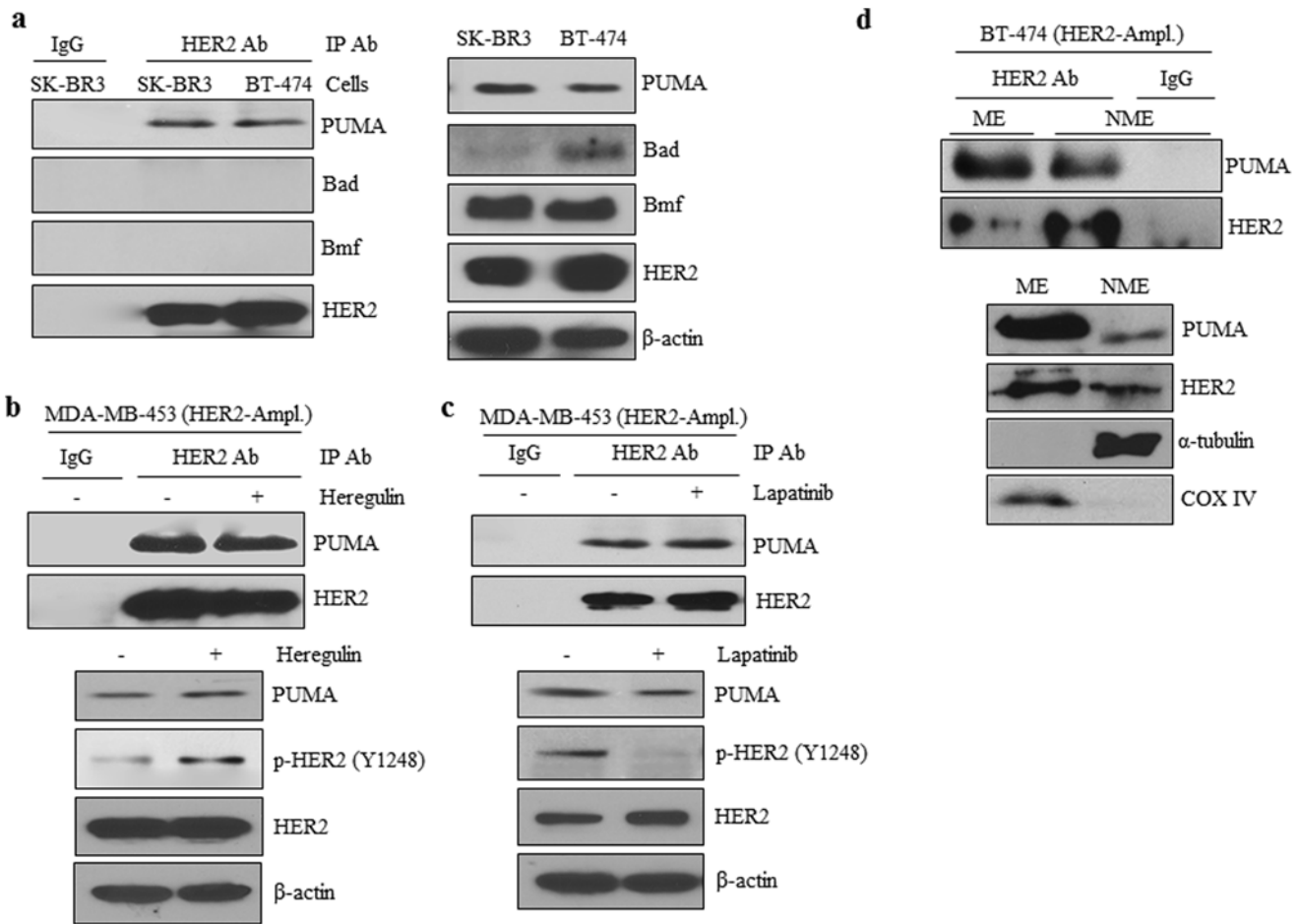


Figure 1. HER2 Directly Interacts with PUMA. a) SKBR3 and BT 474 cells were lysed and total protein subjected to immunoprecipitation with either control IgG or HER2 antibodies followed by immunoblotting with indicated antibodies. Whole cell lysates were also subjected to immunoblotting with indicated antibodies. b) MDA MB 453 cells were incubated in serum free medium for 16 hrs followed by treatment with heregulin (100 ng/mL) for 30 minutes. Cells were then lysed and total protein was subjected to immunoprecipitation with either control IgG or HER2 antibodies followed by immunoblotting with indicated antibodies. Whole cell lysates were also subjected to immunoblotting with indicated antibodies. c) MDA MB 453 cells were incubated with lapatinib (10 μ M) for two hrs. Cells were then lysed and total protein was subjected to immunoprecipitation with either control IgG or HER2 antibodies followed by immunoblotting with indicated antibodies. Whole cell lysates were also subjected to immunoblotting with indicated antibodies. d) The mitochondrial (ME) and non mitochondrial extract (NME) were isolated from BT 474 cells and both extracts were subjected to immunoprecipitation with indicated antibodies. ME and NME were also subjected to immunoblotting with indicated antibodies.

doi:10.1371/journal.pone.0078836.g001

was strongly phosphorylated at tyrosine residues in the presence of HER2. As expected, HER2 underwent auto phosphorylation. In the presence of lapatinib, HER2 phosphorylation was lost, and consequently, there was no tyrosine phosphorylation of PUMA. We also observed a dose response increase in tyrosine phosphorylation of PUMA with increasing levels of PUMA protein in the presence of HER2 (Figure 2e). Using IP WB, we further show that pulldown of recombinant HER2 also results in pulldown of purified PUMA (Figure 2f) confirming HER2 directly associates with PUMA in the context of the cell free kinase assay. These results show for the first time that PUMA can be phosphorylated at tyrosine residues directly by HER2.

HER2 Phosphorylates PUMA at Three Tyrosine Residues

A search of the human PUMA protein sequence revealed the presence of three tyrosine residues, namely Y58, Y152, and Y172 (Figure 3a). All three tyrosine residues in PUMA were found to be conserved across multiple mammalian species (Figure 3a), indi-

cating these residues are potentially functionally important. To determine which specific PUMA tyrosine residue(s) that HER2 phosphorylates, we conducted site directed mutagenesis to mutate each tyrosine (Tyr; Y) to phenylalanine (Phe; F) using an expression vector carrying HA tagged PUMA as the template. Phenylalanine has the same R group as tyrosine without the oxygen to bind phosphate and, thus, cannot be phosphorylated. These PUMA mutants (Y58F, Y152F, Y172F PUMA), along with wild type PUMA (WT PUMA), were expressed in cells, immunoprecipitated using an HA tag antibody, and subjected to the HER2 kinase assay. As shown in Figure 3B, WT PUMA was strongly phosphorylated by recombinant HER2 while all of the mutants showed a low level of phosphorylation, indicating that all three tyrosines can be phosphorylated. To fully understand the biological consequences of PUMA tyrosine phosphorylation we created an additional PUMA mutant, a triple mutant PUMA (TM PUMA), in which all three tyrosines (Y58, Y152, and Y172) were mutated to phenylalanine. Using the cell free HER2 kinase

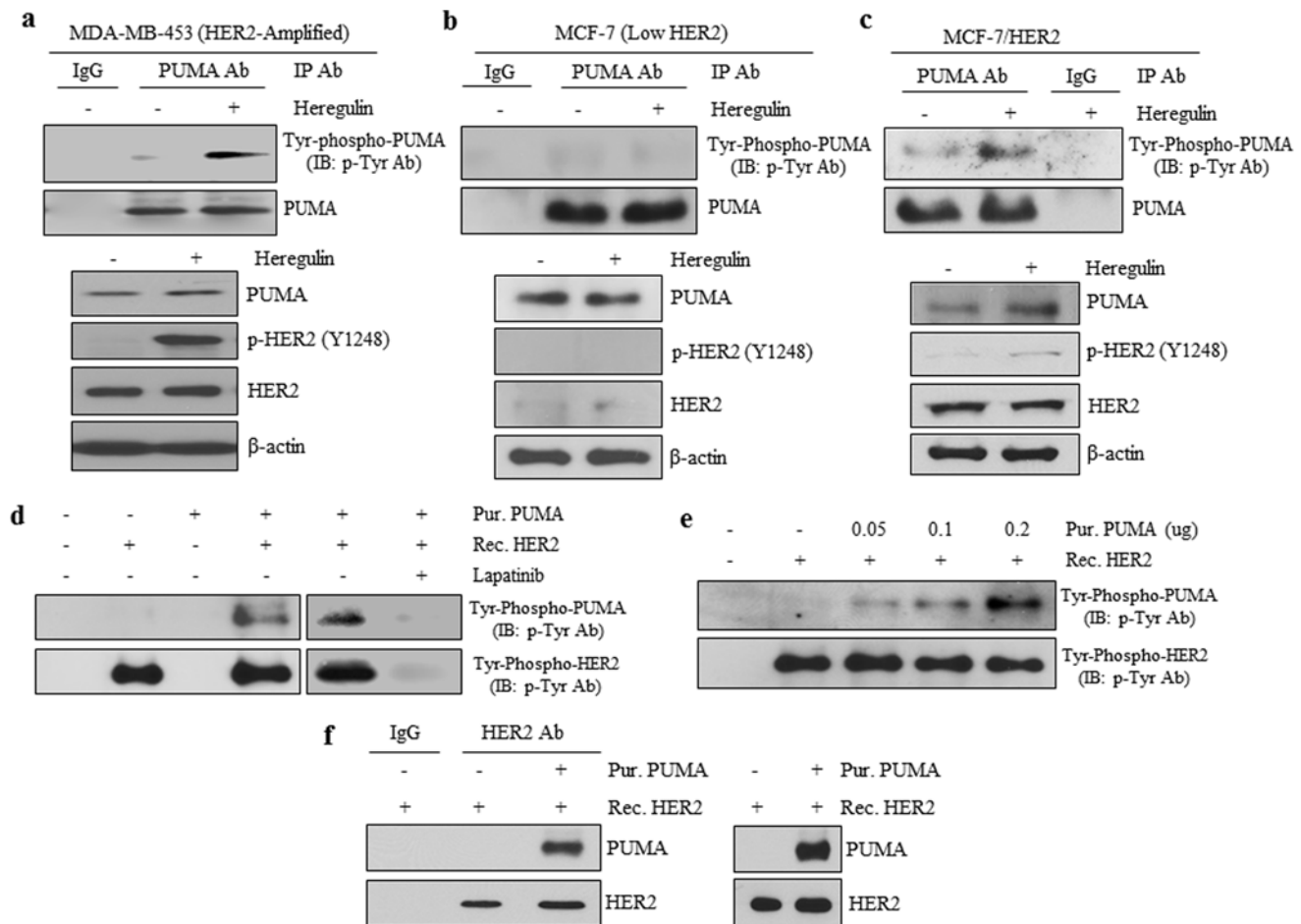


Figure 2. HER2 Directly Phosphorylates PUMA. MDA MB 453 (a), or MCF 7 (b), or MCF 7/HER2 (c) cells were incubated in serum free medium for 16 hrs followed by treatment with heregulin (100 ng/mL) for 30 min. Cells were then lysed and total protein was subjected to immunoprecipitation with either control IgG or PUMA antibodies followed by immunoblotting with indicated antibodies. Whole cell lysates were also subjected to immunoblotting with indicated antibodies. Tyrosine phosphorylated PUMA was detected with 4G10 phospho tyrosine antibodies. Recombinant PUMA protein was subjected to the HER2 kinase assay (as indicated in the Methods & Materials) in the presence or absence of lapatinib (d) or with increasing levels of recombinant PUMA protein (e). f) Recombinant HER2 was immunoprecipitated in the presence or absence of purified PUMA followed by immunoblotting with indicated antibodies.
doi:10.1371/journal.pone.0078836.g002

assay (Figure 3b), WT PUMA showed phospho tyrosine bands whereas none were detected with TM PUMA, indicating the TM PUMA is not phosphorylated by HER2. To rule out the possibility that TM PUMA cannot be tyrosine phosphorylated due to its inability to interact with HER2, we next determined whether TM PUMA can physically interact with HER2. IP/WB with a HER2 antibody (Figure 3c) demonstrated that HER2 interacted with both WT PUMA and TM PUMA equally indicating the lack of TM PUMA phosphorylation by HER2 is not due to decreased interaction between the two proteins. Taken together, the results in Figures 2 and 3 are the first evidence showing that PUMA undergoes tyrosine phosphorylation and that HER2 can directly phosphorylate PUMA.

TM-PUMA has a Longer Half-life than WT-PUMA

We next wanted to determine whether PUMA phosphorylation by HER2 altered PUMA stability. To this end, we assessed protein half life using cycloheximide, which inhibits protein synthesis allowing detection of when proteins are degraded. Cycloheximide is a common method to determine protein stability as several relevant papers have used this method in recent years [31–34].

Thus, HER2 overexpressing MDA MB 453 cells were treated with cycloheximide for up to 16 hrs in the presence or absence of heregulin to activate HER2. As shown in Figure 4a, heregulin induced activation of HER2 in these cells and also led to enhanced PUMA protein degradation. To further examine the stability of PUMA, we assessed PUMA half life using MCF 7 cells, which have low HER2 expression, or MCF 7/HER2 cells, which have stable overexpression of HER2. Figure 4b shows that PUMA is degraded faster in MCF 7/HER2 cells compared to MCF 7 cells indicating HER2 overexpression reduces PUMA stability. We next determined whether the half life of TM PUMA, which cannot be tyrosine phosphorylated, differs from that of WT PUMA. Cells were transfected with either WT PUMA or TM PUMA followed by cycloheximide treatment. As shown in Figure 4c, WT PUMA levels significantly decreased at 16 hrs whereas TM PUMA levels did not substantially decline. Following quantification of PUMA band signals and plotting them over time, we found that the half life for WT PUMA was approximately 7 hrs whereas that of TM PUMA was longer than 16 hrs. It has been previously shown that PUMA can be targeted to the proteasome for degradation [31]. To determine if WT PUMA or

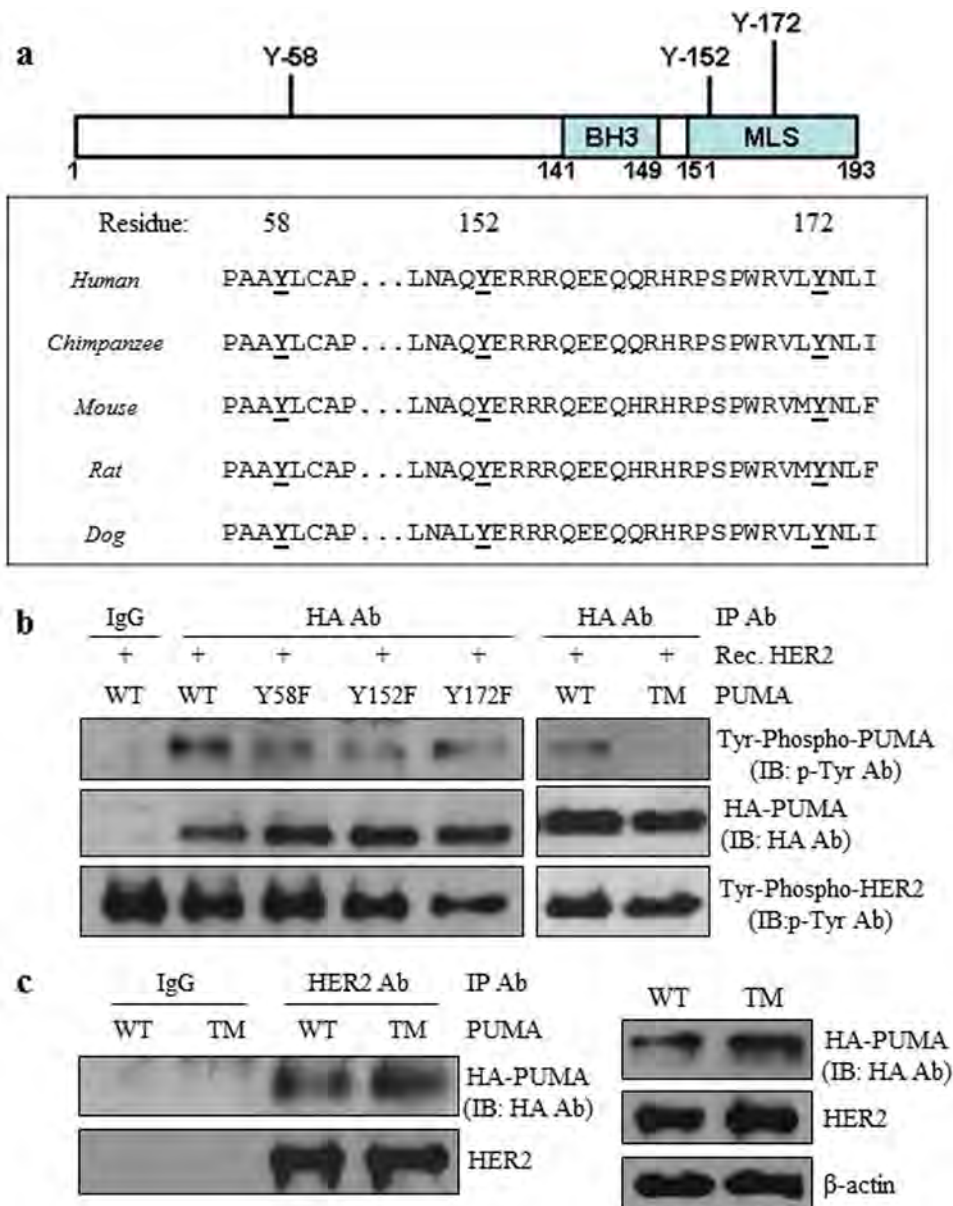


Figure 3. HER2 Phosphorylates Three Tyrosine Residues on PUMA. a) Linear representation of the PUMA protein with each tyrosine, the BH3 domain, and mitochondrial localization signal (MLS) domain indicated (upper panel). Tyrosines 58, 152, and 172 in the PUMA protein is conserved across multiple mammalian species, which are indicated (lower panel). b) Wild type HA tagged PUMA protein was mutated so that each tyrosine was changed to phenylalanine (Y58F, Y152F, Y172F) or all tyrosines were mutated (triple mutant: TM). MCF 7 cells were transfected with WT PUMA or each PUMA mutant and whole cell lysate was subjected immunoprecipitation with either control IgG or HA directed antibodies. Following immunoprecipitation, the product was subjected to the HER2 kinase assay as indicated in the Materials and Methods section. c) WT PUMA or TM PUMA were transfected into MDA MB 453 cells. Cells were lysed and total protein subjected to immunoprecipitation and immunoblotting with indicated antibodies. Whole cell lysates were also subjected to immunoblotting with indicated antibodies.
doi:10.1371/journal.pone.0078836.g003

TM PUMA is regulated by the proteasome, we performed the half life experiment in the presence of the proteasome inhibitor MG132. As shown in Figure 4d, we observed that WT PUMA half life could be extended with inhibition of the proteasome confirming previous results [31]. These results suggest HER2 mediated phosphorylation reduces the half life of PUMA.

We next asked whether TM PUMA retains the ability to undergo translocation to the mitochondria where PUMA promotes apoptosis. Thus, WT PUMA or TM PUMA were transfected into cells followed by isolation of the ME and NME with subsequent immunoblotting. As Figure 4e indicates, TM

PUMA retained the ability to undergo mitochondrial localization. Furthermore, we observed greater levels of TM PUMA compared to WT PUMA in the ME, which was confirmed by calculation of the mtPUMA Index (see Materials and Methods) resulting in 3.3 times more TM PUMA in the mitochondria than WT PUMA. A greater TM PUMA level in the mitochondria is likely the result of enhanced protein stability of TM PUMA protein in the presence of HER2. Together, these data show that PUMA protein stability is decreased with HER2 activation and blocking PUMA tyrosine phosphorylation enhances PUMA stability and results in greater mitochondrial levels of PUMA.

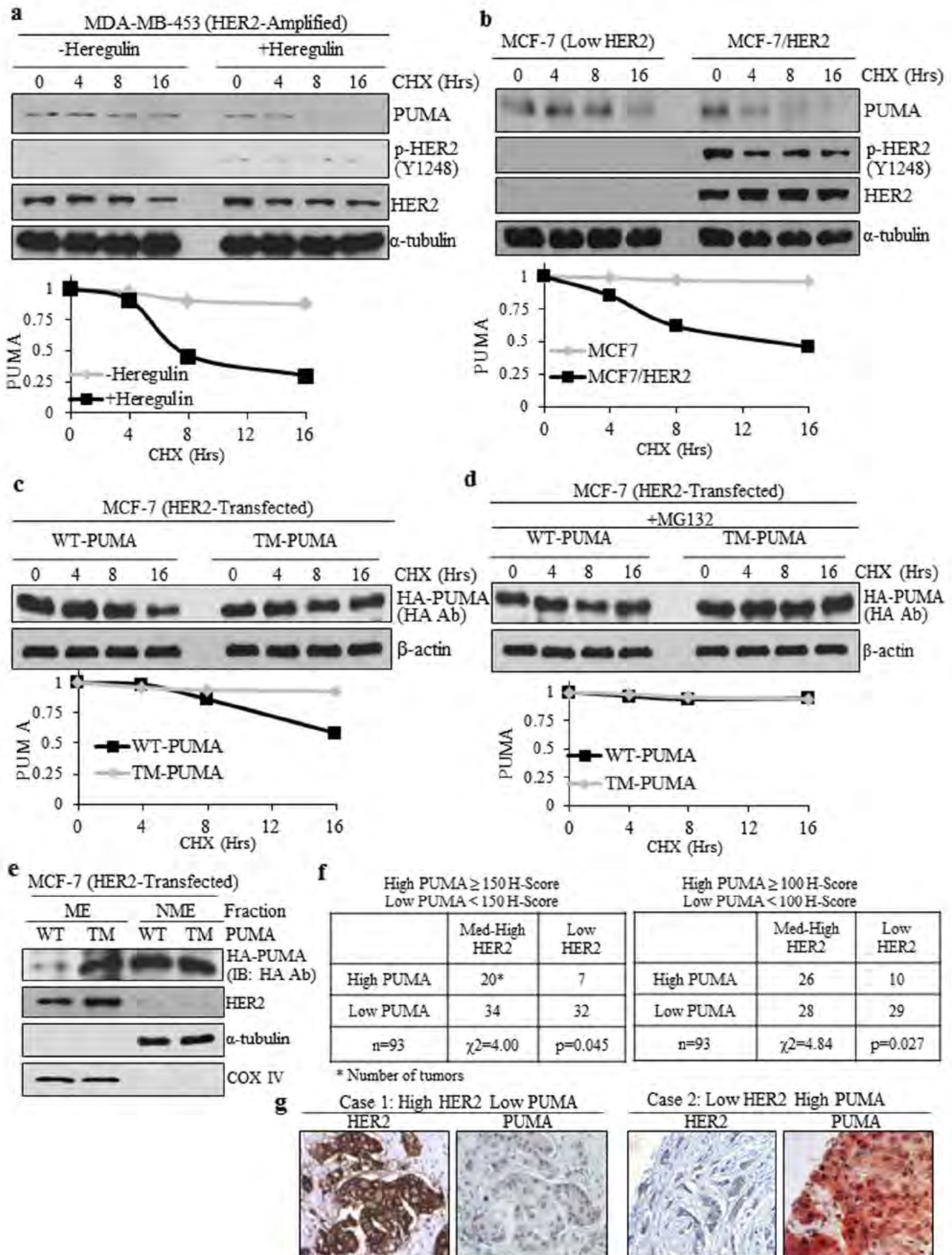


Figure 4. HER2 Phosphorylation Regulates Half Life and Mitochondrial Levels. a) MDA MB 453 cells were incubated in serum free medium for 16 hrs followed by treatment with heregulin (100 ng/mL) and cycloheximide (10 ug/mL). Whole cell lysate was subjected to immunoblotting with indicated antibodies. b) MCF 7 and MCF 7/HER2 cells were incubated in serum free medium for 16 hrs followed by treatment with heregulin (100 ng/mL) and cycloheximide (10 ug/mL). Whole cell lysate was subjected to immunoblotting with indicated antibodies. c,d) MCF 7 cells were transfected with HER2 and either WT PUMA or TM PUMA. Cells were incubated in serum free medium for 16 hrs followed by treatment with heregulin (100 ng/mL) and cycloheximide (10 ug/mL) without (c) or with MG132 (10 μ M) co treatment (d). Whole cell lysate was subjected to immunoblotting with indicated antibodies. e) MCF 7 cells were transfected with WT PUMA or TM PUMA and mitochondria were isolated. ME and NME were subjected to immunoblotting with indicated antibodies. f) Chi square tables for analysis of clinical cancer samples. Med High HER2 = 2–3+. Low HER2 = 0–1+. g) Sample IHC images of clinical cancer samples for High HER2+ Low PUMA (case 1) and Low HER2+ High PUMA (case 2). doi:10.1371/journal.pone.0078836.g004

To assess whether this relationship is maintained *in vivo*, we performed immunohistochemistry on a set of clinical cancer samples (n = 93) to detect HER2 and PUMA. After scoring, we divided the samples into low HER2 (0–1+ intensity) or medium to high HER2 (2–3+ intensity). PUMA was divided into high PUMA (either ≥ 150 H Score or ≥ 100 H Score) or low PUMA (either < 150 H Score or < 100 H Score). We then performed a chi square analysis to determine the relationship between HER2 and PUMA expression (Figure 4f). The chi square analysis using either PUMA barrier (150 H Score or 100 H Score) resulted in statistical significance (p = 0.045 and p = 0.027, respectively). These data suggest the tissues with high HER2 expression tend to have lower PUMA expression *in vivo* (Figure 4g) supporting our data from cell lines that HER2 can downregulate PUMA expression.

TM-PUMA has a Stronger Effect than WT-PUMA on Suppressing Clonogenic Growth

Figure 4 indicated that TM PUMA had greater protein stability and greater protein levels in the mitochondria, which may indicate that TM PUMA has an enhanced ability to promote apoptosis. To examine the effect of TM PUMA on cell viability, we expressed an empty vector, WT PUMA or TM PUMA in two different HER2 overexpressing breast cancer cell lines, namely BT 474 (Figure 5e) and MDA MB 453 (Figure 5f) cells, and monitored the ability of these cells to form colonies. As shown by the anchorage dependent colony assay (Figures 5a and 5b), TM PUMA significantly decreased colony formation compared to WT PUMA, indicating that TM PUMA had a stronger growth suppression than WT PUMA. As expected, compared to the empty vector, WT PUMA had a stronger propensity to decrease the colony formation ability of both cell lines. Both of these cells are aggressive and will grow independent of attachment. Therefore, a similar experiment was also performed with the same cell lines but using an anchorage independent soft agarose colony assay. TM PUMA significantly reduced soft agarose colony formation compared to WT PUMA (Figures 5c and 5d). WT PUMA also reduced colony formation compared to vector in both cell lines. Together, these data demonstrate that TM PUMA has a greater effect than WT PUMA on decreasing clonogenic growth of breast cancer cells and suggests tyrosine phosphorylation of PUMA decreases the ability of PUMA to suppress cell growth.

TM-PUMA Induces Apoptosis to a Greater Degree than WT-PUMA

We observed that TM PUMA has a greater effect on cell growth than WT PUMA in the context of HER2 overexpressing cells. However, whether this decrease in cell growth with TM PUMA was due to enhanced apoptosis cannot be determined from analysis of the colony assays. To determine the effect of TM PUMA on apoptosis, BT 474 cells were transfected with an empty vector, WT PUMA, or TM PUMA followed by treatment with heregulin to ensure HER2 activation. We then assessed the extent of apoptosis in the treated cells by the Annexin V binding assay

using flow cytometry. Figures 6a and 6c show that TM PUMA induced the greatest levels of apoptosis compared to WT PUMA or empty vector. PUMA has been shown previously to sensitize cancer cells to treatment with apoptosis inducing chemotherapeutic agents [21]. Therefore, we next assessed whether TM PUMA could further enhance apoptosis in the presence of a low dose of anisomycin, an apoptosis inducer [35]. To this end, cancer cells were transfected with vector, WT PUMA, or TM PUMA followed by exposure to heregulin and anisomycin with subsequent assessment of Annexin V binding. As shown in Figures 6b and 6c, TM PUMA expression significantly promoted apoptosis in the presence of anisomycin compared to vector and WT PUMA. As expected, we observed modest increases in apoptosis in anisomycin treated cells expressing vector or WT PUMA compared to untreated cells.

To confirm the effects of WT PUMA and TM PUMA on apoptosis, cell lysates were analyzed by WB for the presence of PARP 1 cleavage. Consistent with the results of the Annexin V staining, the results revealed that TM PUMA induced the greatest levels of cleaved PARP 1 (Figure 6d). Together, results presented in Figure 6 indicate TM PUMA as a stronger apoptosis inducer than WT PUMA and that tyrosine phosphorylation of PUMA reduces the ability of PUMA to promote apoptosis.

Discussion

We report in this study that HER2 directly phosphorylates PUMA and this leads to PUMA degradation and suppression of apoptosis (Figure 7). This finding is novel and significant because HER2 mediated negative regulation of PUMA is direct and distinctly different than previously reported mechanisms by which HER2 can indirectly antagonize apoptosis. Furthermore, PUMA was recently shown to be required for HER2 inactivation induced apoptosis [36] and our data suggest a direct method whereby HER2 downregulates PUMA protein levels. Overexpression of HER2 occurs in 15–20% of breast cancers and is a marker for poor patient outcome [2–4]. HER2 promotes several characteristics common to cancer cells including activation of downstream signaling, especially PI3K/AKT and MAPK pathways, promotion of cell division, inhibition of apoptosis, and promotion cell motility among others [4]. HER2 regulation of apoptosis can be mediated by indirect upregulation of anti apoptotic proteins such as Bcl 2 and Bcl xL [7,11]. Also, HER2 mediated activation of AKT leads to phosphorylation and down regulation of Bad, another pro apoptotic BH3 only protein [10]. In addition, our lab recently found that EGFR, another ErbB family member, could physically interact with PUMA, which prevented PUMA localization to the mitochondria and suppressed apoptosis [26]. These studies and the current data indicate that ErbB receptor tyrosine kinases regulate apoptosis at multiple levels including indirect regulation, via downstream signaling components, and direct regulation, such as post translational regulation of PUMA by HER2.

The current study is the first evidence that PUMA can be phosphorylated on tyrosine residues. In 2010, Fricker et al. first

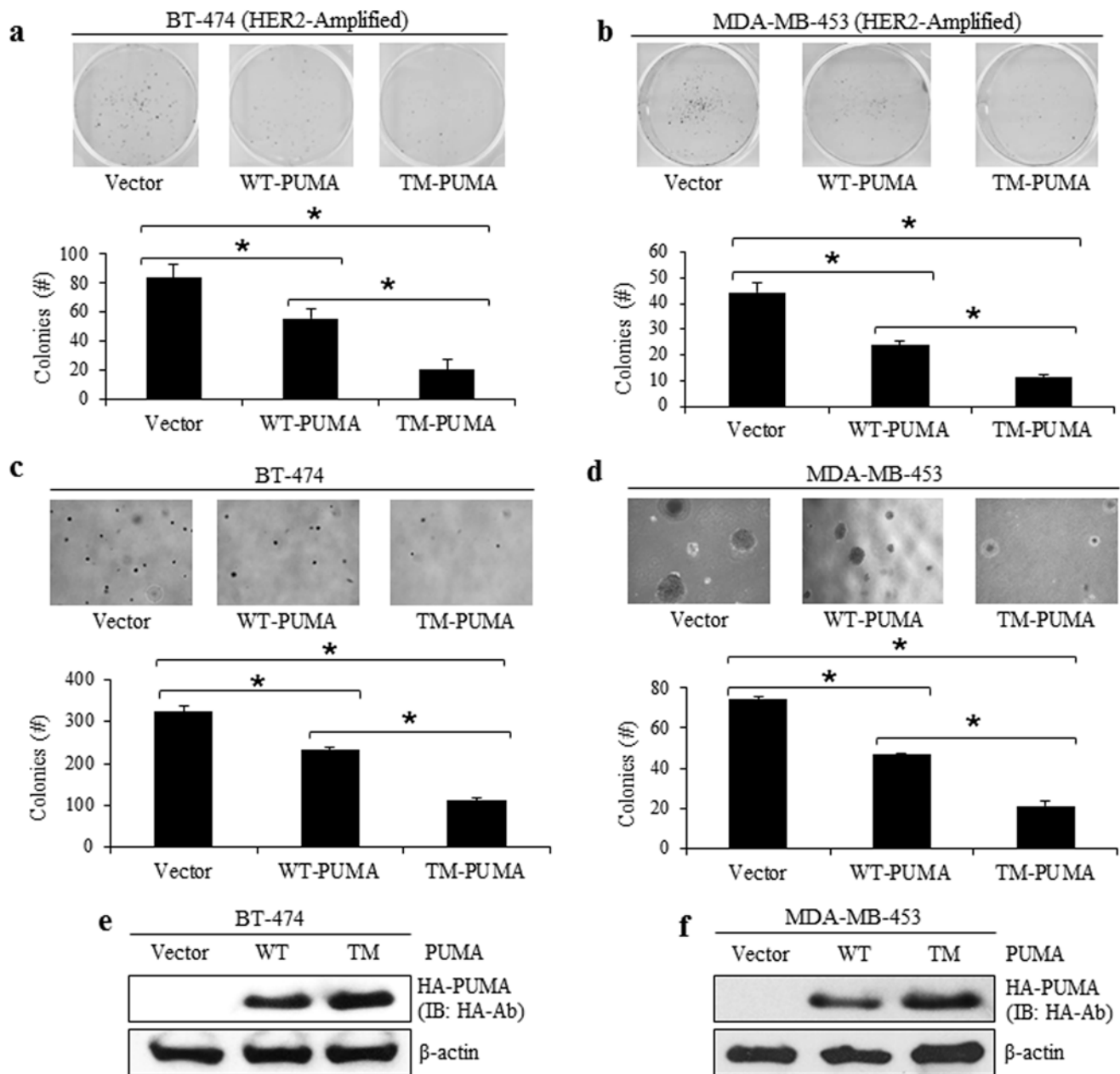


Figure 5. TM PUMA Decreases Clonogenic Growth in HER2 Overexpressing Cells. BT 474 cells (a, c, e) and MDA MB 453 cells (b, d, f) were transfected with an empty vector, WT PUMA, or TM PUMA for 48 hrs (e, f). Transfected cells were then seeded into 6 well plates either without (a and b) or with soft agarose (c and d) and incubated at 37°C for 14–21 days. Colonies were then counted, stained with crystal violet blue, and images were taken.

doi:10.1371/journal.pone.0078836.g005

observed that PUMA protein could incorporate labeled ^{32}P suggesting it could be phosphorylated [31]. Their analysis indicated it was primarily serine residues that were phosphorylated with serine 10 being the major target. Mutation of serine 10 to alanine resulted in a PUMA mutant protein that showed greater induction of apoptosis than wild type PUMA, which was the result of an extended protein half life [31]. Investigators were not able to identify any kinase that mediated serine 10 phosphorylation of PUMA. However, another group soon found that IL 3 signaling induced phosphorylation at serine 10 and enhanced PUMA protein degradation [34]. These results ultimately identified I κ B kinase 1 (IKK1) as the kinase that directly phosphorylates serine

10 of PUMA in response to IL 3 signaling [34]. Results of the current study and these recent studies indicate phosphorylation and degradation of PUMA provide cells an escape from apoptosis under conditions replete with growth promoting signals. Future identification of other kinases that phosphorylate PUMA will provide a greater understanding of what cellular contexts PUMA phosphorylation may be important.

PUMA expression enhances apoptosis induction by chemotherapy [21]. Chemotherapy treatment has been shown to induce PUMA expression in breast cancer cells [21,37,38] and PUMA is a primary mediator of apoptosis in response to tamoxifen in breast cancer cells [39]. Forced HER2 expression in HER2 negative cells

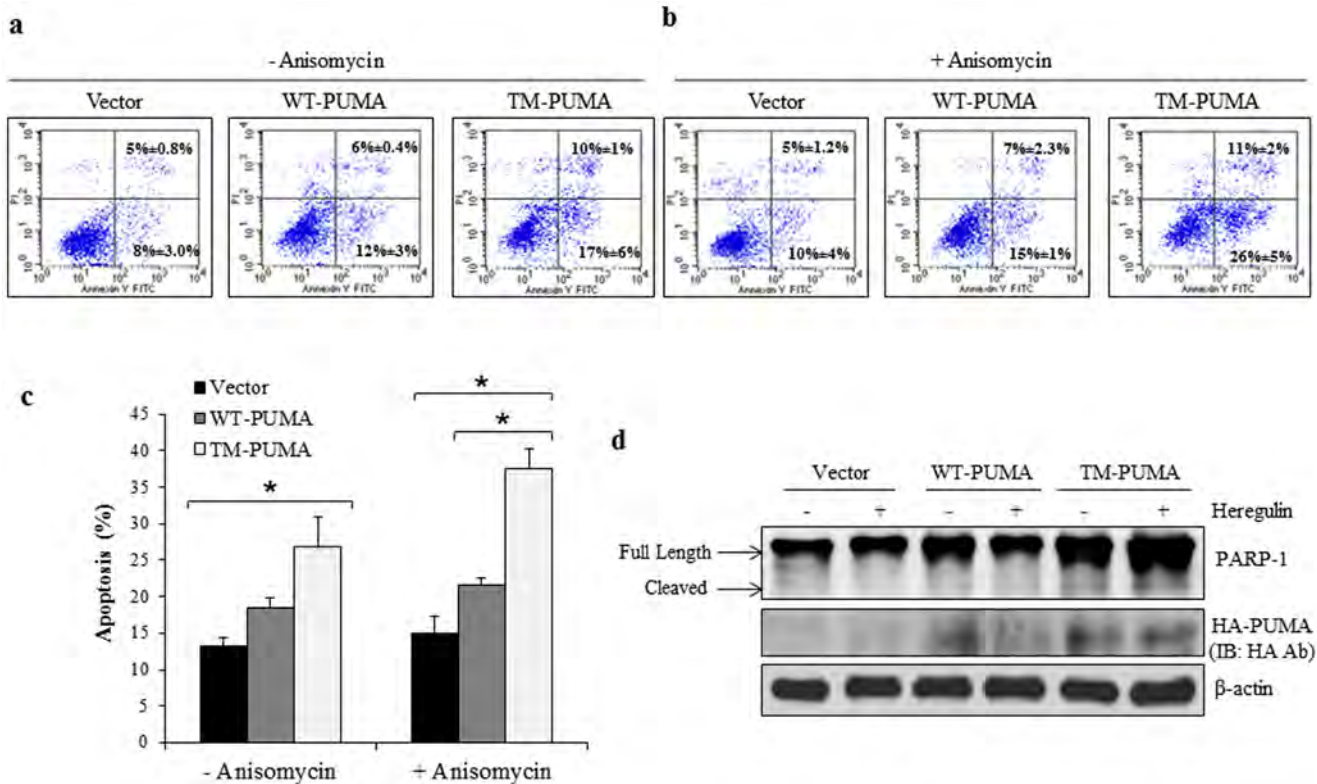


Figure 6. TM PUMA Induces Apoptosis in HER2 Overexpressing Cells. a) and b) BT 474 cells were transfected with an empty vector, WT PUMA, or TM PUMA. Cells were treated with heregulin (100 ng/mL) and with or without anisomycin (25 ng/mL) for 16 hrs. Cells were detached and incubated with annexin V FITC and PI according to manufacturer's instructions followed by analysis by flow cytometry. c) Graph representing measurements of apoptosis from (a and b). d) BT 474 cells were transfected with an empty vector, WT PUMA, or TM PUMA. Cells were incubated in serum free medium for 16 hrs followed by treatment with heregulin (100 ng/mL) for 4 hrs. Cells were then lysed and total protein was subjected to immunoblotting with indicated antibodies. doi:10.1371/journal.pone.0078836.g006

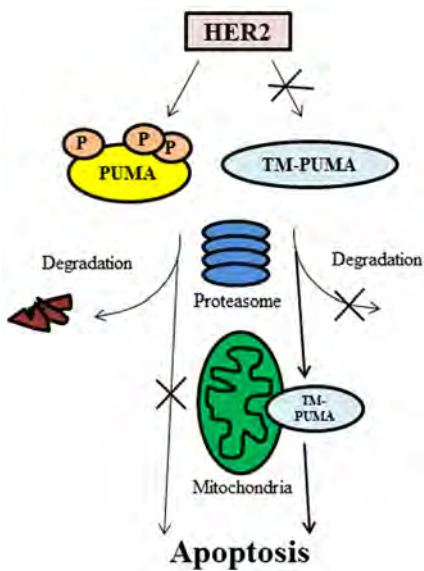


Figure 7. HER2 Downregulates PUMA by Phosphorylation. HER2 phosphorylates PUMA on three tyrosine residues leading to degradation by the proteasome reducing apoptosis. TM PUMA, which cannot be phosphorylated by HER2, has an extended half life and localizes to the mitochondria and promotes apoptosis. doi:10.1371/journal.pone.0078836.g007

suppressed apoptosis and induced tamoxifen resistance because of increased expression of anti apoptotic proteins such as Bcl 2 [7]. Here we show that HER2 can additionally regulate apoptosis by phosphorylating tyrosine residues on PUMA leading to its degradation. HER2 mediated down regulation of PUMA via phosphorylation and HER2 mediated upregulation of anti apoptotic Bcl 2 proteins creates a cellular environment highly resistant to apoptosis.

We also observed that TM PUMA, which is resistant to HER2 phosphorylation, has increased protein stability and enhanced induction of apoptosis by pro apoptotic agents in the presence of HER2 overexpression compared to WT PUMA. Evidence for the benefits of targeting Bcl 2 family proteins is accumulating as BH3 only mimicking agents can promote apoptosis and enhance apoptosis with chemotherapy [40-42]. Specifically, ABT 737 was recently observed to sensitize primary breast tumors overexpressing Bcl 2 to chemotherapy [42]. Also, tumor specific PUMA gene transfer enhanced radiosensitivity of breast cancer cells, although this result was in cells that do not overexpress HER2 [43]. TM PUMA would likely be a more beneficial gene therapy in HER2 overexpressing cells as our results suggest HER2 overexpression decreases WT PUMA induced apoptosis. Together, these results indicate that targeting Bcl 2 family proteins in addition to chemotherapy may provide greater breast cancer cell death.

Our data, and others [31,34], indicate that inhibition of the proteasome extends the half life of PUMA (Figure 4) whereas

inhibition of lysosomal proteases has little effect on PUMA degradation [33]. This would suggest the proteasome is the primary mediator of PUMA protein degradation. Considering that our TM PUMA, which cannot undergo tyrosine phosphorylation, is not degraded by the proteasome it is likely that tyrosine phosphorylation allows for further modifications that target PUMA to the proteasome. Given the nascent understanding of PUMA post translational modifications, further investigation is needed to elucidate the specific modifications required to target PUMA to the proteasome and to determine what enzymes make these modifications.

To extend the findings reported in this study, there should be further investigation into whether other tyrosine kinases can phosphorylate PUMA as this could indicate other cellular and disease contexts in which PUMA phosphorylation is important. Also, the role of phosphorylation of each tyrosine residue on

PUMA should be determined. Our results indicate all three tyrosine residues can be phosphorylated by HER2 but the role of each tyrosine residue on PUMA function cannot be determined herein. Lastly, it should be determined whether tyrosine phosphorylation resistant TM PUMA and BH3 mimetics can enhance the effectiveness of chemotherapeutics in HER2 over-expressing breast tumors. These future studies will elucidate the importance of BH3 only proteins, especially PUMA, in breast cancer and advance the search for therapeutic targets in HER2 positive tumors.

Author Contributions

Conceived and designed the experiments: RLC HWL. Performed the experiments: RLC WH IP. Analyzed the data: RLC. Contributed reagents/materials/analysis tools: RLC. Wrote the paper: RLC HWL.

References

- Society AC (2013) Cancer Facts & Figures 2013. Atlanta, GA.
- Slamon DJ, Clark GM, Wong SG, Levin WJ, Ullrich A, et al. (1987) Human breast cancer: correlation of relapse and survival with amplification of the HER-2/neu oncogene. *Science* 235: 177–182.
- Slamon DJ, Godolphin W, Jones LA, Holt JA, Wong SG, et al. (1989) Studies of the HER-2/neu proto-oncogene in human breast and ovarian cancer. *Science* 244: 707–712.
- Yarden Y, Sliwkowski MX (2001) Untangling the ErbB signalling network. *Nat Rev Mol Cell Biol* 2: 127–137.
- Wallasch C, Weiss FU, Niederfellner G, Jallal B, Issing W, et al. (1995) Heregulin-dependent regulation of HER2/neu oncogenic signaling by heterodimerization with HER3. *EMBO J* 14: 4267–4275.
- Henson ES, Hu X, Gibson SB (2006) Hereceptin sensitizes ErbB2-overexpressing cells to apoptosis by reducing antiapoptotic Mcl-1 expression. *Clin Cancer Res* 12: 845–853.
- Kumar R, Mandal M, Lipton A, Harvey H, Thompson CB (1996) Overexpression of HER2 modulates bcl-2, bcl-XL, and tamoxifen-induced apoptosis in human MCF-7 breast cancer cells. *Clin Cancer Res* 2: 1215–1219.
- Siziopikou KP, Khan S (2005) Correlation of HER2 gene amplification with expression of the apoptosis-suppressing genes bcl-2 and bcl-x-L in ductal carcinoma in situ of the breast. *Appl Immunohistochem Mol Morphol* 13: 14–18.
- Tuna M, Chavez-Reyes A, Tari AM (2005) HER2/neu increases the expression of Wilms' Tumor 1 (WT1) protein to stimulate S-phase proliferation and inhibit apoptosis in breast cancer cells. *Oncogene* 24: 1648–1652.
- Datta SR, Dudek H, Tao X, Masters S, Fu H, et al. (1997) Akt phosphorylation of BAD couples survival signals to the cell-intrinsic death machinery. *Cell* 91: 231–241.
- Siddiqi A, Long LM, Li L, Marciniak RA, Kazhdan I (2008) Expression of HER-2 in MCF-7 breast cancer cells modulates anti-apoptotic proteins Survivin and Bcl-2 via the extracellular signal-related kinase (ERK) and phosphoinositide-3 kinase (PI3K) signalling pathways. *BMC Cancer*. 2008/05/06 ed. 129.
- Nakano K, Vousden KH (2001) PUMA, a novel proapoptotic gene, is induced by p53. *Mol Cell* 7: 683–694.
- Yu J, Zhang L, Hwang PM, Kinzler KW, Vogelstein B (2001) PUMA induces the rapid apoptosis of colorectal cancer cells. *Mol Cell* 7: 673–682.
- Han J, Flemington C, Houghton AB, Gu Z, Zambetti GP, et al. (2001) Expression of bbbc3, a pro-apoptotic BH3-only gene, is regulated by diverse cell death and survival signals. *Proc Natl Acad Sci U S A* 98: 11318–11323.
- Yee KS, Vousden KH (2008) Contribution of membrane localization to the apoptotic activity of PUMA. *Apoptosis* 13: 87–95.
- Yu J, Wang Z, Kinzler KW, Vogelstein B, Zhang L (2003) PUMA mediates the apoptotic response to p53 in colorectal cancer cells. *Proc Natl Acad Sci U S A* 100: 1931–1936.
- Ming L, Wang P, Bank A, Yu J, Zhang L (2006) PUMA Dissociates Bax and Bcl-X(L) to induce apoptosis in colon cancer cells. *J Biol Chem* 281: 16034–16042.
- Hoque MO, Begum S, Sommer M, Lee T, Trink B, et al. (2003) PUMA in head and neck cancer. *Cancer Lett* 199: 75–81.
- Yu J, Zhang L (2008) PUMA, a potent killer with or without p53. *Oncogene* 27 Suppl 1: S71–83.
- Goh AM, Coffill CR, Lane DP (2011) The role of mutant p53 in human cancer. *J Pathol* 223: 116–126.
- Yu J, Yue W, Wu B, Zhang L (2006) PUMA sensitizes lung cancer cells to chemotherapeutic agents and irradiation. *Clin Cancer Res* 12: 2928–2936.
- Luo X, He Q, Huang Y, Sheikh MS (2005) Transcriptional upregulation of PUMA modulates endoplasmic reticulum calcium pool depletion-induced apoptosis via Bax activation. *Cell Death Differ* 12: 1310–1318.
- Ming L, Sakaïda T, Yue W, Jha A, Zhang L, et al. (2008) Sp1 and p73 activate PUMA following serum starvation. *Carcinogenesis* 29: 1878–1884.
- Wu B, Qiu W, Wang P, Yu H, Cheng T, et al. (2007) p53 independent induction of PUMA mediates intestinal apoptosis in response to ischaemia reperfusion. *Gut* 56: 645–654.
- You H, Pellegrini M, Tsuchihara K, Yamamoto K, Hacker G, et al. (2006) FOXO3a-dependent regulation of Puma in response to cytokine/growth factor withdrawal. *The Journal of Experimental Medicine* 203: 1657–1663.
- Zhu H, Cao X, Ali-Osman F, Keir S, Lo HW (2010) EGFR and EGFRvIII interact with PUMA to inhibit mitochondrial translocalization of PUMA and PUMA-mediated apoptosis independent of EGFR kinase activity. *Cancer Lett* 294: 101–110.
- Cao X, Zhu H, Ali-Osman F, Lo HW (2011) EGFR and EGFRvIII undergo stress- and EGFR kinase inhibitor-induced mitochondrial translocalization: a potential mechanism of EGFR-driven antagonism of apoptosis. *Mol Cancer*. 2011/03/11 ed. 26.
- Lo HW, Zhu H, Cao X, Aldrich A, Ali-Osman F (2009) A novel splice variant of GLI1 that promotes glioblastoma cell migration and invasion. *Cancer Res* 69: 6790–6798.
- Xia W, Mullin RJ, Keith BR, Liu LH, Ma H, et al. (2002) Anti-tumor activity of GW572016: a dual tyrosine kinase inhibitor blocks EGF activation of EGFR/erbB2 and downstream Erk1/2 and AKT pathways. *Oncogene* 21: 6255–6263.
- Ding Y, Liu Z, Desai S, Zhao Y, Liu H, et al. (2012) Receptor tyrosine kinase ErbB2 translocates into mitochondria and regulates cellular metabolism. *Nat Commun*. 2012/12/13 ed. 1271.
- Fricker M, O'Prey J, Tolkovsky AM, Ryan KM (2010) Phosphorylation of Puma modulates its apoptotic function by regulating protein stability. *Cell Death Dis*. 2011/03/03 ed. pp. e59.
- Ji Z, Mei FC, Xie J, Cheng X (2007) Oncogenic KRAS activates hedgehog signaling pathway in pancreatic cancer cells. *J Biol Chem* 282: 14048–14055.
- Lakhter AJ, Sahu RP, Sun Y, Kaufmann WK, Androphy EJ, et al. (2013) Chloroquine Promotes Apoptosis in Melanoma Cells by Inhibiting BH3 Domain-Mediated PUMA Degradation. *J Invest Dermatol* 133: 2247–2254.
- Sandow JJ, Jabbour AM, Condina MR, Daunt CP, Stomski FC, et al. (2012) Cytokine receptor signaling activates an IKK-dependent phosphorylation of PUMA to prevent cell death. *Cell Death Differ* 19: 633–641.
- Faris M, Kokot N, Latinis K, Kasibhatla S, Green DR, et al. (1998) The c-Jun N-Terminal Kinase Cascade Plays a Role in Stress-Induced Apoptosis in Jurkat Cells by Up-Regulating Fas Ligand Expression. *The Journal of Immunology* 160: 134–144.
- Bean GR, Ganesan YT, Dong Y, Takeda S, Liu H, et al. (2013) PUMA and BIM are required for oncogene inactivation-induced apoptosis. *Sci Signal* 6: ra20.
- Hernandez-Vargas H, Ballestar E, Carmona-Saez P, von Kobbe C, Banon-Rodriguez I, et al. (2006) Transcriptional profiling of MCF7 breast cancer cells in response to 5-Fluorouracil: relationship with cell cycle changes and apoptosis, and identification of novel targets of p53. *Int J Cancer* 119: 1164–1175.
- Middelburg R, de Haas RR, Dekker H, Kerkhoven RM, Pohlmann PR, et al. (2005) Induction of p53 up-regulated modulator of apoptosis messenger RNA by chemotherapeutic treatment of locally advanced breast cancer. *Clin Cancer Res* 11: 1863–1869.
- Roberts CG, Millar EK, O'Toole SA, McNeil CM, Lehrbach GM, et al. (2011) Identification of PUMA as an estrogen target gene that mediates the apoptotic response to tamoxifen in human breast cancer cells and predicts patient outcome and tamoxifen responsiveness in breast cancer. *Oncogene* 30: 3186–3197.
- Arisan ED, Kutuk O, Tezil T, Bodur C, Telci D, et al. (2010) Small inhibitor of Bcl-2, HA14 1, selectively enhanced the apoptotic effect of cisplatin by modulating Bcl-2 family members in MDA-MB-231 breast cancer cells. *Breast Cancer Res Treat* 119: 271–281.
- Liu Y, Li Y, Wang H, Yu J, Lin H, et al. (2009) BH3-based fusion artificial peptide induces apoptosis and targets human colon cancer. *Mol Ther* 17: 1509–1516.

42. Oakes SR, Vaillant F, Lim E, Lee L, Breslin K, et al. (2012) Sensitization of BCL-2-expressing breast tumors to chemotherapy by the BH3 mimetic ABT-737. *Proc Natl Acad Sci U S A* 109: 2766–2771.
43. Wang R, Wang X, Li B, Lin F, Dong K, et al. (2009) Tumor-specific adenovirus-mediated PUMA gene transfer using the survivin promoter enhances radiosensitivity of breast cancer cells in vitro and in vivo. *Breast Cancer Res Treat* 117: 45–54.

ORIGINAL ARTICLE

Akt phosphorylates and activates HSF-1 independent of heat shock, leading to Slug overexpression and epithelial–mesenchymal transition (EMT) of HER2-overexpressing breast cancer cells

RL Carpenter¹, I Paw¹, MW Dewhirst^{2,3} and H-W Lo^{1,3}

Epithelial–mesenchymal transition (EMT) is an essential step for tumor progression, although the mechanisms driving EMT are still not fully understood. In an effort to investigate these mechanisms, we observed that heregulin (HRG)-mediated activation of HER2, or HER2 overexpression, resulted in EMT, which is accompanied with increased expression of a known EMT regulator Slug, but not TWIST or Snail. We then investigated how HER2 induced Slug expression and found, for the first time, that there are four consensus HSF sequence-binding elements (HSEs), the binding sites for heat shock factor-1 (HSF-1), located in the *Slug* promoter. HSF-1 bound to and transactivated the *Slug* promoter independent of heat shock, leading to Slug expression in breast cancer cells. Mutation of the putative HSEs ablated Slug transcriptional activation induced by HRG or HSF-1 overexpression. Knockdown of HSF-1 expression by siRNA reduced Slug expression and HRG-induced EMT. The positive association between HSF-1 and Slug was confirmed by immunohistochemical staining of a cohort of 100 invasive breast carcinoma specimens. While investigating how HER2 activated HSF-1 independent of heat shock, we observed that HER2 activation resulted in concurrent phosphorylation of Akt and HSF-1. We then observed, also for the first time, that Akt directly interacted with HSF-1 and phosphorylated HSF-1 at S326. Inhibition of Akt using siRNA, dominant-negative Akt mutant, or small molecule inhibitors prevented HRG-induced HSF-1 activation and Slug expression. Conversely, constitutively active Akt induced HSF-1 phosphorylation and Slug expression. HSF-1 knockdown reduced the ability of Akt to induce Slug expression, indicating an essential role that HSF-1 plays in Akt-induced Slug upregulation. Altogether, our study uncovered the existence of a novel Akt-HSF-1 signaling axis that leads to Slug upregulation and EMT, and potentially contributes to progression of HER2-positive breast cancer.

Oncogene advance online publication, 27 January 2014; doi:10.1038/onc.2013.582

Keywords: Slug; EMT; Akt; HSF-1; HER2; phosphorylation

INTRODUCTION

Epithelial–mesenchymal transition (EMT) is a cellular process whereby epithelial cells are reprogrammed to mesenchymal cells. Both EMT and the reverse process MET (mesenchymal–epithelial transition) are critically important in multiple stages of development in vertebrates and invertebrates.¹ Both EMT and MET are also important processes in tumor progression and metastasis whereby EMT facilitates the migration of epithelial tumor cells from the primary site to distant locations, whereas MET allows for extravasation and subsequent colonization at the secondary sites.² Direct evidence for these models has been established using animal models of different cancer types, including breast cancer.^{3,4}

The transcription factor Slug (SNAI2) promotes EMT by binding to the *E-cadherin* promoter and repressing *E-cadherin* expression in epithelial cells,⁵ which is accompanied by changes in cell morphology indicating EMT.⁶ Slug is considered a marker for malignancy.⁷ Another member of the SNAI family, Snail (SNAI1), also binds to the *E-cadherin* promoter and represses *E-cadherin* expression in epithelial cells, leading to EMT.^{8,9} Additional EMT

transcription factors (for example, TWIST1, ZEB1 and ZEB2) can also repress *E-cadherin* promoter causing dissolution of cell junctions, loss of cell polarity and enhanced cell migration.^{10,11}

HER2 is a member of the ErbB family of receptor tyrosine kinases.¹² HER2 is expressed in 15–20% of breast cancers and HER2-positivity is associated with poor clinical prognosis.^{13–15} Overexpression of HER2 results in overactivation of several pathways in cells, including PI3K-Akt and Ras-MAPK among others. HER2 utilizes these pathways to support tumor growth by promoting cell proliferation, cell survival, tumor angiogenesis and metastasis.¹⁶ Overexpression of HER2 has been shown to associate with *E-cadherin* downregulation.^{17,18} There is also clinical evidence indicating that patients with HER2-positive metastatic breast cancer have circulating tumor cells that have undergone EMT.¹⁹ However, the mechanisms by which HER2 promotes EMT have not been fully elucidated and are likely complex.

To provide new mechanistic insights into the relationship between HER2 and EMT, we undertook the current study using breast cancer as the study model, and our study provided

¹Division of Surgical Sciences, Department of Surgery, Duke University School of Medicine, Durham, NC, USA; ²Department of Radiation Oncology, Duke University School of Medicine, Durham, NC, USA and ³Duke Cancer Institute, Duke University School of Medicine, Durham, NC, USA. Correspondence: Professor H W Lo, Division of Surgical Sciences, Department of Surgery (Box 3156), Duke Cancer Institute, Duke University School of Medicine, 423 MSRB I, 103 Research Drive, Durham, NC 27710, USA. E mail: huiwen.lo@duke.edu

Received 10 September 2013; revised 26 November 2013; accepted 3 December 2013

evidence showing that activation of HER2 induces EMT by upregulating Slug expression in the human breast cancer cells we had examined. A search of the human *Slug* gene promoter revealed the existence of several putative binding sites for the transcription factor, heat shock factor-1 (HSF-1). HSF-1 is classically activated by heat stress leading to the induction of heat shock proteins (HSPs), which are molecular chaperones that permit repair and refolding to damaged proteins. HSF-1 is constitutively expressed in most tissues but activation can be regulated by post-translational modification, specifically phosphorylation at S326 upon heat stress.²⁰ Active HSF-1 trimerizes allowing the recognition of HSF sequence-binding elements (HSEs) and upregulation of target genes.²¹ Activation of HSF-1 is enhanced in several cancer types, which is associated with a poor prognosis.^{22–24} Subsequently, we found, for the first time, that HSF-1 directly binds to the *Slug* promoter to induce Slug expression independent of heat shock, and that HER2-activated Akt directly phosphorylates HSF-1 at S326 and activates HSF-1 transcriptional activity. Through these observations, we uncovered a novel HER2-Akt-HSF-1 signaling axis that induces Slug expression and promotes EMT in breast cancer cells, thereby shedding new light on the molecular basis by which HER2-overexpressing breast cancer cells undergo EMT and potentially subsequent metastasis.

RESULTS

Heregulin (HRG) induces EMT and Slug expression in HER2-amplified breast cancer cells

We first investigated whether HRG induced EMT of two HER2-amplified breast cancer cell lines, MDA-MB-453 and BT-474. Both cell lines displayed typical epithelial morphology after serum starvation overnight (day 0) and underwent changes to the mesenchymal-like morphology after HRG treatment (Figure 1a). To determine which of the EMT regulators may be involved in the observed EMT, we determined levels of Slug, Snail and TWIST with HRG stimulation for 0–120 min, and the results (Figure 1b) showed that the *Slug* transcripts were significantly induced by HRG in both cell lines. This observation was further confirmed at the protein levels using western blotting (WB; Figure 1c). Consistent with increased expression of Slug, a transcriptional repressor of E-cadherin,⁵ E-cadherin expression level was reduced by HRG. In agreement with observed EMT-like morphological changes in Figure 1a, the mesenchymal marker Vimentin was elevated after HRG treatment (Figure 1c). We further show that levels of Slug and Vimentin were elevated, whereas E-cadherin expression was suppressed after prolonged HRG treatment (Figure 1d).

Using a luciferase reporter under the control of the human *Slug* promoter, we found the *Slug* promoter was significantly activated by HRG in all three breast cancer cell lines with HER2 amplification (Figure 1e). Altogether, these observations indicate that HRG induces EMT and Slug expression in HER2-amplified breast cancer cells.

HER2 overexpression enhances Slug expression, leading to EMT in breast cancer cells

We next asked whether HER2 overexpression induced EMT using MCF-7 (with normal HER2 expression level) and MCF-7/HER2 (MCF-7 cells stably expressing ectopic HER2). As shown by reverse transcription (RT)-PCR in Figure 2a, forced expression of HER2 upregulated Slug expression which led to reduced E-cadherin expression. WB in Figure 2b confirmed the RT-PCR data and HER2 overexpression in MCF-7/HER2 cells. We further show that HER2 overexpression converted the epithelial appearance of MCF-7 cells into the mesenchymal morphology (Figure 2c). In the presence of HRG, MCF-7 cells (with normal HER2 expression) also underwent

EMT-like morphological changes (Figure 2d). This observation is consistent with the results in Figure 2e showing that HRG induced *Slug* promoter activity in MCF-7 cells. Figure 2e also shows that HER2 transient transfection induced *Slug* promoter activation, which is in agreement with the results with MCF-7/HER2 stable transfectant cells. Conversely, we observed that Lapatinib, a small molecule HER2/EGFR inhibitor reduced Slug expression in HER2-amplified MDA-MB-453 and SK-BR-3 cells (Figure 2f). Altogether, these results demonstrate that HER2 overexpression enhances Slug expression, leading to EMT in breast cancer cells.

HSF-1 binds to and transactivates the *Slug* gene promoter, leading to Slug expression in breast cancer cells

To investigate the mechanisms by which Slug expression is upregulated by HER2/HRG, we searched the *Slug* promoter using TFSearch, a web-based search engine for transcription factor binding sites. Our search revealed that there are four putative HSF-1-binding sites, HSEs, within the *Slug* promoter (Figure 3a). Of note, HSF-1 proteins form trimers and recognize three repeats of HSEs, nGAAAn or nTTCn (Figure 3a).²¹ Using chromatin immunoprecipitation (ChIP) assay, we found that HSF-1 bound to the *Slug* promoter and this binding was enhanced by HRG (Figure 3b). As a positive control, we observed HSF-1 also bound to the *Hsp70* promoter, a known HSF-1 target gene. In ChIP assay, immunoglobulin G (IgG) was used as negative controls for IP, whereas chromatin inputs were used as loading controls for PCR. Using the luciferase reporter assay and WB, we found that HSF-1 expression significantly induced *Slug* promoter activity (Figure 3c) and expression (Figure 3d), respectively.

To determine whether the putative HSEs are essential for HSF-1-mediated Slug expression, we created two mutant promoters, each with mutations at two of the four putative sites, in order to destroy the three tandem repeats required for binding to HSF-1 trimers (Figure 3a). The analysis of the wild-type and mutant *Slug* promoter reporters showed that both mutant reporters lost the ability to respond to HRG induction, indicating the identified HSEs are important for HRG induction of *Slug* promoter activation (Figure 3e). Both mutant reporters also lost substantial responsiveness to HSF-1 (Figure 3f). Finally, we showed that levels of p-HSF-1 (S326) were directly associated with those of Slug in invasive breast carcinoma specimens (Figure 3g; $N=100$, $R=0.56$, $P<0.000001$). In summary, results in Figure 3 indicate that HSF-1 transcriptionally upregulates *Slug* gene expression in breast cancer cells.

HSF-1 knockdown prevents HRG-induced EMT and suppresses growth of breast cancer cells

To complement the HSF-1 upregulation results, we knocked down HSF-1 expression using siRNA to determine its impact on Slug expression and EMT. Our results showed that HSF-1 siRNA reduced the expression of Slug in BT-474 cells (Figure 4a). The reduction was accompanied with increased expression of E-cadherin and decreased expression of Vimentin. HSF-1 expression was effectively downregulated by HSF-1 siRNA. Moreover, HSF-1 knockdown partially prevented HRG-induced EMT of BT-474 cells, as indicated by the presence of both clustered epithelial-like cells and spindle-shaped mesenchymal-like cells (Figure 4b). Using the soft agar colony formation assay, we further found that HSF-1 siRNA reduced the propensity of BT-474 cells to grow in an anchorage-independent manner (Figure 4c).

To further examine whether HSF-1 knockdown will promote MET of mesenchymal post-EMT breast cancer cells, we used MDA-MB-231 cells, a mesenchymal breast cancer cell line. The results showed that HSF-1 siRNA reduced Slug expression, which was accompanied with increased E-cadherin expression and decreased Vimentin levels (Figure 4d). HSF-1 expression was effectively

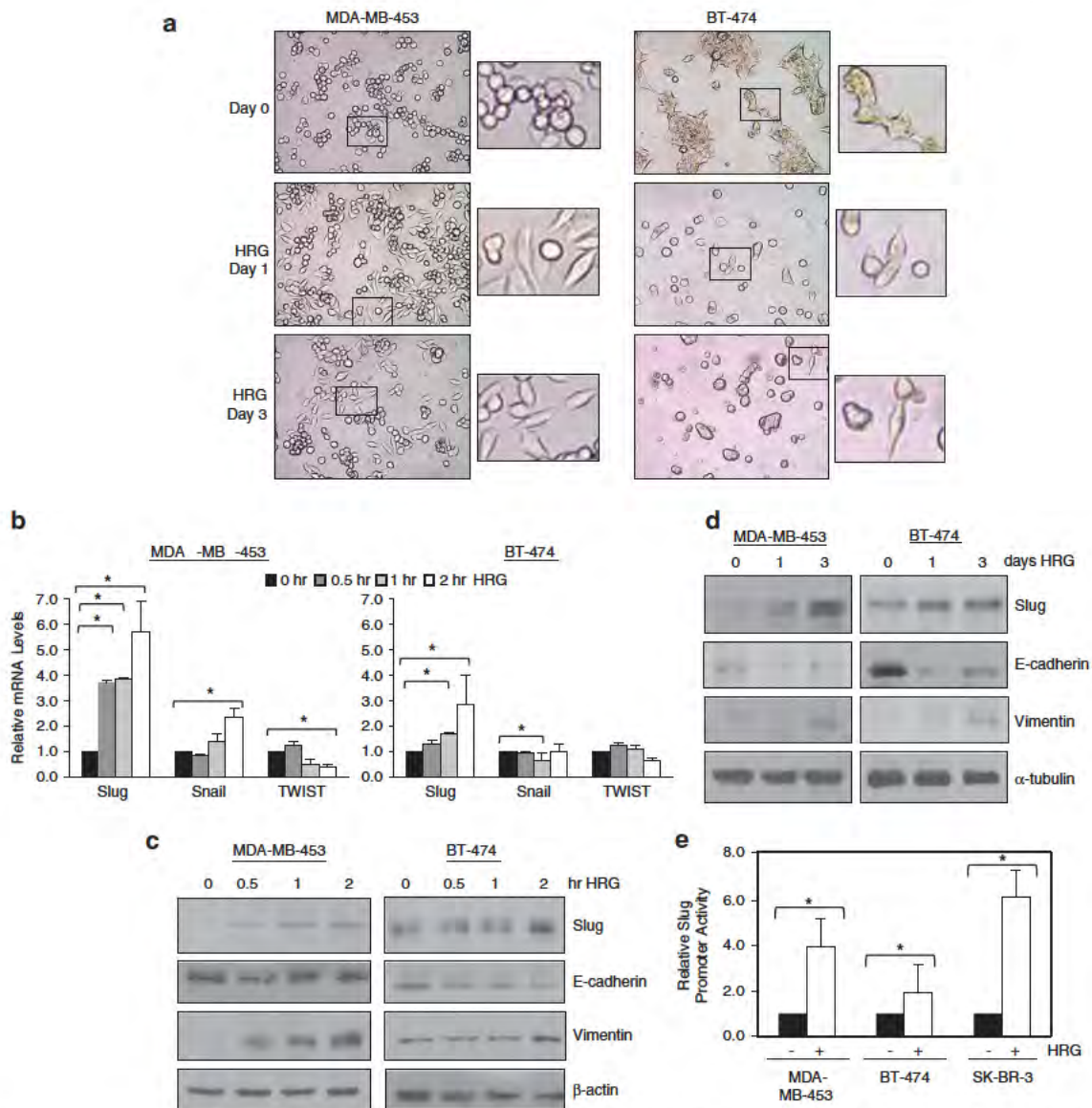


Figure 1. HRG induces EMT and Slug expression in HER2-amplified breast cancer cells. **(a)** HRG induced EMT of HER2-amplified breast cancer cells. MDA-MB-453 and BT-474 were serum-starved overnight (day 0) and then treated with HRG (100 ng/ml) for 1 or 3 days. Cultured cells were imaged using a phase-contrast microscope. Representative images are shown. **(b)** Slug transcripts were induced by HRG in HER2-amplified breast cancer cells. MDA-MB-453 and BT-474 were starved from serum overnight, treated with HRG (100 ng/ml) for 0 120 min and harvested for total RNA extraction and RT-qPCR. Levels of EMT regulators, Slug, Snail and TWIST were determined. * indicates P -values < 0.05. **(c, d)** Slug protein expression was induced by HRG in HER2-amplified breast cancer cells. MDA-MB-453 and BT-474 were starved from serum overnight, treated with HRG (100 ng/ml) for 0 120 min **(c)** or for 1 3 days **(d)**, and harvested for protein extraction and WB. Levels of Slug, E-cadherin (epithelial marker) and Vimentin (mesenchymal marker) were analyzed. **(e)** *Slug* promoter was significantly activated by HRG in breast cancer cells with HER2 amplification. MDA-MB-453, BT-474 and SK-BR-3 cells were transfected with a firefly luciferase reporter under the control of the human *Slug* promoter, serum-starved for 16 h and treated with HRG (100 ng/ml) for 2 h. Treated cells were lysed and subjected to luciferase assay. All cells were cotransfected with the Renilla luciferase expression vector, pRL-CMV, to control for transfection efficiency. The results were derived from at least three experiments. Student's t -test was conducted to compute P -values. * indicates P -values < 0.05.

downregulated by HSF-1 siRNA. However, morphological examination of these cells indicated modest changes indicative of MET (Figure 4e), which is likely due to the observation that knockdown of HSF-1 in MDA-MB-231 cells reduced cell viability. This speculation was consistent with the results of the soft agar colony formation assay, in which we found that HSF-1 siRNA significantly compromised the ability of MDA-MB-231 cells to colonize in an anchorage-independent manner (Figure 4f). Results presented in Figure 4 demonstrate that HSF-1 knockdown prevents HRG-induced EMT and suppresses anchorage-independent growth of breast cancer cells.

Concurrent activation of Akt and HSF-1 by HRG/HER2 in breast cancer cells

We further investigated the relationship between HRG/HER2 and HSF-1. It is known that activated HER2 leads to activation of a number of downstream signaling molecules, such as PI3K/Akt, p38, ERK, JNK and mTOR. Thus, we asked which of the HER2 downstream signaling molecule(s) are activated by HRG in concordance with HSF-1 activation. Our results indicated that HRG induced HSF-1 phosphorylation in both HER2-amplified breast cancer cell lines, MDA-MB-453 and BT-474. HSF-1 phosphorylation at S326 has been shown to activate HSF-1

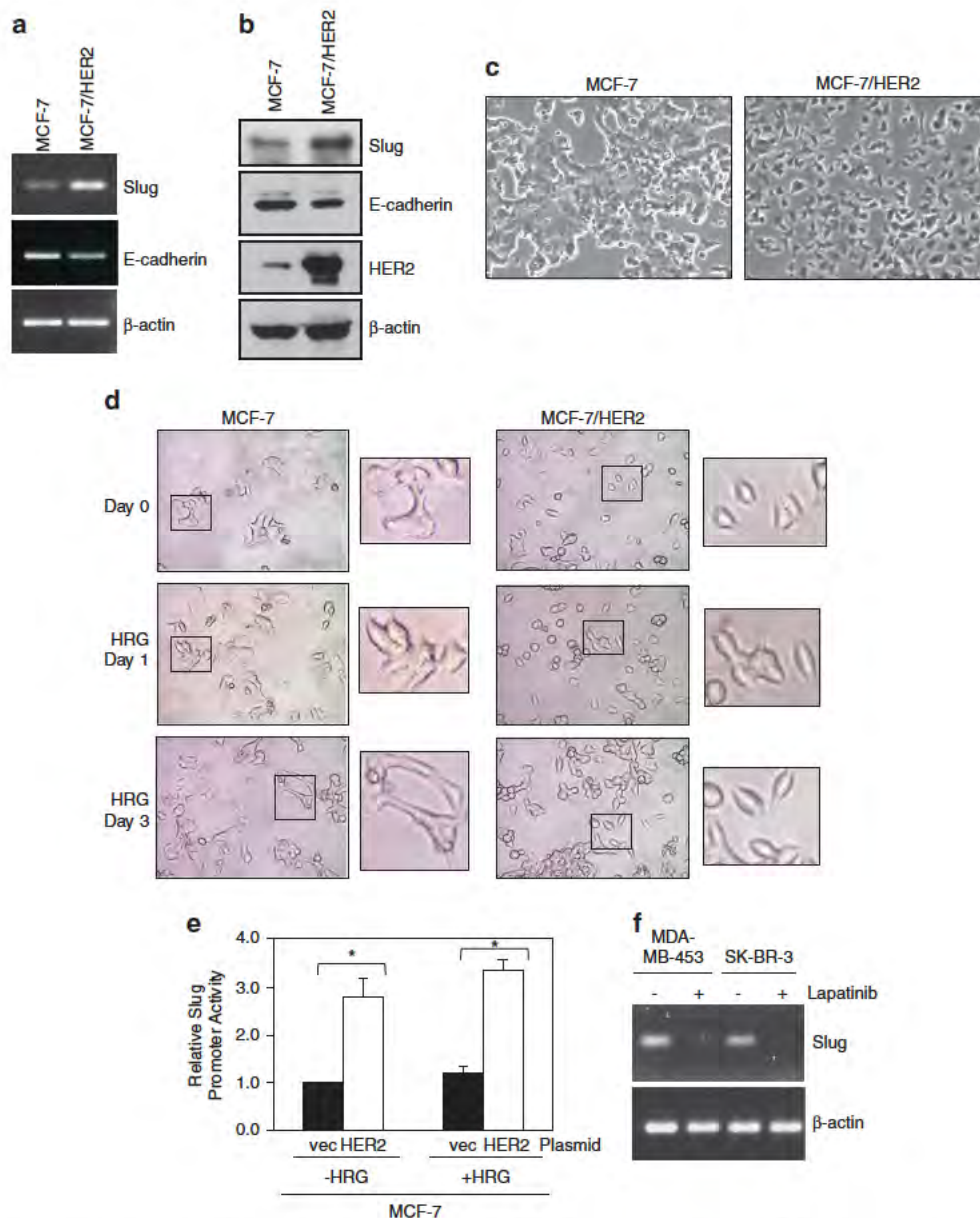


Figure 2. HER2 overexpression enhances Slug expression, leading to EMT in breast cancer cells. **(a, b)** Ectopic HER2 expression induced Slug expression in breast cancer cells. MCF-7 (with normal HER2 expression level) and MCF-7/HER2 (MCF-7 cells stably expressing ectopic HER2) were analyzed for Slug and E-cadherin expression using **(a)** RT-PCR and **(b)** WB. Enhanced HER2 expression in MCF-7/HER2 cells is indicated by WB. **(c, d)** Ectopic HER2 expression induced EMT-like morphology changes in breast cancer cells. **(c)** Both cell lines were cultured in normal growth condition with fetal calf serum. **(d)** Cells were serum-starved and treated with HRG (100 ng/ml) for 0–3 days. Representative images are shown. **(e)** Ectopic HER2 expression induced *Slug* promoter activity in breast cancer cells. MCF-7 cells (with normal HER2 levels) were transiently transfected with HER2 and the *Slug* luciferase reporter, serum-starved, and then stimulated with HRG (100 ng/ml) for 2 h. All cells were cotransfected with the Renilla luciferase expression vector, pRL-CMV, to control for transfection efficiency. The results were derived from at least three experiments, and analyzed by Student's *t*-test to compute *P*-values. **P*-values < 0.05. **(f)** Lapatinib, a small molecule HER2/EGFR inhibitor reduced *Slug* expression in HER2-amplified MDA-MB-453 and SK-BR-3 cells. Cells were pretreated with lapatinib (5 μM) for 24 h and subjected to total RNA extraction and RT-PCR for *Slug* transcript levels.

transcriptional activity.²⁰ As shown in Figure 5a, HSF-1 phosphorylation status is in concordance with Akt phosphorylation, but not with the other kinases we examined. As expected, *Slug* expression was enhanced by HRG in both the cell lines.

To confirm the results with concurrent activation of HSF-1 and Akt, we treated the two cell lines with HRG for 0–240 min and determined levels of p-HSF-1 (S326) and p-Akt (S473). The results showed that the kinetics for HSF-1 activation is in concordance with that for Akt (Figure 5b). Using MCF-7 and MCF-7/HER2 cell lines, we further observed that ectopic HER2 expression led to

increased activation of both HSF-1 and Akt in the cells (Figure 5c). Results in Figure 5 indicate, for the first time, that HSF-1 and Akt are concurrently activated by HRG/HER2 in breast cancer cells.

Akt directly interacts with and phosphorylates HSF-1 at S326
In light of the observation with concurrent activation of Akt and HSF-1, we asked whether these two proteins physically associated. Using IP followed by WB, we found that Akt constitutively interacted with HSF-1 independent of HRG treatment (Figure 6a).

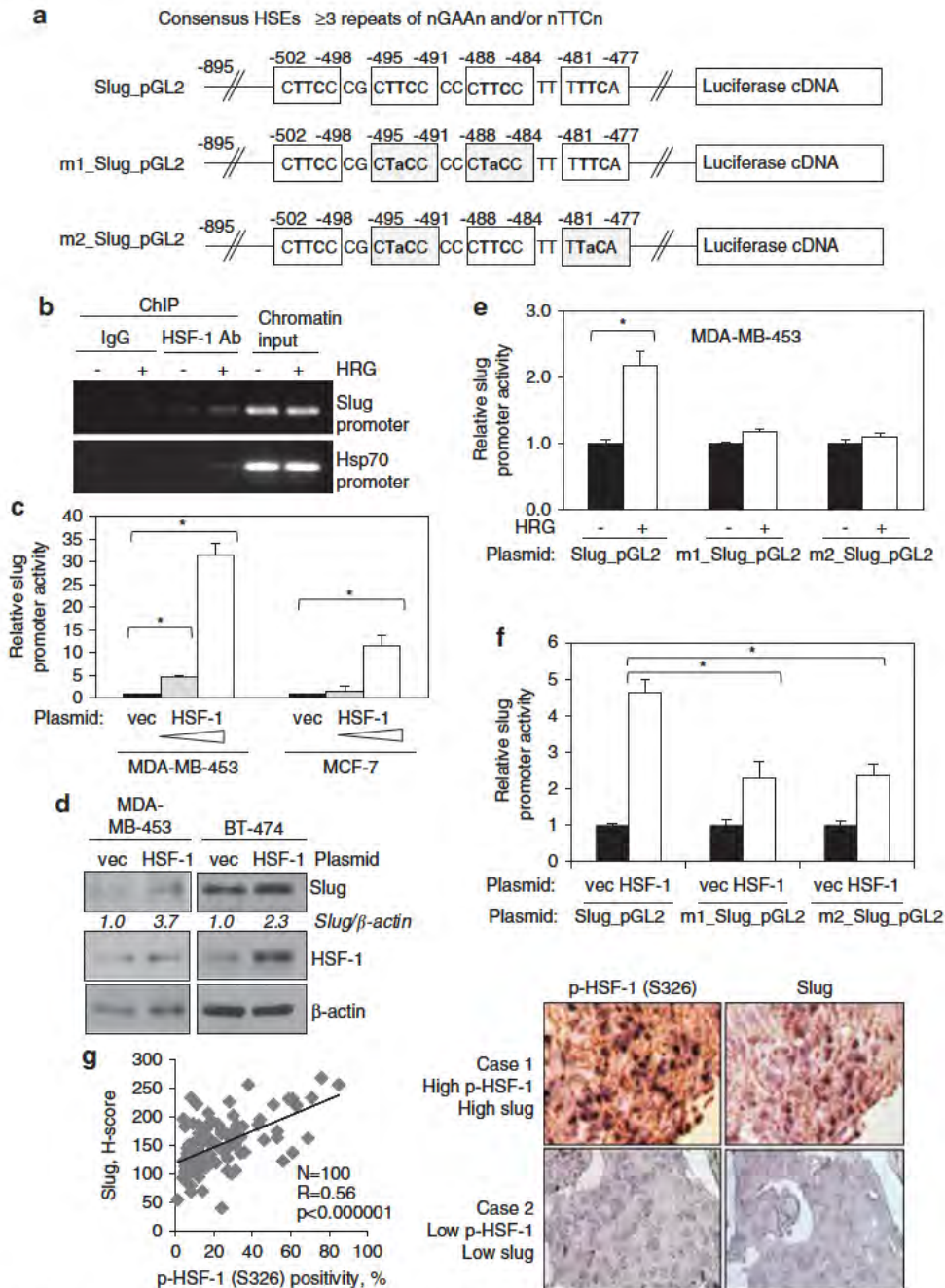


Figure 3. HSF-1 binds to and transactivates the *Slug* gene promoter, leading to *Slug* expression in breast cancer cells. **(a)** Identification of four putative HSEs within the human *Slug* gene promoter. TFSearch, a web-based search engine for transcription factor binding sites, was used to search for HSEs within the *Slug* promoter. Consensus HSEs are shown on the top. Structures of the wildtype *Slug* promoter reporter and two mutant reporters are shown. Each of the two mutant promoters contain mutations at two of the four putative sites, to destroy the three repeats required for binding to HSF-1 trimers. Clear boxes mark the putative HSEs. Lower case letters indicate mutated bases. **(b)** HSF-1 binds to the *Slug* promoter and the binding was enhanced by HRG. Serum-starved BT-474 cells treated with and without HRG (100 ng/ml) were used in the ChIP assay. HSF-1 antibody (Ab) was used to immunoprecipitate HSF-1, whereas IgG served as the negative controls. Chromatin input was used to control for loading. PCR was conducted to detect HSF-1 binding to *Slug* promoter and a known HSF-1 target gene, *Hsp70*. **(c)** Ectopic HSF-1 expression significantly induced *Slug* promoter activity. Cells were transfected with the control vector or the HSF-1 vector, and the *Slug* luciferase reporter for 48 h and subjected to luciferase assay. All cells were cotransfected with the Renilla luciferase expression vector, pRL-CMV, to control for transfection efficiency. The results represent means and s.d from at least three experiments, and were analyzed by Student's *t*-test to compute *P*-values. **P*-values < 0.05. **(d)** Ectopic HSF-1 expression enhanced *Slug* expression. BT-474 and MDA-MB-453 cells transfected with the control vector or the HSF-1 vector were analyzed by WB to determine *Slug* and HSF-1 expression levels. **(e, f)** Identified HSEs are important for HRG- and HSF-1-mediated induction of *Slug* promoter activation. MDA-MB-453 cells transfected with the wild-type and mutant slug reporters were serum-starved and treated with HRG for 2 h, and then subjected to luciferase assay. All cells were cotransfected with the Renilla luciferase reporter, pRL-CMV, to control for transfection efficiency. The results were derived from at least three experiments, and analyzed by Student's *t*-test to compute *P*-values. **P*-values < 0.05. **(g)** Levels of p-HSF-1 (S326) were directly associated with those of *Slug* in invasive breast carcinoma specimens. immunohistochemistry was conducted to analyze 100 invasive carcinomas. Linear regression was used to compute *R* and *P* values (*R* = 0.56, *P* < 0.000001). Right, representative images.

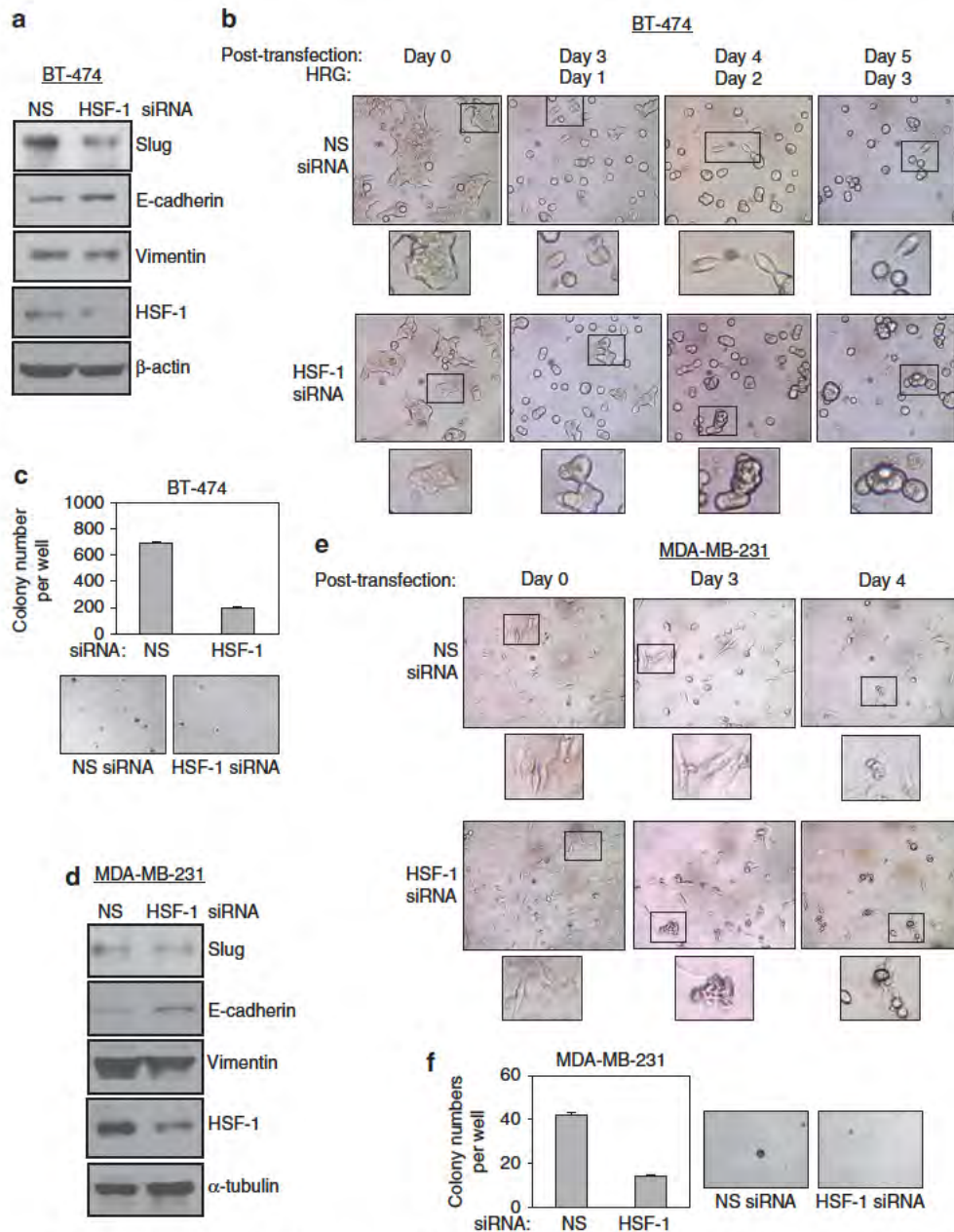


Figure 4. HSF-1 expression knockdown prevents HRG-induced EMT and suppresses growth of breast cancer cells. **(a)** HSF-1 siRNA reduced expression of Slug in epithelial BT-474 cells. BT-474 cells transfected with non-specific (NS) siRNA or Slug siRNA were analyzed by WB. **(b)** HSF-1 knockdown has in part prevented HRG-induced EMT. BT-474 cells transfected NS siRNA or Slug siRNA were serum-starved and treated with HRG (100 ng/ml) for 0 3 days. Representative images are shown. **(c)** HSF-1 siRNA reduced the propensity of BT-474 cells to grow in an anchorage-independent manner. BT-474 cells transfected NS siRNA or Slug siRNA were seeded into 6-well culture plates with agarose (2000 cells/well). After colonies were formed to the appropriate size, colonies were counted under a microscope. Data represent means and s.d. of three independent experiments. Student's *t*-test was performed to calculate *P*-values. **P*-values < 0.05. **(d)** HSF-1 siRNA reduced Slug expression in mesenchymal MDA-MB-231 cells. MDA-MB-231 cells transfected with NS siRNA or Slug siRNA were examined by WB. **(e)** HSF-1 knockdown resulted in modest MET of mesenchymal, post-EMT MDA-MB-231 cells, but induced significant cell death. MDA-MB-231 cells transfected NS siRNA or Slug siRNA imaged for 0 4 days post transfection. Representative images are shown. **(f)** HSF-1 siRNA reduced the ability of MDA-MB-231 cells to grow in an anchorage-independent manner. MDA-MB-231 cells transfected NS siRNA or Slug siRNA were seeded into six-well culture plates with agarose (2000 cells/well). After colonies have formed to the appropriate size, colonies were counted. Results represent means and s.d. of three independent experiments, and were analyzed by Student's *t*-test. **P*-values < 0.05.

Recombinant Akt directly interacted with recombinant HSF-1 (Figure 6b). Next, we investigated whether the Akt-HSF-1 interaction resulted in HSF-1 phosphorylation. Using the cell-free Akt kinase assay followed by WB, we showed that recombinant Akt directly phosphorylated recombinant GST-HSF-1 protein at S326 (Figure 6c). The same assay further showed that GST-HSF-1

protein was phosphorylated by Akt in time- and dose-dependent manners (Figures 6d-f).

We further investigated whether HSF-1 immunoprecipitated from MCF-7 cells was phosphorylated by recombinant Akt, and the results indicated that cellular HSF-1 was directly phosphorylated by Akt at S326 (Figure 6g). In agreement with these

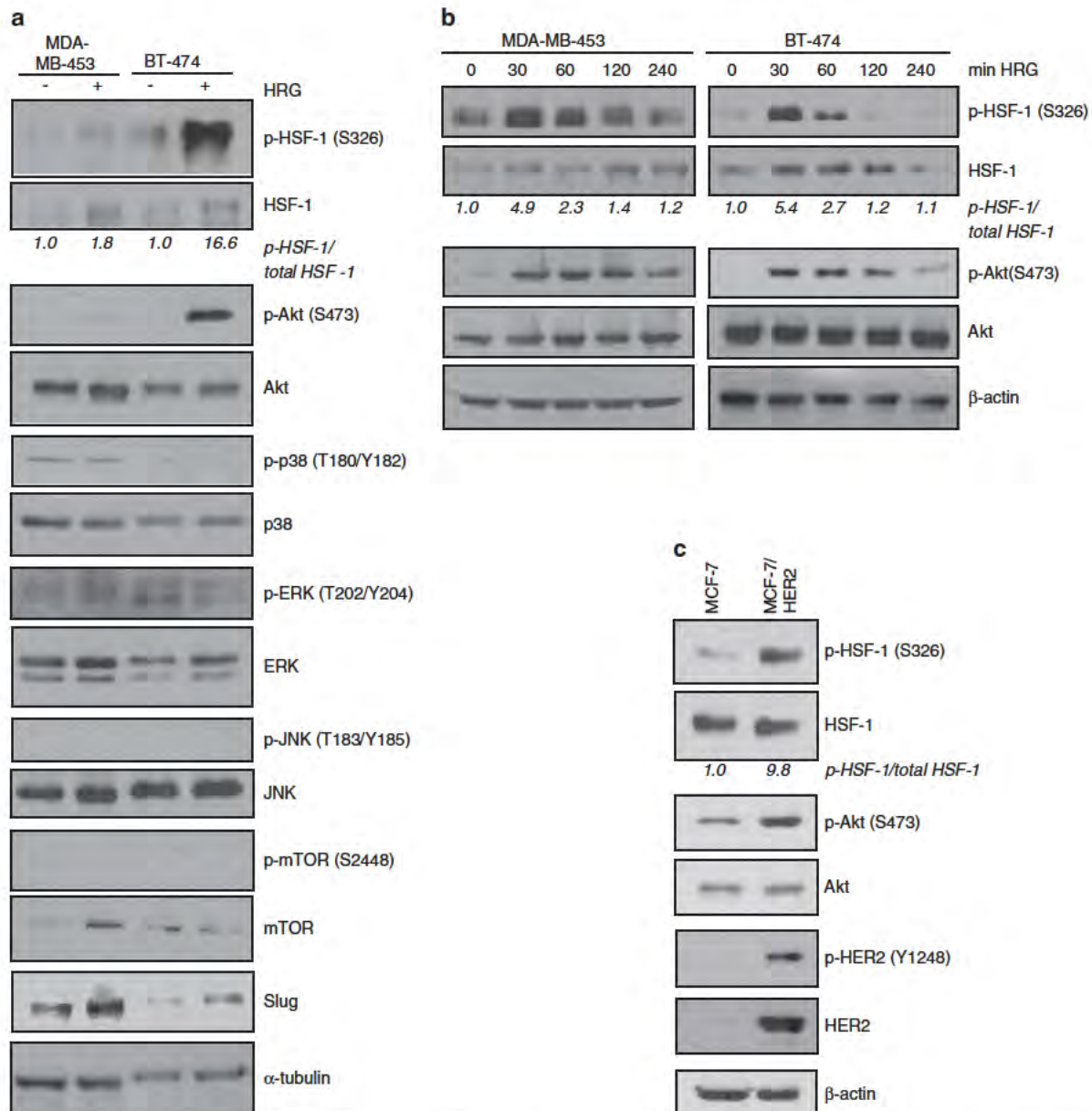


Figure 5. Concurrent activation of Akt and HSF-1 by HRG/HER2 in breast cancer cells. **(a)** HRG induced phosphorylation of both HSF-1 and Akt in HER2-amplified breast cancer cell lines. MDA-MB-453 and BT-474 cells were treated with and without HRG (100 ng/ml) for 2 h and the whole cell lysates were analyzed by WB for levels of HER2 downstream kinases and Slug. **(b)** Kinetics for HSF-1 activation was in concordance with that for Akt. The two cell lines were treated with HRG for 0–240 min and the whole cell lysates were analyzed by WB to determine levels of p-HSF-1 (S326) and p-Akt (S473). **(c)** Ectopic HER2 expression led to increased activation of both HSF-1 and Akt. MCF-7 and MCF-7/HER2 cell lines were examined using WB.

observations, we found that ectopic expression of CA-Akt significantly enhanced HSF-1 phosphorylation in MCF-7 cells (Figure 6h). Conversely, ectopic expression of dominant-negative Akt (DN-Akt) substantially reduced HSF-1 phosphorylation in MCF-7/HER2 and BT-474 cells (Figure 6h). Altogether, these results demonstrate, for the first time, that Akt directly interacts with HSF-1 and phosphorylates HSF-1 at S326.

Slug expression is suppressed by blocking the HER2–Akt–HSF-1 signaling axis; HSF-1 is essential for Akt-induced Slug expression. We further investigated the link between Slug and the HER2–Akt–HSF-1 signaling axis. We observed that small molecule inhibitors to PI3K (LY294002, LY) and HER2 (lapatinib, Lap) suppressed Slug

protein and transcription expression in BT-474 cells, as shown in Figures 7a and b respectively. Both LY294002 and lapatinib effectively inhibited phosphorylation of Akt and HSF-1 (Figure 7a), which is consistent with our earlier observation that Akt phosphorylates HSF-1. As positive controls for HSF-1 activity, we found that expression of *Hsp70*, a known HSF-1 target gene, was reduced in cells with lower levels of p-HSF-1 (Figure 7a). Using *Slug* promoter luciferase reporter assay, we further found that both LY294002 and Lapatinib blocked HRG induction of *Slug* promoter activity (Figure 7c).

HSF-1 and Akt siRNAs reduced Slug protein expression in BT-474 cells (Figure 7d). Consistent with this observation, HSF-1 and Akt siRNAs prevented HRG-induced activation of *Slug* promoter in BT-474 cells (Figure 7e). Ectopic expression of DN-

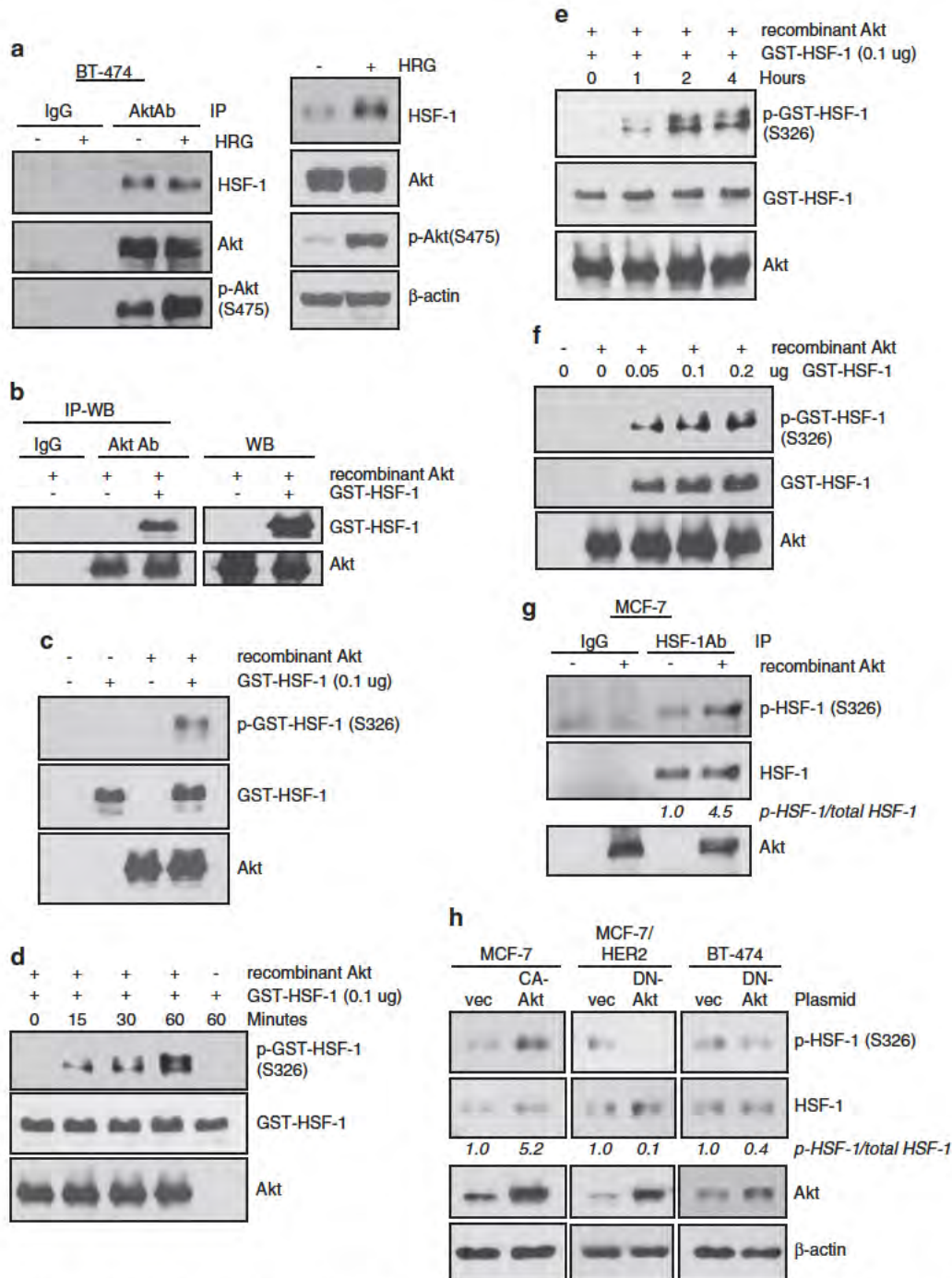


Figure 6. Akt directly interacts with and phosphorylates HSF-1 at S326. **(a)** Akt interacts with HSF-1 constitutively, independent of HRG treatment. IP WB were conducted using whole cell lysates extracted from BT-474 cells treated with and without HRG. An Akt Ab was used to immunoprecipitate Akt, whereas IgG was used as negative controls. WB results are shown in the right panel. **(b)** Recombinant Akt directly interacts with recombinant HSF-1. IP-WB was conducted. **(c)** Recombinant Akt directly phosphorylated recombinant HSF-1 protein at S326. Cell-free Akt kinase assay was conducted followed by WB. **(d, e)** HSF-1 protein was phosphorylated by Akt in a time-dependent manner. **(f)** HSF-1 protein was phosphorylated by Akt in a dose-dependent manner. **(g)** Cellular HSF-1 was directly phosphorylated by Akt at S326. HSF-1 immunoprecipitated from MCF-7 cells was subjected to the cell-free Akt kinase assay followed by WB. **(h)** Ectopic expression of constitutively activated Akt (CA-Akt) significantly enhanced HSF-1 phosphorylation, whereas ectopic expression of DN-Akt substantially reduced HSF-1 phosphorylation. Transfected cells were lysed and subjected to WB.

Akt blocked HRG-induced Slug protein expression and HSF-1 activation (Figure 7f). Both Akt siRNA and DN-Akt inhibited Slug transcription in BT-474 cells (Figure 7g). DN-Akt reduced activity of the *Slug* promoter in MCF-7/HER2 cells, whereas constitutively activated Akt (CA-Akt) enhanced its activity in MCF-7 cells

(Figure 7h). Finally, we observed that HSF-1 siRNA significantly reduced the ability of CA-Akt to induce *Slug* promoter activity (Figure 7i; left panel) and Slug protein expression (right panel), indicating that HSF-1 has an essential role in Akt-induced Slug expression. Altogether, results presented in Figure 7 indicate that

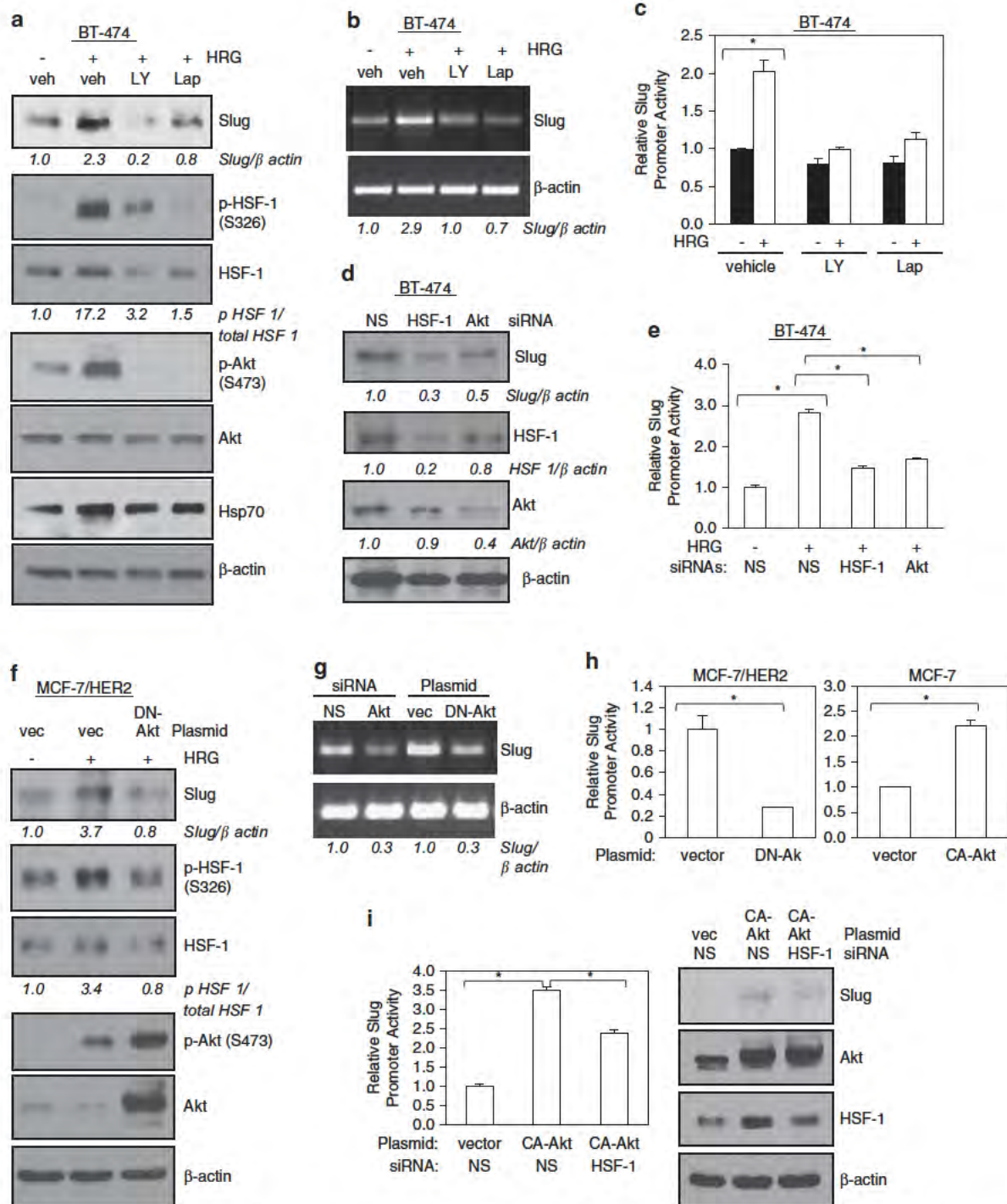


Figure 7. Slug expression is suppressed by blocking the HER2-Akt-HSF-1 signaling axis; HSF-1 is essential for Akt-induced Slug expression. In luciferase assays (**b**, **d** and **e**), three independent experiments were performed to derive means and s.d. All cells were cotransfected with the Renilla luciferase reporter, pRL-CMV, to control for transfection efficiency. The results were analyzed by Student's *t*-test to compute *P*-values. **P*-values < 0.05. (**a**, **b**) Small molecule inhibitors to PI3K/Akt (LY294002; LY; 50 μ M) and HER2 (Lapatinib; Lap; 25 μ M) pretreatment for 1–2 h suppressed HRG-induced Slug expression in BT-474 cells. In panel (**a**), WB was conducted. Hsp70 served as positive controls for HSF-1 activity. HRG exposure was for 1 h at 100 ng/ml. In panel (**b**), total RNA was analyzed by RT-PCR. Veh, vehicle (1% DMSO). (**c**) Both LY294002 and Lapatinib blocked HRG induction of *Slug* promoter activity. BT-474 cells transfected with the *Slug* luciferase reporter were serum-starved, treated with vehicle or indicated inhibitor (50 μ M LY294002 or 25 μ M Lapatinib) for 2 h, and then treated with and without HRG for 4 h. Harvested cells were lysed and subjected to luciferase assay. (**d**) HSF-1 and Akt siRNAs reduced *Slug* expression in BT-474 cells, as shown by WB. (**e**) HSF-1 and Akt siRNAs prevented HRG-induced activation of *Slug* promoter in BT-474 cells. BT-474 cells cotransfected with siRNA and the *Slug* luciferase reporter were serum-starved and treated with HRG for 4 h, and then subjected to luciferase assay. (**f**) DN-Akt blocked HRG-induced *Slug* expression and HSF-1 activation in MCF-7/HER2 cells, as shown by WB. (**g**) Akt siRNA and DN-Akt inhibited *Slug* transcription in BT-474 cells as shown by RT-PCR. (**h**) DN-Akt reduced activity of the *Slug* promoter in MCF-7/HER2 cells, whereas CA-Akt enhanced its activity in MCF-7 cells. Luciferase assay was conducted to measure *Slug* promoter activity. (**i**) HSF-1 is essential for CA-Akt-induced *Slug* expression. MCF-7 cells were used. Left, luciferase assay. Right, WB.

a novel HER2-Akt-HSF-1 signaling axis positively regulates expression of the EMT-promoting transcription factor Slug, and that HSF-1 plays an essential role in Akt-induced Slug expression.

DISCUSSION

Slug participates in several physiological and pathological processes from development to re-epithelialization during wound healing, and to EMT and tumor progression.⁷ However, the regulation of Slug expression is still not well understood. In this study, we provide evidence uncovering a novel HER2-Akt-HSF-1 signaling axis that acts to promote Slug expression and EMT whereby HSF-1 directly binds to the *Slug* promoter to induce transcription.

Our results indicate HSF-1 directly upregulates Slug transcription to promote EMT. This novel observation is in agreement with a recent study suggesting an association between HSF-1 and Slug expression as HER2⁺HSF-1^{+/+} mice showed greater Slug expression in mammary tumors than HER2⁺HSF-1^{+/-} mice, which was also accompanied with reduced E-cadherin.²⁵ We further confirmed this *in vitro* observation *in vivo* as we found a strong correlation between active HSF-1 and Slug expression in a sample of 100 invasive breast carcinoma specimens. These experimental findings led us to propose a model whereby overexpression of HER2 activates the PI3K-Akt pathway, which leads to HSF-1 activation/phosphorylation that upregulates Slug expression and promotes EMT of breast cancer cells.

Our results demonstrated that HER2-induced Akt activation leads to Akt phosphorylation of HSF-1 at S326, which results in enhanced HSF-1 transcriptional activity. Interestingly, HRG has been shown to upregulate expression of HSF-1,²⁶ although the underlying mechanisms are still unclear. It has also been observed that activation of HER2 can upregulate HSF-1 expression whereas loss of HSF-1 reduces HER2-driven tumorigenesis.^{26,27} On the basis of these observations, the relationship between HER2 and HSF-1 appears to be complex warranting further investigations.

Our discovery of HSF-1 being a target of Akt is an important finding. Akt is frequently dysregulated in human cancers and is consequently an important target for cancer therapeutics. Although Akt-targeted therapy has shown promising clinical results, identification of new Akt downstream effectors will help us develop new biomarkers for the aberrant Akt pathway and potentially, novel drug targets for tumors with hyperactive Akt signaling. In light of these notions, the HSF-1 pathway could serve as a new biomarker and a novel therapeutic target for human cancers with high Akt activity, such as, those with PTEN loss, constitutively activated PI3K, or with overexpression of receptor tyrosine kinases, HER2 and EGFR.

In addition to Akt, several other Ser/Thr kinases have been shown to phosphorylate HSF-1 to regulate HSF-1 transcriptional activity, stability and intracellular trafficking.²⁸ Phosphorylation of HSF-1 at S326 was reported to be a key step in the ability of HSF-1 to regulate gene expression in response to heat stress.²⁰ However, to date, little evidence has been provided as to what kinases mediate phosphorylation at S326. In this study, we provide conclusive evidence demonstrating that Akt can directly phosphorylate HSF-1 on S326. Interestingly, it was recently reported that mTOR could phosphorylate HSF-1 on S326 in HeLa cells under proteotoxic stress.²⁹ However, it is worth noting that we did not observe detectable activation of mTOR in the context of HER2 activation in the breast cancer cells we examined. Although Akt has been shown to activate mTOR,³⁰ we did not observe substantial involvement of mTOR in the Akt-HSF-1-Slug-mediated promotion of EMT in the HER2-amplified breast cancer cells that we have examined. These differences could be explained by several potential mechanisms. First, mTOR-induced phosphorylation of HSF-1 may require mTOR activation from increased cell stress via heat stress or exposure to noxious substances as was observed in a previous study.²⁹ Second,

Akt may act as the predominant regulator of HSF-1 over mTOR in cancer cells with HER2 amplification, as suggested by the data presented in this study. Third, the choice of Akt or mTOR for HSF-1 S326 phosphorylation may differ in a cancer- and/or cell-type dependent manner. Finally, it is likely that HSF-1 S326 residue can be targeted by other Ser/Thr kinases besides Akt and mTOR, which may influence the accessibility of HSF-1 by Akt and/or mTOR.

Our results showed the transcriptional activity of HSF-1 can be activated by the HER2-Akt signaling axis independent of heat shock. This is in agreement with emerging evidence suggesting that HSF-1 can induce a transcriptional program independent of the heat shock program.²³ Importantly, our results further linked HSF-1 to EMT, independent of heat shock, which is clearly a novel, important observation. This observation plus previous reports showing that HSF-1 promotes cell cycle progression and antagonizes apoptosis,²³ together, could help define HSF-1 as a mediator of aggressive tumor phenotypes. These observations also raise the possibility that HSF-1 may have wide-ranging oncogenic functions, thus warranting future in-depth investigations. In support of this possibility, our data suggest that HSF-1 may support HER2-mediated breast cancer cell growth (Figures 4c and f). This interesting observation is in accordance with several earlier studies.^{25,27,31} We speculate that the effects of HSF-1 on tumor growth and progression are likely due to a combination of the effects of HSF-1 on the induction of the heat shock program,²² the induction of genes unrelated to heat shock that support malignant growth²³ and the promotion of EMT as indicated by our results, all three of which can support cell survival and resistance to therapy.

In summary, our study uncovered a novel role for HSF-1 in promoting EMT via direct upregulation of Slug in HER2-amplified breast cancer cells independent of heat shock. Our data also revealed, for the first time, that Akt can directly phosphorylate and activate HSF-1 to induce the expression of Slug. Understanding other post-translational modifications of HSF-1, along with which proteins mediate those modifications, and what role they have in tumor progression, will further elucidate the role that HSF-1 plays in the progression of cancer. It is becoming increasingly apparent that HSF-1 can regulate a vast array of genes outside of the heat shock program. Identification and functional investigations into these HSF-1-targeted genes and cellular mechanisms are certainly warranted to fully understand the role of HSF-1 in cancer. Investigation into the impact of inhibiting HSF-1 is also needed. There are several compounds that have been developed and observed to inhibit HSF-1, including, KRIBB11,³² KNK437³³ and triptolide.³⁴ However, the potential therapeutic impact of these compounds in HER2-positive breast cancer models is largely unknown. Thus, there is much left to understand regarding the role of HSF-1 in cancer as evidence continues to suggest that HSF-1 has a much broader biological function than mediating the cellular heat shock response.

MATERIALS AND METHODS

Reagents, cell lines and primary specimens

All chemicals were purchased from Sigma (St Louis, MO, USA) unless otherwise stated. All human breast cancer cell lines used in this study were obtained from ATCC (Manassas, VA, USA), and maintained according to ATCC's instructions. Tissue microarray slides (BC081116) were purchased from US Biomax (Rockville, MD, USA) that contained 100 invasive breast carcinomas. MCF 7/HER2 stable transfectant cell line was a generous gift from Dr Mien Chie Hung at MD Anderson Cancer Center and was maintained in MEM medium supplemented with 10% FBS, 1 mM sodium pyruvate, 0.1 mM non essential amino acids, 10 µg/ml bovine insulin and 350 µg/ml G418. All siRNAs were ordered from Bioneer (Alameda, CA, USA). The siRNA sequences are 5' CCUACGCCACCACUUUCGU(dTdT) 3' (nonspecific control), 5' GACAACCGCAUCCAGACU(dTdT) 3' (Akt) and 5' GAGAU CUAUAAACAGACAG(dTdT) 3' (HSF 1). Lapatinib was purchased from LC Laboratories (Woburn, MA, USA). LY294002 was obtained from Cayman Chemical (Ann Arbor, MI, USA).

RT-PCR and qPCR

Total RNA isolation and RT were conducted using SV Total RNA Isolation System (Promega, Madison, WI, USA) and Superscript II First Strand cDNA synthesis system (Invitrogen, Grand Island, NY, USA), retrospectively. The forward and reverse primers used for regular PCR were: 5' TGATGAAGAGGAAAGACTACAG 3' and 5' GCTCACATATTCCTTGTCACA G 3' (Slug), 5' GGAGTCCGAGCTTACAG 3' and 5' TCTGGAGGACCTG GTAGAGG 3' (TWIST), 5' CGAAAGGCCTCAACTGCAAA 3' and 5' ACTG GTACTTCTTGACATCTG 3' (Snail), 5' GTCTGGGAGAGTGAATTTT 3' and 5' ATTCAGCGTGACTTTGGTGGGA 3' (E cadherin), 5' ACCAACGAGAAGGTGGA GCTG 3' and 5' TCGTTGGTAGCTGGTCCACC 3' (Vimentin), and 5' GGCGG CACCACCATGTACCC 3' and 5' AGGGGCCGGACTCGTCACTACT 3' (β actin). Primers used in qPCR included 5' TCGACCCACACATTACCTT 3' and 5' TG ACCTGTCTGCAAAATGCTC 3' (Slug), 5' CTCAGCTACGCTTCTCG 3' and 5' AC TGCCATTTTCTCTCTCTG 3' (TWIST), 5' GGAAGCCTAACTACAGCGAG 3' and 5' CAGAGTCCAGATGAGCATTG 3' (Snail), and 5' ACCCTGAAGTAC CCCAT 3' and 5' CCACAGCAGCTGATTGT 3' (β actin). In qPCR, β actin gene was used as normalization controls and all experiments were carried out in triplicates. qPCR master mix was purchased from Apex BioResearch Products.

Western Blotting (WB) and immunoprecipitation (IP)

This was performed as described previously.^{35,36} Antibodies used in WB included mouse monoclonal antibodies against β actin (Sigma), α tubulin (Sigma), E cadherin (610404, BD, Franklin Lakes, NJ, USA), p HSF 1/S326 (ab76076, Epitomics/Abcam, Cambridge, MA, USA), p JNK/S63/73 (sc 6254, Santa Cruz, Biotech., Santa Cruz, CA, USA), and rabbit antibodies against Slug (AP2053a, Abgent, Atlanta, GA, USA), HSF 1 (4356, Cell Signaling, Danvers, MA, USA), Hsp70 (4876, Cell Signaling), p38 (9212, Cell Signaling), p p38/T180/Y182 (4511, Cell Signaling), pERK/T202/Y204 (9109, Cell Signaling), Akt/pan (4691, Cell Signaling), p Akt/S473 (4060, Cell Signaling), mTOR (2983, Cell Signaling), p mTOR/S2448 (5536, Cell Signaling), JNK (sc 571, Santa Cruz), HER2 (2165, Cell Signaling), p HER2/Y1278 (2247, Cell Signaling). Rabbit polyclonal HSF 1 antibody used in IP and ChIP assay was from Cell signaling (4356).

Plasmids, transfection and luciferase assay

CA Akt and DN Akt constructs were generous gifts from Dr Mong Hong Lee at MD Anderson Cancer Center.³⁷ The FLAG HSF 1 plasmid was purchased from Addgene (ID 32537, Cambridge MA, USA), which was originally established by Dr Stuart Calderwood.³⁸ Slug pGL2 luciferase reporter construct was obtained from Addgene (ID 31695), originally cloned by Dr Paul Wade.³⁹ HER2 WT plasmid was obtained from Addgene (ID 16257), which was generated by Dr Mien Chie Hung.⁴⁰ All transfections were performed with cells in exponential growth using lipofectamine 2000 (Invitrogen) or XtremeGene HP (Roche, Indianapolis, IN, USA). A Renilla luciferase expression vector, pRL CMV was used to control for transfection efficiency. 48 hr after transfection, the cells were lysed and luciferase activity was measured using the Firefly and Renilla Luciferase Assay Kit (Biotium, Hayward, CA, USA), as we previously described.^{10,35,36,41} Relative promoter activity was computed by normalizing the Firefly luciferase activity against that of the Renilla luciferase.

Mutagenesis

Generation of mutant *Slug* promoter reporter vectors was carried out using a QuikChange Site Directed Mutagenesis kit (Agilent Technologies, Santa Clara, CA, USA) as per the manufacturer's instructions. Primers used for mutagenesis were: 5' CCTTTGTCTTCCCGCTACCCCTACCTTTTCAAAAAGC 3' and 5' GCTTTTAAAAAGGTAGGGGTAGCGGGAAGACAAAAGG 3' (m1 Slug pGL2) and 5' GTCTTCCCGCTACCCCTTCTTTTACAAAAGCCAAG 3' and 5' CTTGCTTTTGTAAAAGGAAGGGGTAGCGGGAAGAC 3' (m2 Slug pGL2) Mutation was confirmed by sequencing.

ChIP Assay to determine binding of HSF-1 to the *Slug* gene promoter

This was performed using a ChIP Assay Kit (Upstate, Billerica, MA, USA) as we described previously.⁴¹ Rabbit polyclonal HSF 1 antibody was used (4356, Cell Signaling). DNA sequences for the primers used to amplify the Slug promoter are 5' TGGAAGTGGCATCTGGAGAG 3' (forward) and 5' GC TAACACGGTGACATGAGT 3' (reverse), and for the Hsp70 promoter, 5' CA CTCCCCCTCTCTCAG 3' (forward) and 5' TTCCCTTCTGAGCCAATCAC 3' (reverse).

Immunohistochemistry (IHC)

This was conducted as we described previously.⁴² The slides were incubated with p HSF 1 (S326) (Abcam) and Slug (Abgent) antibodies. Histologic scores (H Scores) were computed from both percent positivity (A%, A 1 100) and intensity (B 0 3) using the equation, H Score A \times B.

Determination of anchorage-independent growth by colony formation assays

Clonogenic growth assays were performed in six well cell culture plates with 2000 cells per well, as we previously described.^{41,43} All wells were precoated with 0.5% agarose at the bottom layer whereas the top layer is consisted of 0.3% agarose and tumor cells. After 6–8 weeks, colonies were stained with crystal violet blue solution (Sigma) for 1 h and counted under a microscope. Triplicate wells were used for each cell line and three independent experiments were performed.

Akt kinase assay

Recombinant AKT and recombinant HSF 1 were purchased from Sigma. Indicated amounts of recombinant GST HSF 1 (0.1–0.4 μ g) was incubated with or without 0.1 μ g recombinant AKT for up to 60 min at 37 °C in the presence of ATP in kinase assay buffer (20 mM HEPES, 10 mM MgCl₂, 10 mM MnCl₂, 1 mM DTT). Samples were then boiled and subjected to SDS PAGE and WB with indicated antibodies.

Statistical analysis

Student's *t* test and linear regression analysis were performed using STATISTICA (StatSoft Inc., Tulsa, OK, USA) and Microsoft Excel, as we previously described.^{35,42,44}

CONFLICT OF INTEREST

The authors declare no conflict of interest.

ACKNOWLEDGEMENTS

We are thankful to Dr Mong Hong Lee at MD Anderson Cancer Center who provided CA Akt and DN Akt constructs. This study was supported by the NIH grant K01 CA118423, and W81XWH 11 1 0600 from the US Department of Defense, the Beez Foundation and the Intramural Division of Surgical Sciences grants, Dani P. Bolognesi PhD Award and Clarence Gardner PhD Award.

REFERENCES

- 1 Thierry JP, Aclouque H, Huang RY, Nieto MA. Epithelial mesenchymal transitions in development and disease. *Cell* 2009; **139**: 871–890.
- 2 De Craene B, Bex G. Regulatory networks defining EMT during cancer initiation and progression. *Nat Rev Cancer* 2013; **13**: 97–110.
- 3 Rhim AD, Mirek ET, Aiello NM, Maitra A, Bailey JM, McAllister F *et al*. EMT and dissemination precede pancreatic tumor formation. *Cell* 2012; **148**: 349–361.
- 4 Trimboli AJ, Fukino K, de Bruin A, Wei G, Shen L, Tanner SM *et al*. Direct evidence for epithelial mesenchymal transitions in breast cancer. *Cancer Res* 2008; **68**: 937–945.
- 5 Hajra KM, Chen DY, Fearon ER. The SLUG zinc finger protein represses E cadherin in breast cancer. *Cancer Res* 2002; **62**: 1613–1618.
- 6 Savagner P, Yamada KM, Thierry JP. The zinc finger protein slug causes desmosome dissociation, an initial and necessary step for growth factor induced epithelial mesenchymal transition. *J Cell Biol* 1997; **137**: 1403–1419.
- 7 Cobaleda C, Perez Caro M, Vicente Duenas C, Sanchez Garcia I. Function of the zinc finger transcription factor SNAI2 in cancer and development. *Annu Rev Genet* 2007; **41**: 41–61.
- 8 Battle E, Sancho E, Franci C, Dominguez D, Monfar M, Baulida J *et al*. The transcription factor snail is a repressor of E cadherin gene expression in epithelial tumour cells. *Nat Cell Biol* 2000; **2**: 84–89.
- 9 Cano A, Perez Moreno MA, Rodrigo I, Locascio A, Blanco MJ, del Barrio MG *et al*. The transcription factor snail controls epithelial mesenchymal transitions by repressing E cadherin expression. *Nat Cell Biol* 2000; **2**: 76–83.
- 10 Lo HW, Hsu SC, Xia W, Cao X, Shih JY, Wei Y *et al*. Epidermal growth factor receptor cooperates with signal transducer and activator of transcription 3 to induce epithelial mesenchymal transition in cancer cells via up regulation of TWIST gene expression. *Cancer Res* 2007; **67**: 9066–9076.

- 11 Yang J, Mani SA, Donaher JL, Ramaswamy S, Itzykson RA, Come C *et al*. Twist, a master regulator of morphogenesis, plays an essential role in tumor metastasis. *Cell* 2004; **117**: 927–939.
- 12 Hynes NE, MacDonald G. ErbB receptors and signaling pathways in cancer. *Curr Opin Cell Biol* 2009; **21**: 177–184.
- 13 Slamon DJ, Clark GM, Wong SG, Levin WJ, Ullrich A, McGuire WL. Human breast cancer: correlation of relapse and survival with amplification of the HER2/neu oncogene. *Science* 1987; **235**: 177–182.
- 14 Slamon DJ, Godolphin W, Jones LA, Holt JA, Wong SG, Keith DE *et al*. Studies of the HER2/neu proto oncogene in human breast and ovarian cancer. *Science* 1989; **244**: 707–712.
- 15 Yarden Y, Sliwkowski MX. Untangling the ErbB signalling network. *Nat Rev Mol Cell Biol* 2001; **2**: 127–137.
- 16 Ursini Siegel J, Schade B, Cardiff RD, Muller WJ. Insights from transgenic mouse models of ERBB2 induced breast cancer. *Nat Rev Cancer* 2007; **7**: 389–397.
- 17 Cheng JC, Qiu X, Chang HM, Leung PC. HER2 mediates epidermal growth factor induced down regulation of E cadherin in human ovarian cancer cells. *Biochem Biophys Res Commun* 2013; **434**: 81–86.
- 18 D'Souza B, Taylor Papadimitriou J. Overexpression of ERBB2 in human mammary epithelial cells signals inhibition of transcription of the E cadherin gene. *Proc Natl Acad Sci USA* 1994; **91**: 7202–7206.
- 19 Giordano A, Gao H, Anfossi S, Cohen E, Mego M, Lee BN *et al*. Epithelial mesenchymal transition and stem cell markers in patients with HER2 positive metastatic breast cancer. *Mol Cancer Ther* 2012; **11**: 2526–2534.
- 20 Guettouche T, Boellmann F, Lane WS, Voellmy R. Analysis of phosphorylation of human heat shock factor 1 in cells experiencing a stress. *BMC Biochem* 2005; **6**: 4.
- 21 Kroeger PE, Morimoto RL. Selection of new HSF1 and HSF2 DNA binding sites reveals difference in trimer cooperativity. *Mol Cell Biol* 1994; **14**: 7592–7603.
- 22 Cocca DR, Arrigo AP, Calderwood SK. Heat shock proteins and heat shock factor 1 in carcinogenesis and tumor development: an update. *Arch Toxicol* 2013; **87**: 19–48.
- 23 Mendillo ML, Santagata S, Koeva M, Bell GW, Hu R, Tamimi RM *et al*. HSF1 drives a transcriptional program distinct from heat shock to support highly malignant human cancers. *Cell* 2012; **150**: 549–562.
- 24 Santagata S, Hu R, Lin NU, Mendillo ML, Collins LC, Hankinson SE *et al*. High levels of nuclear heat shock factor 1 (HSF1) are associated with poor prognosis in breast cancer. *Proc Natl Acad Sci USA* 2011; **108**: 18378–18383.
- 25 Xi C, Hu Y, Buckhaults P, Moskophidis D, Mivechi NF. Heat shock factor Hsf1 cooperates with ErbB2 (Her2/Neu) protein to promote mammary tumorigenesis and metastasis. *J Biol Chem* 2012; **287**: 35646–35657.
- 26 Khaleque MA, Bharti A, Sawyer D, Gong J, Benjamin IJ, Stevenson MA *et al*. Induction of heat shock proteins by heregulin beta1 leads to protection from apoptosis and anchorage independent growth. *Oncogene* 2005; **24**: 6564–6573.
- 27 Meng L, Gabai VL, Sherman MY. Heat shock transcription factor HSF1 has a critical role in human epidermal growth factor receptor 2 induced cellular transformation and tumorigenesis. *Oncogene* 2010; **29**: 5204–5213.
- 28 Ankar J, Sistonen L. Regulation of HSF1 function in the heat stress response: implications in aging and disease. *Annu Rev Biochem* 2011; **80**: 1089–1115.
- 29 Chou SD, Prince T, Gong J, Calderwood SK. mTOR is essential for the proteotoxic stress response, HSF1 activation and heat shock protein synthesis. *PLoS One* 2012; **7**: e39679.
- 30 Sekulic A, Hudson CC, Homme JL, Yin P, Otterness DM, Kamitz LM *et al*. A direct linkage between the phosphoinositide 3 kinase AKT signaling pathway and the mammalian target of rapamycin in mitogen stimulated and transformed cells. *Cancer Res* 2000; **60**: 3504–3513.
- 31 Gabai VL, Meng L, Kim G, Mills TA, Benjamin IJ, Sherman MY. Heat shock transcription factor Hsf1 is involved in tumor progression via regulation of hypoxia inducible factor 1 and RNA binding protein HuR. *Mol Cell Biol* 2012; **32**: 929–940.
- 32 Yoon YJ, Kim JA, Shin KD, Shin DS, Han YM, Lee YJ *et al*. KRIBB11 inhibits HSP70 synthesis through inhibition of heat shock factor 1 function by impairing the recruitment of positive transcription elongation factor b to the hsp70 promoter. *J Biol Chem* 2011; **286**: 1737–1747.
- 33 Ohnishi K, Takahashi A, Yokota S, Ohnishi T. Effects of a heat shock protein inhibitor KNK437 on heat sensitivity and heat tolerance in human squamous cell carcinoma cell lines differing in p53 status. *Int J Radiat Biol* 2004; **80**: 607–614.
- 34 Westerheide SD, Kawahara TL, Orton K, Morimoto RL. Triptolide, an inhibitor of the human heat shock response that enhances stress induced cell death. *J Biol Chem* 2006; **281**: 9616–9622.
- 35 Lo HW, Cao X, Zhu H, Ali Osman F. Constitutively activated STAT3 frequently coexpresses with epidermal growth factor receptor in high grade gliomas and targeting STAT3 sensitizes them to lressa and alkylators. *Clin Cancer Res* 2008; **14**: 6042–6054.
- 36 Lo HW, Stephenson L, Cao X, Milas M, Pollock R, Ali Osman F. Identification and Functional Characterization of the Human Glutathione S Transferase P1 Gene as a Novel Transcriptional Target of the p53 Tumor Suppressor Gene. *Mol Cancer Res* 2008; **6**: 843–850.
- 37 Zhao R, Yang HY, Shin J, Phan L, Fang L, Yeung SC *et al*. CDK inhibitor p57 (Kip2) is downregulated by Akt during HER2 mediated tumorigenicity. *Cell Cycle* 2013; **12**: 935–943.
- 38 Wang X, Grammatikakis N, Siganou A, Calderwood SK. Regulation of molecular chaperone gene transcription involves the serine phosphorylation, 14-3-3 epsilon binding, and cytoplasmic sequestration of heat shock factor 1. *Mol Cell Biol* 2003; **23**: 6013–6026.
- 39 Fujita N, Jaye DL, Kajita M, Geigerman C, Moreno CS, Wade PA. MTA3, a Mi-2/NuRD complex subunit, regulates an invasive growth pathway in breast cancer. *Cell* 2003; **113**: 207–219.
- 40 Li YM, Pan Y, Wei Y, Cheng X, Zhou BP, Tan M *et al*. Upregulation of CXCR4 is essential for HER2 mediated tumor metastasis. *Cancer Cell* 2004; **6**: 459–469.
- 41 Lo H W, Hsu S C, Ali Seyed M, Gunduz M, Xia W, Wei Y *et al*. Nuclear Interaction of EGFR and STAT3 in the Activation of iNOS/NO Pathway. *Cancer Cell* 2005; **7**: 575–589.
- 42 Lo HW, Zhu H, Cao X, Aldrich A, Ali Osman F. A novel splice variant of GLI1 that promotes glioblastoma cell migration and invasion. *Cancer Res* 2009; **69**: 6790–6798.
- 43 Lo HW, Cao X, Zhu H, Ali Osman F. Cyclooxygenase 2 is a novel transcriptional target of the nuclear EGFR STAT3 and EGFRvIII STAT3 signaling axes. *Mol Cancer Res* 2010; **8**: 232–245.
- 44 Zhu H, Cao X, Ali Osman F, Keir S, Lo HW. EGFR and EGFRvIII interact with PUMA to inhibit mitochondrial translocation of PUMA and PUMA mediated apoptosis independent of EGFR kinase activity. *Cancer Lett* 2010; **294**: 101–110.